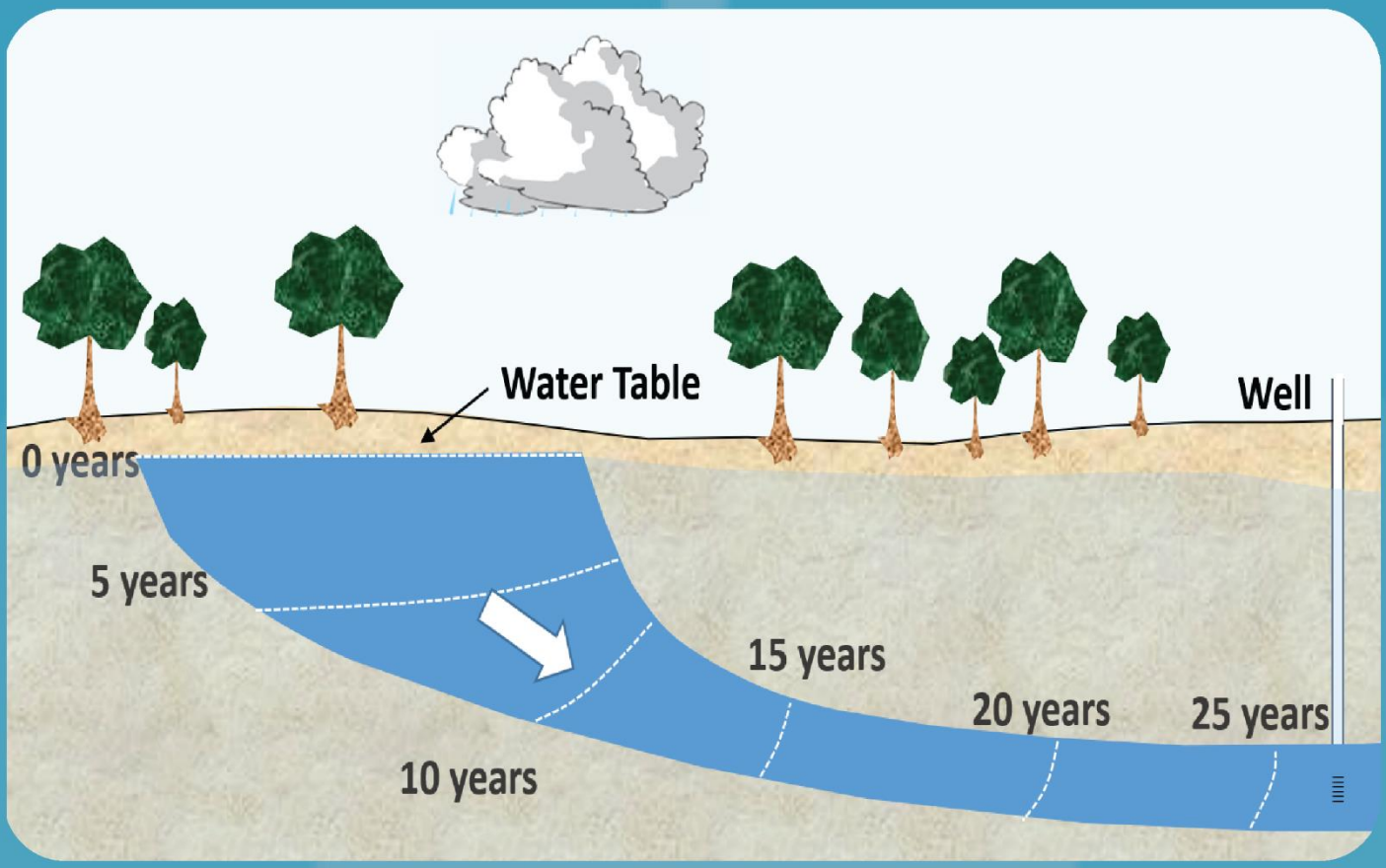

Introduction to Isotopes and Environmental Tracers as Indicators of Groundwater Flow

Peter Cook

THE GROUNDWATER PROJECT

Introduction to Isotopes and Environmental Tracers as Indicators of Groundwater Flow

The Groundwater Project

Peter Cook

Professorial Research Fellow,
National Center for Groundwater Research and Training,
Flinders University
Bedford Park, South Australia, Australia

Introduction to Isotopes and Environmental Tracers as Indicators of Groundwater Flow

The Groundwater Project
Guelph, Ontario, Canada

Published by the Groundwater Project, Guelph, Ontario, Canada, 2020.

Cook, Peter

Introduction to Isotopes and Environmental Tracers as Indicators of Groundwater Flow / Peter Cook - Guelph, Ontario, Canada, 2020.

74 pages

ISBN: 978-1-7770541-8-2

Please consider signing up to the Groundwater Project mailing list and stay informed about new book releases, events and ways to participate in the Groundwater Project. When you sign up to our email list it helps us build a global groundwater community. Sign-up↗.

Cover Image: Peter Cook, 2020

The Groundwater Project Foreword

The United Nations Water Members and Partners establish their annual theme a few years in advance. The theme for World Water Day of March 22, 2022, is "Groundwater: making the invisible visible." This is most appropriate for the debut of the first Groundwater Project (GW-Project) books in 2020, which have the goal of making groundwater visible.

The GW-Project, a non-profit organization registered in Canada in 2019, is committed to contribute to advancement in education and brings a new approach to the creation and dissemination of knowledge for understanding and problem solving. The GW-Project operates the website https://gw-project.org as a global platform for the democratization of groundwater knowledge and is founded on the principle that:

"Knowledge should be free and the best knowledge should be free knowledge." Anonymous

The mission of the GW-Project is to provide accessible, engaging, high-quality, educational materials, free-of-charge online in many languages, to all who want to learn about groundwater and understand how groundwater relates to and sustains ecological systems and humanity. This is a new type of global educational endeavor in that it is based on volunteerism of professionals from different disciplines and includes academics, consultants and retirees. The GW-Project involves many hundreds of volunteers associated with more than 200 hundred organizations from over 14 countries and six continents, with growing participation.

The GW-Project is an on-going endeavor and will continue with hundreds of books being published online over the coming years, first in English and then in other languages, for downloading wherever the Internet is available. The GW-Project publications also include supporting materials such as videos, lectures, laboratory demonstrations, and learning tools in addition to providing, or linking to, public domain software for various groundwater applications supporting the educational process.

The GW-Project is a living entity, so subsequent editions of the books will be published from time to time. Users are invited to propose revisions.

We thank you for being part of the GW-Project Community. We hope to hear from you about your experience with using the books and related material. We welcome ideas and volunteers!

The GW-Project Steering Committee

October 2020

Foreword

This book is focused on the use of isotope analysis of groundwater samples to better understand the origin, travel time, residence time (often referred to as 'groundwater age') and recharge of groundwater. Isotopes serve as indicators or inherent tracers that occur within all groundwater systems. The analyses are done on groundwater molecules or on dissolved constituents in the water. The methods for sampling wells and springs are not complicated and there are many commercial and other laboratories across the globe available for analysis of the most useful isotopes. Isotopes in the study of groundwater systems began in the 1950's and there is now a large literature showing how they can be helpful. Given and relatively low cost per analysis and the many ways in which isotope data provide useful insights unobtainable in other ways, isotopes should be viewed as indispensable 'tools' for nearly all types of groundwater investigations. However, in standard practice, isotopes are not yet used to full advantage. An objective of the GW-Project is to correct this situation by providing education about isotopes in many books in various levels of detail. Peter Cook, the author of this book that provides a broad overview of as the starting point for this topic, is a leader in the field who has co-authored many of the seminal papers across a broad spectrum of isotope applications.

John Cherry, The Groundwater Project Leader

Guelph, Ontario, Canada, October 2020

Preface

This book addresses the use of environmental tracers and environmental isotopes for identifying groundwater sources and quantifying rates of groundwater recharge, discharge, flow, and mixing. Its goal is to present the application of the techniques in a form that can be readily understood and appreciated by groundwater professionals who do not have a background in the use of isotopes or other environmental tracers. The aim is to raise awareness of the potential of these tools, not to present all of the information that is required for their application in particular studies. Consequently, the details of sampling requirements, which sometimes involve specialized equipment, are not discussed. For most of the examples, the techniques were successfully applied. However, not all studies are so successful. Some of the limitations of the various tracers that contribute to failed studies are briefly discussed toward the end of this book and are widely discussed elsewhere.

In this book, emphasis is given to techniques that provide information on groundwater residence times, as these facilitate estimation of groundwater flow rates. The focus is on water quantity rather than quality, so the use of compound-specific isotopic techniques to determine sources of anthropogenic contamination is not considered. Also, the use of isotopes to determine geochemical reactions and pathways is not the focus of this book, although some of the examples demonstrate how residence time indicators have been used in conjunction with measurement of contaminant concentration to determine rates of plume movement or changes in contaminant concentrations over time. This book is focused on the saturated zone, thus does not discuss the use of environmental tracers to estimate soil evaporation or rates of plant water use.

While not the focus of this book, these other topics are of great interest. Isotopes and environmental tracers are being used more widely in groundwater science, and this book aims to facilitate the continuation of this increased use.

Acknowledgements

I deeply appreciate the thorough and useful reviews of and contributions to this book by the following individuals:

- Warren Wood (Michigan State University, East Lansing, Michigan, USA);
- Kip Solomon (University of Utah, Salt Lake City, Utah, USA);
- Andrew Herczeg (Adelaide, Australia);
- Kamini Singha (Colorado School of Mines, Golden, Colorado, USA);
- Roger Diamond (University of Pretoria, Hatfield, South Africa);
- Didier Gastmans (Sao Paulo State University, Rio Claro, Brazil); and,
- David Poulsen (Flinders University, Adelaide, South Australia, Australia).

I appreciate the contributions of Eileen Poeter and John Cherry. I am grateful for Amanda Sills' oversight of this book and to Elhana Dyck for copyediting, both of the Groundwater Project, Guelph, Ontario, Canada. I thank Eileen Poeter (Colorado School of Mines, Golden, Colorado, USA) for copyediting, layout editing and production of this book.

Table of Contents

THE GROUNDWATER PROJECT FOREWORD **4**
FOREWORD **5**
PREFACE **6**
ACKNOWLEDGEMENTS **7**
TABLE OF CONTENTS **8**
1 INTRODUCTION **1**
2 TYPES OF TRACERS **2**
2.1 Introduction 2
2.2 Groundwater Age 3
2.3 Radioactive Tracers 5
2.4 Radiogenic Tracers 7
2.5 Event Markers 8
2.6 Stable Isotopes 9
2.7 Noble Gases 14
2.8 Dissolved Gas Tracers and Liquid-Vapor Partitioning 15
3 TRACER APPLICATIONS **17**
3.1 Investigating Groundwater Mixing 17
3.2 Quantifying Rates of Groundwater Recharge 21
3.3 Quantifying Groundwater Velocities in Confined Aquifers 27
3.4 Identifying Recharge Processes 32
3.5 Estimating the Recharge Rate of River Infiltration 36
3.6 Identifying Groundwater Discharge to Rivers 38
3.7 Identifying Groundwater Flow through Fractures 39
3.8 Reconstructing Climatic Conditions 42
3.9 Reconstructing Contamination History 44
3.10 Calibrating Groundwater Models 46
4 EFFECTS OF MIXING ON GROUNDWATER AGES **49**
4.1 Diffusion and Dispersion 51
4.2 Diffusive Exchange with Aquitards 52
5 PRACTICAL CONSIDERATIONS **54**
5.1 Non-Conservative Tracer Behavior 54
5.2 Planning Field Investigations 57
Availability of Piezometers *57*
The Expected Age of the Groundwater and Required Precision *58*
Local Geology and Geochemical Environment *58*
Sampling Requirements and Analytical Facilities *58*
Ancillary Information Requirements *59*
The Potential for Site Contamination *59*
6 EXERCISES **62**
Exercise 1 62
Exercise 2 62
Exercise 3 63
Exercise 4 63

7 REFERENCES 64
8 EXERCISE SOLUTIONS 71
EXERCISE 1 SOLUTION 71
EXERCISE 2 SOLUTION 71
EXERCISE 3 SOLUTION 72
EXERCISE 4 SOLUTION 72
9 ABOUT THE AUTHOR 73
MODIFICATIONS FROM ORIGINAL RELEASE ..... A

1 Introduction

The most direct way to obtain information on groundwater flow is to follow (or *trace*) the movement of a dissolved substance within groundwater. This approach is most straightforward when a substance is added to the groundwater that was not originally present, and this tracer is added only for a short period of time. Substances like this that are deliberately added for the purpose of studying groundwater movement are referred to as *artificial tracers* and are not discussed here. However, because groundwater movement is often very slow (sometimes only a few meters per year or less), artificial tracers are of limited use for understanding large groundwater systems. Fortunately, there are several *environmental tracers* that can provide similar information. Often, these environmental tracers have been added to the groundwater by natural processes operating over long periods of time. Measurement of these tracers can therefore provide information on processes that have operated over large spatial and temporal scales. This is particularly useful for understanding natural flow systems in large basins.

Here, environmental tracers are defined as geogenic (natural to the Earth) or anthropogenic (human created) isotopes, elements or compounds that are widely distributed in the near-surface environment of the earth, such that variations in their abundances can be used to infer environmental processes. *Isotopes* are a particular category of environmental tracers and are variants of chemical elements that have the same atomic number but differ in their mass number due to different numbers of neutrons in their nucleus. An ideal tracer of water flow is one which is soluble, mobile, relatively unreactive, and easily measured. However, while tracers that behave conservatively (that is, do not cling to subsurface materials nor undergo chemical change) in the environment yield information on water sources or transport processes, tracers that readily undergo chemical reactions can be used to determine hydrochemical conditions in aquifers and reaction pathways. Several environmental tracers also provide information on timescales of subsurface processes. These include *radioactive tracers*, which decay at a known rate; *radiogenic tracers*, which are produced and accumulate in the subsurface; and *event markers*, which are neither produced nor consumed in the subsurface but have a variable and well-known history as to when they entered the groundwater. These tracers can be used to estimate the age of groundwater, which can be used to determine groundwater velocities. Applications of environmental tracers in groundwater therefore include estimation of:

- Mixing between different water sources (Section 3.1);
- Processes and rates of groundwater recharge (Sections 3.2, 3.4 and 3.5);
- Groundwater flow rates (Section 3.3);
- Flow of groundwater to rivers (Section 3.6);
- Groundwater flow through fractures (Section 3.7);
- Palaeoclimate and palaeohydrology (Section 3.8);

- Sources of salinity and other contaminants (Section 3.9); and,
- Calibration of groundwater models (Section 3.10).

The starting point for interpreting environmental tracers is that transport is dominated by advection (transport of a substance by the bulk motion of the groundwater), rather than diffusion and dispersion. This assumption means that as the tracer moves along a flow line water gets progressively older. Within a relatively homogeneous aquifer, it also means that water gets older with depth (Figure 1). There are, of course, several qualifications and exceptions to this general principle, but it provides a good starting point for us to think about the behavior of tracers.

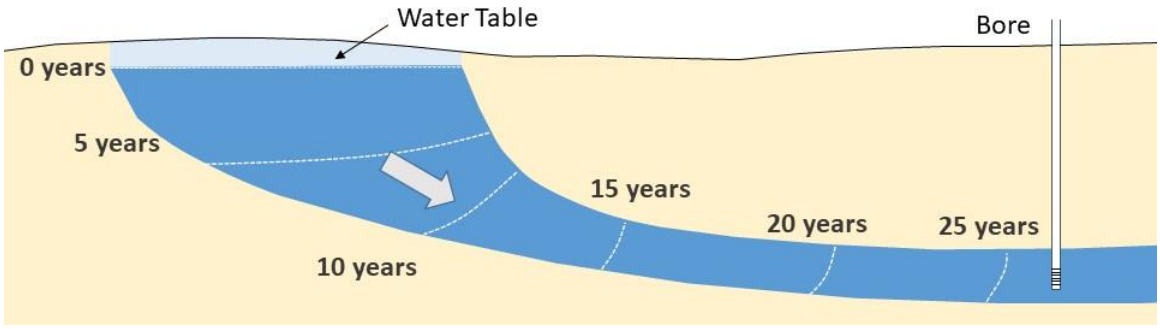

Figure 1 - Schematic illustration of the layering of groundwater age in a simple aquifer system. Groundwater age increases in the direction of groundwater flow, and also increases with depth in the aquifer (Cook, 2020).

2 Types of Tracers

2.1 Introduction

There are numerous tracers that have application to hydrogeology. Three groups of tracers are described here:

- Tracers that provide information on the age of groundwater and that are principally used for determining water velocities and aquifer recharge rates. Types of tracers that fit into this group include radioactive tracers (Section 2.3), radiogenic tracers (Section 2.4) and event markers (Section 2.5).
- Tracers that provide information on reaction processes and phase changes (e.g., evaporation, and condensation). Stable isotopes (Section 2.6) are one of the most important tracers in this group.
- Tracers that are used for identifying water sources and groundwater flow and mixing. In addition to the tracers mentioned above, this group of tracers includes noble gases (Section 2.7) and ion concentrations. Ionic tracers (such as chloride) are not discussed.

The following sections summarizes key principles of these different types of environmental tracers. Sampling and measurement techniques are not discussed in this book but can be found in several specialist texts (e.g., Fritz and Fontes, 1980; Clark and Fritz, 1997; Cook and Herczeg, 2000; Clark, 2015). The most commonly used units for measurement for many of the environmental tracers are summarized in Table 1. In general, stable isotope abundances are reported as deviations from a standard, rather than absolute values, whereas tracers used for groundwater dating can be reported in units of radioactivity or concentration.

Table 1 - Different approaches to reporting tracer concentrations in groundwater, together with the most commonly used units for the most widely used tracers. (The examples include chemical elements, with the number to the upper left indicating the number of protons in the nucleus. Rn is Radon, Kr is Krypton, C is Carbon, Ar is Argon, H is Hydrogen (the form with 3 protons is called Tritium and the form with 2 protons is called Deuterium), Cl is chlorine, Sr is Strontium, O is oxygen, CFC is Chlorofluorocarbon, SF_6 is Sulfur Hexafluoride, N_2 is Nitrogen gas, He is Helium. CFC and SF_6 concentrations in water are usually reported as grams or moles of substance per kg of water. However, atmospheric concentrations are reported in parts per trillion, by volume, often abbreviated as ppt or pptv.)

Reporting Method	Example	Units	Abbreviation
Radioactivity per water volume	^{222}Rn ^{85}Kr	Becquerels per litre	Bq/L
Radioactivity relative to standard	^{14}C	Percent modern carbon	pmC
	^{39}Ar	Percent modern argon	pmA
Atom ratio to more abundant isotope	$^{3}H/^{1}H$ $^{36}Cl/^{35}Cl$ $^{87}Sr/^{86}Sr$	Tritium (^{3}H) is measured in tritium units (TU), where one tritium unit represents one atom of tritium in 10^{18} atoms of hydrogen. For other tracers, this ratio is dimensionless and does not have units.	
Deviation of atom ratio from standard	$^{2}H/^{1}H$ $^{18}O/^{16}O$ $^{13}C/^{12}C$	Per mille (per thousand)	‰
Mass or molar concentration in water	CFC	Picograms per kilogram	pg/kg
	SF_6	Picomoles per kilogram	pmol/kg
Atom concentration in water	^{36}Cl	Atoms per litre of water	atoms/L
Volume of gas at standard temperature and pressure (STP) per water volume	N_2 Ar He	Micro-cm^3 at STP per m^3	μcm^3 (STP) m^{-3}

2.2 Groundwater Age

The *age* of groundwater refers to the time that has elapsed since a water particle entered the saturated zone as groundwater recharge. This is also called the *residence time* of the water particle in the aquifer. The *advective travel time* is the time required for a particle of water to move from one location to another. Residence time and advective travel time are equal when the starting point for the advective travel time is the point of recharge. The

mean age or *mean residence time* refers to a group of water particles. This might be the mean age of a water sample pumped from a well (all the individual water particles need not have the same age) or the mean residence time of water in the entire aquifer. This is perhaps best understood by analogy to human age, where we can talk about the age of an individual or the mean age of a group of individuals. The mean residence time of water in the aquifer (average age at discharge) is then analogous to the life expectancy of the population (average age at death).

It needs to be recognized that while groundwater age may be estimated using environmental tracers, it is only an estimate because measured tracer concentrations are also affected by other processes. Therefore, some authors prefer to use terms such as *apparent groundwater age* or *piston-flow groundwater age* so that this distinction is clear, although these terms are somewhat cumbersome. However, it is useful to refer to *tracer ages* in general, or for example to *CFC-12 ages* or *^{14}C ages* in particular, to differentiate between the concept of age and the estimate obtained with a specific tracer.

Environmental tracers that can be used for estimating groundwater age can be divided into *radioactive isotopes*, *event markers* and *radiogenic tracers*. The most commonly used of these tracers, and the approximate age ranges that they can be used to estimate are illustrated in Figure 2.

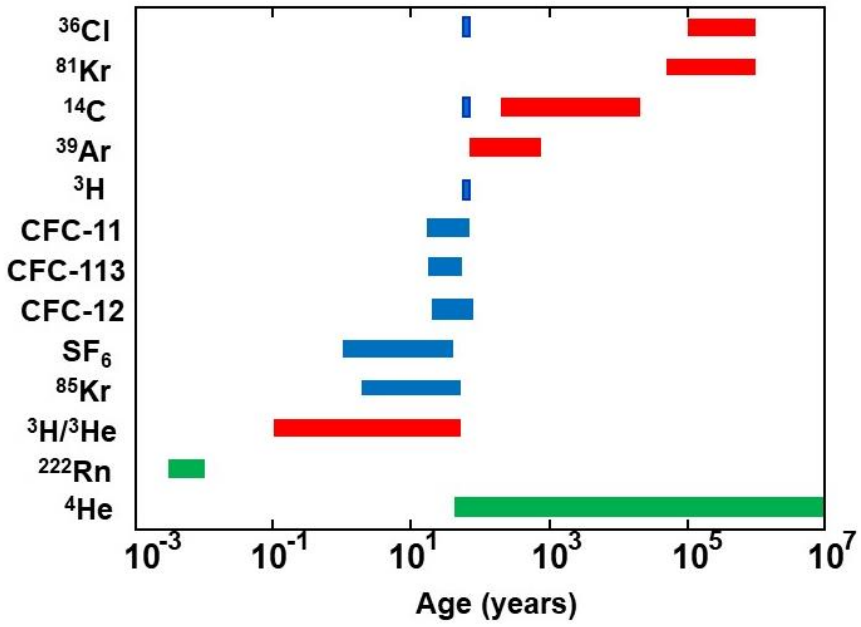

Figure 2 - Approximate age ranges over which different environmental tracers can provide information on groundwater age. Radioactive tracers are indicated in red, event markers in blue and radiogenic tracers in green. Note that while ^{36}Cl and ^{14}C can be used to determine groundwater ages over long timescales as radioactive tracers, they can also be used as event markers for water from the 1950s and 1960s, due to elevated concentrations in the atmosphere at that time from atomic bomb testing. While ^{4}He can potentially be used to date groundwater over a large age range, radiogenic tracers are limited by accurate estimates of production rates (Cook, 2020).

2.3 Radioactive Tracers

A radioactive tracer is any of several species of the same chemical element with different masses that have an unstable nucleus that dissipates excess energy by spontaneously emitting radiation in the form of alpha, beta, and/or gamma rays. If radioactive decay is the dominant process causing changes in the concentration of a tracer, then these changes can be used to infer timescales of groundwater movement. If the concentration of the radioactive element that serves as the tracer in groundwater recharge has been relatively constant, then its concentration will decrease exponentially over time (Figure 3). Assuming no other process is reducing the concentration of the element, the age of a groundwater sample is given by Equation 1.

$$t = -\lambda^{-1} ln\left(\frac{c}{c_0}\right) \quad (1)$$

where:

c = measured concentration of radioactive tracer

c_0 = initial concentration of radioactive tracer (same dimension as c)

λ = decay constant (T^{-1})

The decay constant and half-life are related by Equation 2.

$$\lambda = \frac{-\ln (0.5)}{t_{1/2}} \quad (2)$$

where:

$t_{1/2}$ = half-life of radioactive tracer (T)

A number of different radioactive isotopes have been used to estimate the age of groundwater in this way, including ^{14}C ($t_{1/2}$= 5,730 years), ^{32}Si ($t_{1/2}$= 140 years), ^{35}S ($t_{1/2}$= 88 days), ^{36}Cl ($t_{1/2}$= 301,000 years), ^{39}Ar ($t_{1/2}$= 269 years) and ^{81}Kr ($t_{1/2}$ = 229,000 years), with ^{14}C the most commonly used. These isotopes are produced by cosmic ray interactions with various elements in the atmosphere and dissolve in rain and enter the hydrologic cycle.

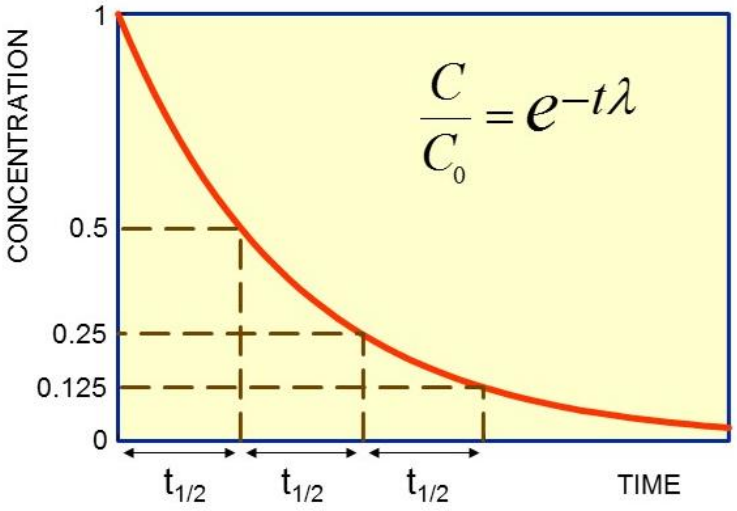

Figure 3 - In the radioactive decay process, the concentration of the radioactive element will be reduced to half of its initial value after one half-life, and the concentration will continue to halve after every subsequent half-life until it is no longer measurable. The equation in the Figure is a re-arrangement of Equation 1 in the text (Cook, 2020).

If the input concentration of a radioactive tracer is variable or not well known, it is sometimes possible to measure the concentrations of both the *radioactive parent* (the radioactive element that originally entered the groundwater) and the *daughter product* (the element that is produced by the radioactive decay), and to sum these to determine the initial concentration of the parent. This is generally only possible when the daughter product is not itself radioactive. This is the basis of the $^{3}H/^{3}He$ method of groundwater dating (the parent ^{3}H decays to the stable daughter ^{3}He; Figure 4), but it cannot be used for some of the other radioactive tracers (e.g., ^{14}C, ^{35}S, ^{36}Cl, ^{39}Ar) as their decay products are difficult to measure, in some cases due to high background concentrations (elemental symbols are defined in the caption of Table 1). A background concentration is the concentration of a substance unrelated to that input by the source of the tracer (e.g., ^{14}C decays to stable nitrogen, which is widespread in the environment).

Where both parent and daughter concentrations are measured, the daughter is stable, and background concentrations are low, then the age of a groundwater sample is given by Equation 3.

$$t = -\lambda^{-1} ln\left(\frac{c_p}{c_p + c_d}\right) \quad (3)$$

where:

c_p = parent concentration

c_d = daughter concentration (same dimension as c_p)

λ = decay constant of the parent (T^{-1})

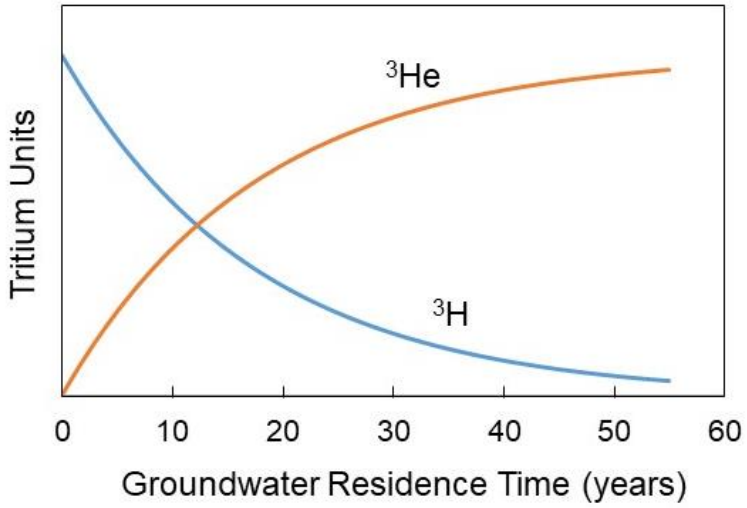

Figure 4 - Schematic illustration of the decay of ^{3}H and growth of ^{3}He over time. The ratio of ^{3}He to ^{3}H increases with time and can be used to estimate the groundwater age. After 12.3 years, the half-life of ^{3}H, exactly half of the ^{3}H has decayed to ^{3}He (Cook, 2020).

2.4 Radiogenic Tracers

Radiogenic tracers are atoms of a chemical element that are produced by radioactive decay and may themselves be radioactive or stable. Information about groundwater residence times sometimes can be obtained from the accumulation rates of radiogenic isotopes with low background concentrations. This approach may be applied in aquifers with relatively long groundwater residence times containing components of ^{4}He from radioactive decay of U and Th (e.g., Mazor and Bosch, 1992; Solomon et al., 1996). The technique requires independent estimates of the local production and release rates of the radiogenic isotopes. However, obtaining enough measurements to understand potential spatial variations in production rates is difficult. ^{222}Rn is also produced through U and Th decay, but its short half-life (3.8 days) means that secular equilibrium concentrations are achieved after a relatively short time (~20 days). (*Secular equilibrium* means that the rate of production is exactly balanced by the rate of decay, and so the concentration does not change.) Thus, over longer timescales, ^{222}Rn concentrations in groundwater are essentially unrelated to residence time and primarily determined by the production rate (Figure 5).

^{222}Rn is only produced by radioactive decay of ^{226}Ra (which is part of the U and Th decay chain). Therefore, in principle, measurements of ^{222}Rn can be used to date groundwater over periods up to approximately 20 days. Helium can be present from other sources. It has a significant concentration in the atmosphere, so is present in water that recharges the groundwater system. Consequently, helium is most useful for dating groundwater over longer timescales, when He produced from radioactive decay of U and Th isotopes within an aquifer (referred to as radiogenic ^{4}He) is likely to dominate helium from other sources, including diffusion from underlying strata.

When groundwater containing accumulated radiogenic tracers is removed from the aquifer that contains the parent materials, for example by discharging to a stream, then concentrations of these tracers no longer increase. ^{222}Rn concentrations will decrease due to radioactive decay, and concentrations of ^{4}He and ^{222}Rn will decrease due to exchange with the atmosphere. If these exchange rates are known, or can be measured, then concentrations of these dissolved gases within surface water bodies can be used to determine the time since groundwater discharged to the surface (Section 3.6).

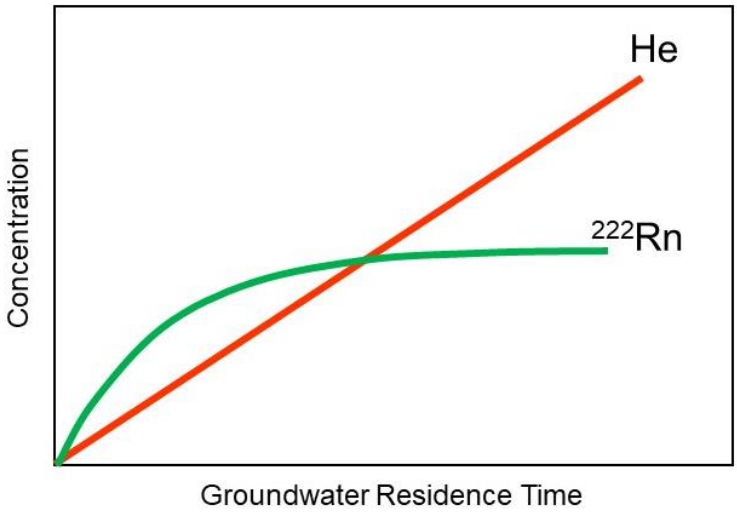

Figure 5 - Schematic illustration of changes in concentration of helium and radon with time after water enters an aquifer system. Both are produced by radioactive decay of other elements. However, as radon is itself radioactive, the rate of increase in concentration decreases over time, until eventually a constant concentration is reached (after approximately 20 days). Helium does not decay or degrade, so its concentration continues to increase over time (Cook, 2020).

2.5 Event Markers

If the input concentration of an environmental tracer has been variable, but is well known, concentrations measured in groundwater may be compared directly with the known input concentrations to provide information on the groundwater age. ^{3}H, ^{36}Cl, ^{85}Kr, CFC and SF_6 concentrations are commonly interpreted in this way. Of course, this method is effective only over the period during which input concentrations have changed and in which they have been measured or can be modelled reliably. It is therefore generally limited to groundwater that entered the subsurface over the past 100 years. Concentrations of ^{3}H, ^{36}Cl and ^{14}C increased in the atmosphere during the 1950s and 1960s as a result of above-ground nuclear bomb testing and have decreased gradually toward natural levels since then. ^{85}Kr, CFCs and SF_6 have been released to the atmosphere from various industrial sources since the middle of the 20th century (Figure 6). CFCs were most useful as a groundwater dating tool until the 1990s, as until that time atmospheric concentrations of

these compounds were increasing monotonically, and so a measured concentration in groundwater could be uniquely assigned a groundwater age. However, international agreements to reduce anthropogenic emissions of these compounds have reduced atmospheric concentrations, so that measured concentrations can no longer be uniquely related to a recharge date. For SF_6 and ^{85}Kr, however, atmospheric concentrations continue to increase, so these tracers still have good resolution for young water samples. Other atmospheric contaminants are also being explored as potential event markers (Busenberg and Plummer, 2008; Beyer et al., 2017).

One of the advantages of CFCs and SF_6 is that their atmospheric concentrations are relatively uniform globally, and so the input concentration is usually known with a high precision. ^{85}Kr shows greater latitudinal variation. ^{3}H and ^{36}Cl show the greatest amount of spatial variation of input concentrations, although the time of peak concentrations was essentially the same at all locations.

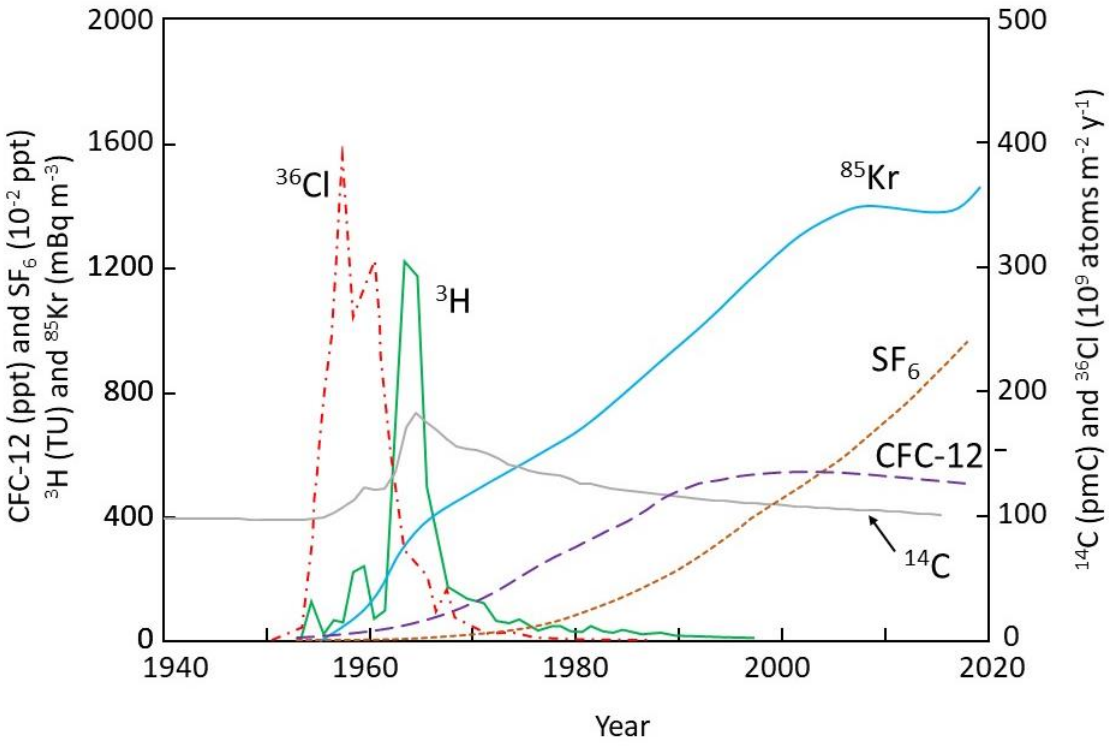

Figure 6 - Annually averaged atmospheric concentrations of some environmental tracers used as event markers to determine ages of groundwater. Unlike Figures 4 and 5, groundwater age decreases towards the right. Data are from Maiss and Brenninkmeifer (1998), Walker et al. (2000), Cook and Böhlke (2000), Graven et al. (2017), Bollhöfer et al. (2019) and HATS (Halocarbons and other Atmospheric Trace Species Group) Global database (Cook, 2020).

2.6 Stable Isotopes

Stable isotopes are atoms of the same chemical element (i.e. the same number of protons and electrons) with a different number of neutrons that do not undergo radioactive

decay, but they may be present as a result of radioactive decay. Ratios of different stable isotopes of the same element can provide useful indicators of water sources and chemical reactions.

The ratios of the less abundant to the most abundant stable isotope of an element (e.g., $^{13}C/^{12}C$, $^{18}O/^{16}O$, $^{15}N/^{14}N$) vary slightly between different materials and vary spatially within the same material. Differences in abundance of the different isotopes are usually caused by small differences in reactivity because of mass differences; lighter isotopes typically being more reactive than heavier isotopes. Natural materials will therefore have different isotopic abundances due to different source materials and different geochemical processes to which they have been exposed. Consequently, changes in isotopic abundance of natural materials can provide information on sources of dissolved substances, and chemical reactions that might have taken place after dissolution. The stable isotope ratios of the water molecule ($^{18}O/^{16}O$ and $^{2}H/^{1}H$) are particularly useful in hydrology, as they can provide information on condensation and evaporation processes. Manufactured chemicals can have different isotopic ratios due to differences in source materials or manufacturing processes. Fractionation is the name given to processes that affect the relative abundance of light and heavy stable isotopes (light being the isotopic form with fewer neutrons).

Some of the key stable isotopes that have application to hydrology are listed in Table 2, along with their relative global abundances. The ratio of heavy to light isotopes can be measured with high accuracy and precision, therefore differences between relative abundances at a local level can be used to infer migration of groundwater and geochemical processes occurring along the flow paths. Isotope ratios can be measured either on individual ions of molecules, for example, $^{15}N/^{14}N$ and $^{18}O/^{16}O$ of NO_3^-, $^{34}S/^{32}S$ or $^{18}O/^{16}O$ of SO_4^{2-}, $^{18}O/^{16}O$ or $^{2}H/^{1}H$ of H_2O, or on groups of molecules, such as with $^{13}C/^{12}C$ of total dissolved inorganic carbon (TDIC). Usually this ratio is expressed relative to a standard using the *delta (δ) notation* as shown in Equation 4.

$$\delta = \frac{R_{sample} - R_{std}}{R_{std}} \times 1000\ ‰ \qquad (4)$$

where:

R = ratio of isotope amount (usually less abundant to most abundant isotope)

Thus, the δ-value of a sample which is identical to the standard would be 0 ‰, positive values indicate a greater proportion of the less abundant isotope than the standard, and negative values indicate a lower proportion of the less abundant isotope (Table 1).

Table 2 - Relative global abundances of some commonly used stable isotopes. From Rosman and Taylor (1998).

Hydrogen (%)		Carbon (%)		Nitrogen (%)	
^{1}H	99.9885	^{12}C	98.93	^{14}N	99.632
^{2}H	0.0115	^{13}C	1.07	^{15}N	0.368
Oxygen (%)		**Sulphur (%)**		**Strontium (%)**	
^{16}O	99.757	^{32}S	94.93	^{84}Sr	0.56
^{17}O	0.038	^{33}S	0.76	^{86}Sr	9.86
^{18}O	0.205	^{34}S	4.29	^{87}Sr	7.00
		^{36}S	0.02	^{88}Sr	82.58

Two of the most widely used stable isotope ratios are those of hydrogen and oxygen in the water molecule. Although there are two common stable isotopes of hydrogen and three of oxygen, giving a total of nine isotopically different water molecules, only three are commonly measured in natural waters: $^{1}H^{1}H^{16}O$, $^{1}H^{2}H^{16}O$ and $^{1}H^{1}H^{18}O$, with the first being the most abundant form. Variations in $^{2}H/^{1}H$ and $^{18}O/^{16}O$ ratios in natural waters arise mostly from isotopic fractionation during evaporation and condensation processes, whereby the heavy isotopes of water preferentially remain in the liquid phase during evaporation or pass into the liquid phase during condensation.

Rainfall everywhere in the world is depleted in the heavy isotopes of water relative to seawater through a process known as *Rayleigh fractionation*. (Seawater is used as the standard for $\delta\,^{2}H$ and $\delta\,^{18}O$ measurement, so it has an isotopic composition of $\delta\,^{2}H = \delta\,^{18}O = 0$ ‰.) Because lighter isotopes evaporate more readily than heavier isotopes, clouds will contain a greater proportion of light isotopes (and thus have negative values for $\delta\,^{2}H$ and $\delta\,^{18}O$). The isotopic composition of rainfall will be heavier than that of clouds, but lighter than the seawater which was the original source of the water vapor forming the clouds. As air masses progressively move inland, rainfall becomes progressively lighter (Coplen et al., 2000). Because ^{2}H and ^{18}O are affected in similar ways, $\delta\,^{2}H$ and $\delta\,^{18}O$ values in precipitation are highly correlated. The *global meteoric water line* (GMWL) is an empirical relationship that expresses the average correlation between $\delta\,^{2}H$ and $\delta\,^{18}O$ values in precipitation, and is given by Equation 5 (Craig, 1961).

$$\delta^{2}H = 8\delta^{18}O + 10 \qquad (5)$$

Often, however, the stable isotopic composition of local rainfall differs from the global mean, and so it is sometimes useful to define a *local meteoric water line* (LMWL; Figure 7).

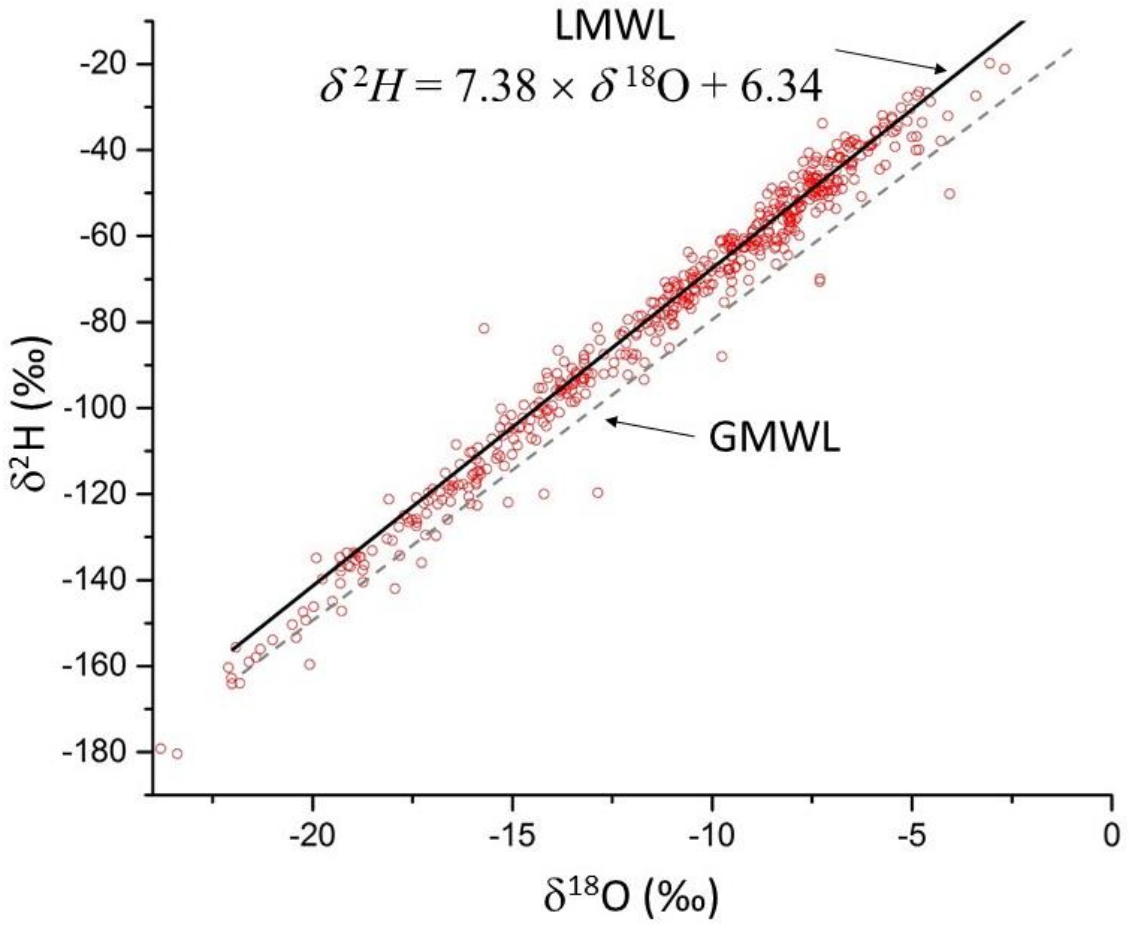

Figure 7 - Monthly rainfall data for Ottawa, Canada, between December 1972 and February 2017, together with the Local Meteoric Water Line (LMWL), calculated as a linear regression on the data. Data from IAEA/WMO (2018). The global meteoric water line (GMWL), given by Equation 5 is shown for comparison (Cook, 2020).

In many cases, the mean δ^2H and δ^{18}O composition of groundwater will be similar to the mean amount-weighted δ^2H and δ^{18}O composition of precipitation within its recharge area. However, fractionation processes result in variations in isotopic composition of precipitation, and sometimes these variations can be used to identify conditions under which the groundwater recharge occurred (Figure 8). Other factors being equal, the isotopic composition will be more depleted in heavy isotopes during heavy rainstorms than during lighter storm events. So, if groundwater recharge primarily occurs during large rain events, it may cause the mean isotopic composition of groundwater to be more depleted than mean rainfall. Also, rainfall at higher elevations will be more depleted than rainfall at lower elevations, and rainfall during cold climatic periods will be more depleted than rainfall during warmer periods (Ingraham, 1998; Mazor, 2004). Subsequent to a rainfall event, the ^{18}O and ^{2}H composition of water may be further modified by evaporation from the soil or from surface water bodies, and these effects are most notable in more arid climates. Water samples affected by evaporation are typically displaced to the right of the meteoric water line, and often fall on a line of lower slope (Figure 8), while transpiration does not

significantly fractionate the stable isotopes. The International Atomic Energy Agency (IAEA) maintains a network of rainfall collection stations around the world, so there is a good database on the $\delta^{2}H$ and $\delta^{18}O$ composition of precipitation for comparison with groundwater samples.

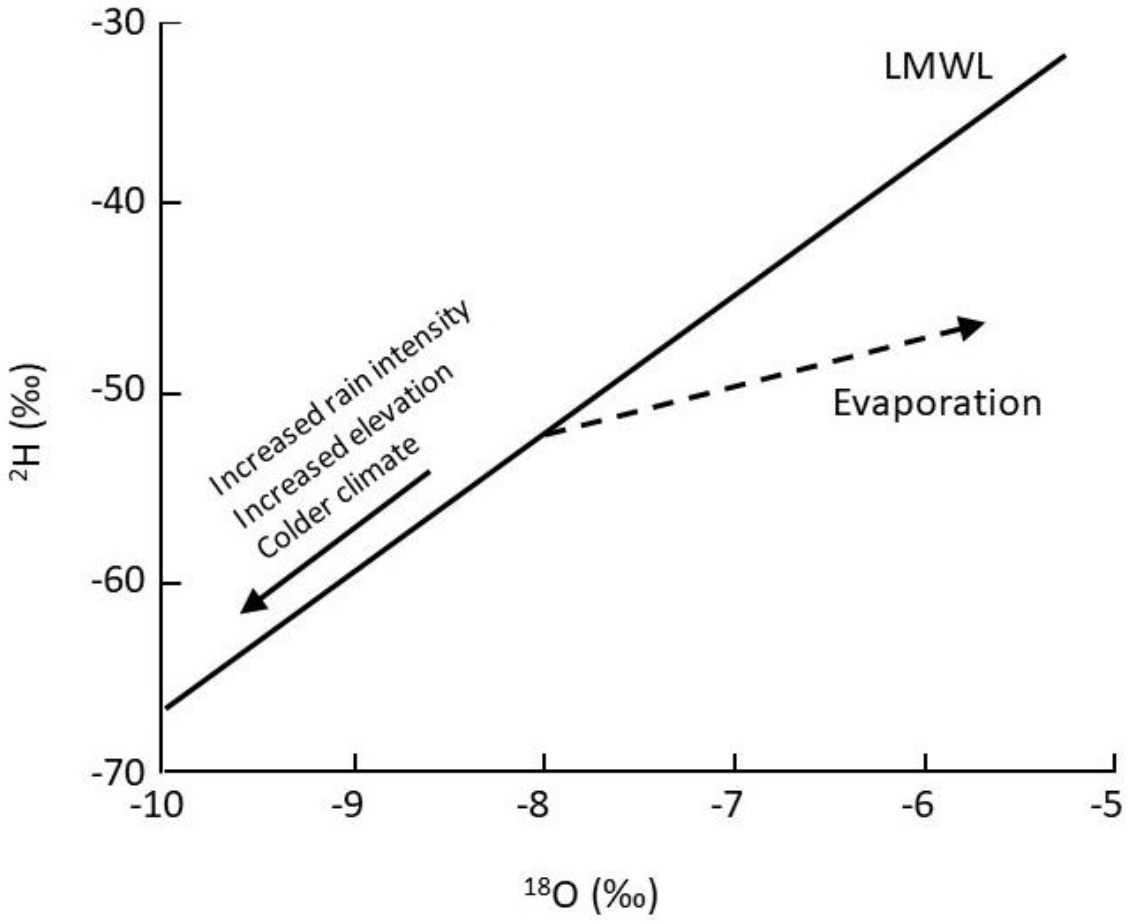

Figure 8 - Schematic representation of the principal processes affecting the ^{2}H and ^{18}O composition of groundwater. The slope of the evaporation line is usually between 4 and 6 for surface water evaporation, and between 2 and 5 for soil evaporation (Barnes and Allison, 1988) (Cook, 2020).

Other stable isotopes that are widely used in hydrogeology include:

- Nitrogen ($^{15}N/^{14}N$) and oxygen ($^{18}O/^{16}O$) isotope ratios on NO_3^-, which are used to determine sources of nitrate contamination in groundwater, and biogeochemical processes that affect nitrate concentrations.
- Strontium isotope ratios ($^{87}Sr/^{86}Sr$) for identifying water sources and geological provenance of groundwater.
- Sulphur ($^{34}S/^{32}S$) and oxygen ($^{18}O/^{16}O$) isotope ratios on SO_4^{2-} are used to trace natural and anthropogenic sources of sulfur, and biogeochemical processes that affect sulfur and sulfate.
- Carbon isotope ratios ($^{13}C/^{12}C$) are used for determining chemical reactions involving dissolved organic and inorganic carbon. $\delta^{13}C$ ratios on dissolved

inorganic carbon are particularly useful for determining chemical reactions that have affected ^{14}C activity, and hence impacted the ability to use ^{14}C as a groundwater age tracer. $\delta^{13}C$ of organic materials can provide evidence for identifying sources of contaminants.

2.7 Noble Gases

Noble gases are a group of chemical elements that are stable (i.e. unreactive) because their outer shell of valence electrons is full. They are also colorless, odorless, tasteless and non-flammable. The six naturally occurring noble gases are the chemical elements helium (He), neon (Ne), argon (Ar), krypton (Kr), xenon (Xe), and radon (Rn). Radon and helium have been discussed above in the context of radiogenic tracers. The common isotopes of the other noble gases are neither radiogenic nor radioactive, and therefore represent the most stable of all tracers. In environmental applications, concentrations of nitrogen are often interpreted together with noble gas concentrations, and so it is also discussed here. (Although nitrogen is more reactive than the noble gases, dissolved N_2 is relatively stable and nitrogen concentrations in water are more easily measured than concentrations of many of the noble gases.)

The atmospheric abundances of the noble gases and nitrogen have been essentially constant throughout geologic time, and so for most of these gases differences in concentrations in water are principally due to differences in gas solubility in water, which is a function of temperature, pressure and salinity (Section 2.8). Solubility is the amount of a substance (the solute) that dissolves in a unit volume of a liquid (the solvent) to form a saturated solution at a specified temperature and pressure. The exceptions are He and Rn, which are produced by radioactive decay in quantities that sometimes overwhelm that resulting from equilibrium solubility with the atmosphere. For the other noble gases (Ne, Ar, Kr and Xe) and N_2, concentrations in water provide information on the temperature and pressure at the time of recharge.

Measurements of noble gas concentrations in groundwater have shown that concentrations in water are often much larger than can be explained by equilibrium solubility. Such 'excess' gas concentrations are referred to as *excess air* and believed to be due to addition of air due to entrapment of air bubbles during recharge and their subsequent dissolution (Heaton and Vogel, 1981). If all the air bubbles completely dissolve, then excess air entrapment is not a function of solubility, and so gas ratios in excess air are different to those due to equilibrium solubility. Measurement of at least two noble gases typically allows both recharge temperature and excess air to be independently quantified (Figure 9). In mountainous terrain, gas concentrations may provide information on elevation (and hence location of recharge; Peters et al., 2018), whereas in large regional aquifers measurement of gas concentrations in conjunction with groundwater dating can provide information on paleo-temperatures (Aeschbach-Hertig and Solomon, 2013; Section

3.8). A few studies have also suggested that excess air might provide information on recharge processes (e.g., Massmann and Sültenfuss, 2008; Hall et al., 2012).

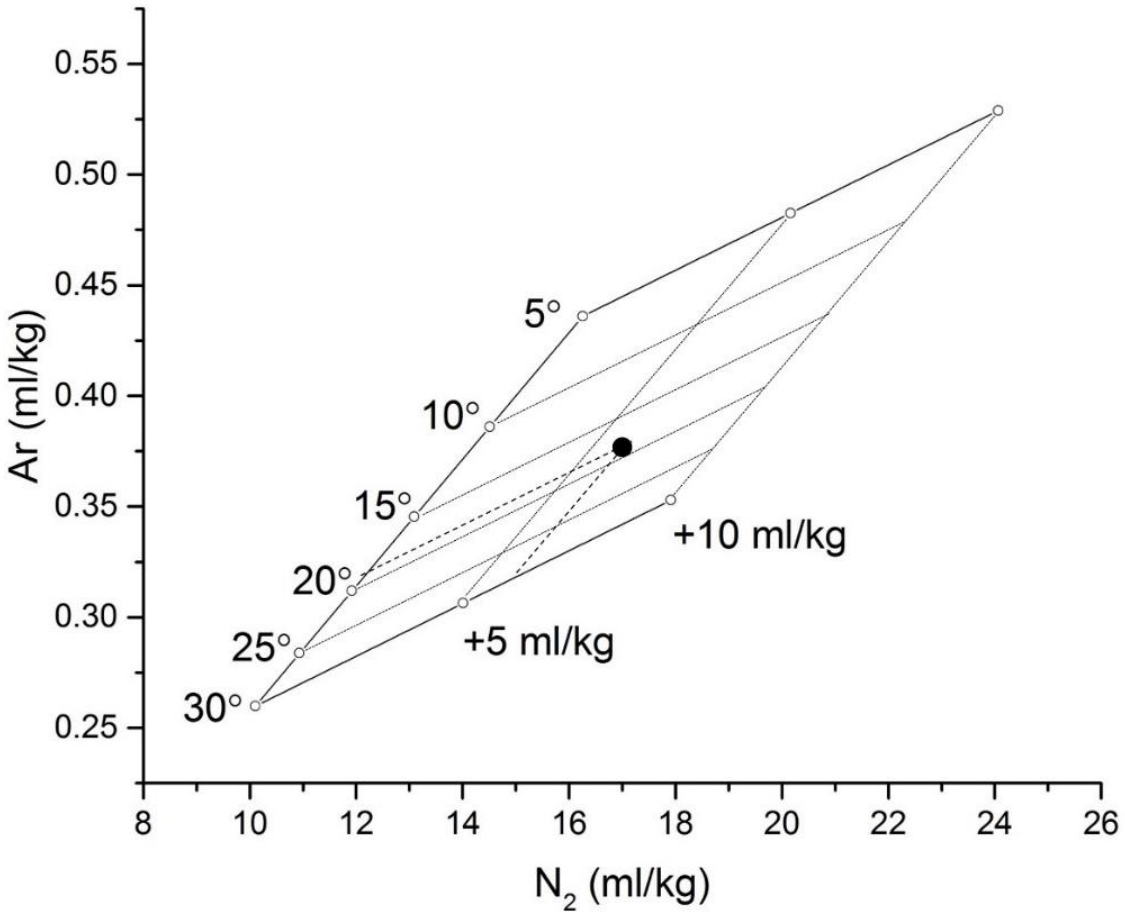

Figure 9 - Comparison of argon and nitrogen concentrations in groundwater as a function of recharge temperature and excess air. Lines depict expected concentrations for water in equilibrium with the atmosphere at temperatures between 5 and 30°C, and with up to 10 ml/kg of excess air. The sample indicated by the circle would therefore represent a recharge temperature of 19°C with 6 ml/kg of excess air. This plot assumes complete dissolution of excess air in groundwater. For partial dissolution models, the reader is referred to Aeschbach-Hertig et al. (1999); Aeschbach-Hertig and Solomon (2013); and Aeschbach-Hertig (2004) (Cook, 2020).

2.8 Dissolved Gas Tracers and Liquid-Vapor Partitioning

Several of the commonly used environmental tracers are gases at natural atmospheric temperatures and pressures. However, all gases will dissolve in water, so they can provide information on groundwater processes. Under equilibrium conditions, the relationship between the concentration of gas in air and its concentration in water is given by Henry's Law. This can be expressed as shown in Equation 6.

$$C_w = K_H C_a \left(P - p_{H_2O}\right) \quad (6)$$

where:

C_w = concentration dissolved in water

C_a = concentration in dry air

K_H = Henry's Law constant (solubility of the gas in water)

P = total atmospheric pressure

p_{H_2O} = water vapor pressure

The solubility of a gas in water will be a function of the water temperature and salinity, and the resultant equilibrium concentration in water will also be a function of the atmospheric pressure. The water vapor pressure is also a function of temperature and salinity. In general, concentrations of dissolved gases will be higher in colder water and in water with lower salinity. Gas solubility as a function of temperature and salinity is well known for most gases of interest in hydrology. Data on gas solubility have been compiled by Cook and Herczeg (2000).

The relationship between a gas's concentration in air and its equilibrium concentration in water can also be expressed in terms of a partition coefficient. The partition coefficient reflects the relative mass of tracer in equivalent volumes of water and air and will be one when equal mass occurs in each phase. Partition coefficients at 10°C and 1 atm pressure for commonly used tracers range from approximately 0.01 for helium and SF_6 to 0.5 for CFC-11 and ^{222}Rn (Figure 10). This means that great care needs to be taken when sampling for helium and SF_6, as contact with the atmosphere can rapidly change concentrations. It also means that transport of helium and SF_6 through the unsaturated zone predominantly occur within the gas phase, whereas transport of CFC-11 and ^{222}Rn occur in both liquid and gas phases. In contrast, dissolved ions such as chloride move exclusively in the liquid phase. Analysis of ^{14}C in inorganic carbon that is dissolved in the water includes dissolved CO_2 and carbonate and bicarbonate ions, so the partition coefficient for total inorganic carbon will be greater than that of CO_2 alone. In areas with thick unsaturated zones, groundwater ages estimated with CFCs, SF_6 and ^{85}Kr may include a component that reflects the travel time through the unsaturated zone (Engesgaard et al., 2004). The effect will be more pronounced for tracers with large partition coefficients, and this can sometimes cause differences between water ages obtained with these tracers (Cook and Solomon, 1997).

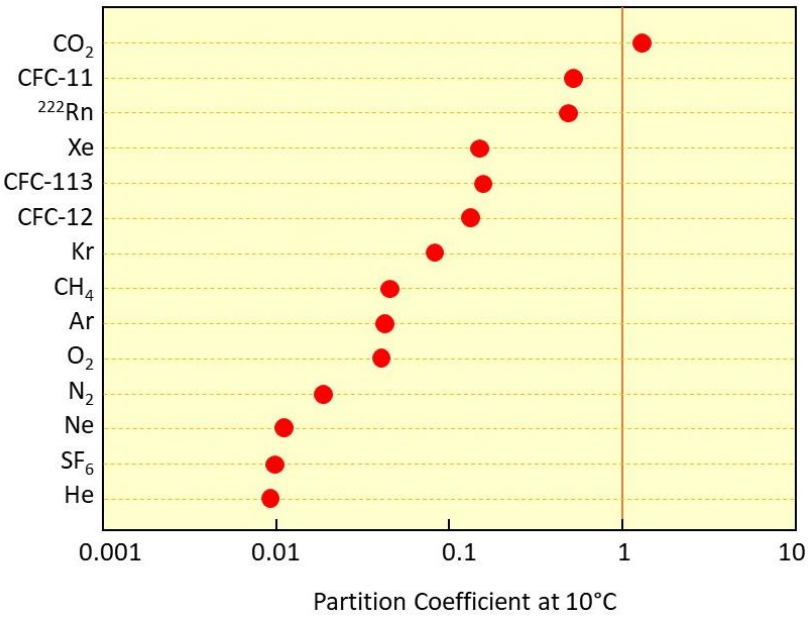

Figure 10 - Partition coefficients (moles per cm^3 of water divided by moles per cm^3 of air under equilibrium conditions) at 1 atm pressure for some commonly used environmental tracers. Low values of the partition coefficient indicate that the tracer occurs predominantly in the gas phase within the unsaturated zone (Cook, 2020).

3 Tracer Applications

3.1 Investigating Groundwater Mixing

Conservative tracers can provide quantitative information on mixing between different water sources. When two or more water sources (often termed *end-members*) that have different isotopic or chemical compositions are mixed, then the chemical composition of the mixture will depend upon the composition of each end-member and the proportion of each end-member in the mixture. Thus, Equation 7 can be written for mixing of two water sources.

$$c_m = c_1 f + c_2(1 - f) \tag{7}$$

where:

c_m = concentration of the mixed water

c_1 = concentration of conservative tracer in end-member water 1

c_2 = concentration of conservative tracer in end-member water 2

f = proportion of end-member 1 in the mixture

$1 - f$ = proportion of end-member 2 in the mixture

Here, the concentrations must be absolute concentrations, and not isotope ratios, as discussed below. Thus, if the concentrations in the two sources (end-members) are known (or assumed), and their concentrations in the mixed sample are measured, then Equation 7 can be re-arranged into Equation 8 and hence the proportions of each end-member in the mixture can be determined.

$$f = \frac{c_m - c_2}{c_1 - c_2} \tag{8}$$

Although concentrations of a single conservative tracer only need be measured to calculate proportions of two end-members in a mixture, it is more common to measure concentrations of more than one tracer. This will give increased confidence in results of the mixing calculations. When two different tracers are measured, then a mixing plot can be constructed showing the concentrations of the two end-members in the mixture, and the concentration of the mixed sample.

The concentration of a conservative element in a mixture of two end-members will lie on a straight line between these end-members (Figure 11). This straight line is often called a *mixing line*. Where several samples fall on mixing line, then this is evidence that they may be the products of mixing. However, if the ratios of elements, or isotope ratios (e.g., $^{87}Sr/^{86}Sr$, $^{13}C/^{12}C$), are plotted then the mixing line can be curved rather than straight. In this case, Equation 7 will also not be correct. This occurs most frequently when an isotope ratio is plotted against the total concentration of the element (e.g., $^{87}Sr/^{86}Sr$ ratio versus total Sr concentration). It occurs because at higher element (e.g., Sr) concentrations, a larger change in isotope concentration (e.g., ^{87}Sr concentration) is required to change the isotope ratio than at lower element concentrations (Section 2.5.3 of Kendall and Caldwell, 1998).

A similar approach can be applied where there are more than two end-members, although more than one conservative tracer will be needed. The mixing equation for 'n' end-members is shown as Equation 9.

$$c_{Am} = c_{A1}f_1 + c_{A2}f_2 + \cdots + c_{An}f_n \tag{9}$$

where:

c_{Am} = concentration of tracer A in mixture

c_{Ai} = concentration of tracer A in end-member water n (same dimension as c_{Am})

f_n = proportion of end-member 'n' (dimensionless)

In this case there are 'n' proportions: f_1, f_2, ..., f_n. However, since the proportion of the last end-member, f_n, can be calculated from the other proportions (i.e., $f_n = 1 - f_1 - f_2 - \ldots - f_{n-1}$), there are only n-1 unknowns. To solve this equation, n-1 equations are needed, which means that n-1 different conservative tracers need to be measured. The equations for the

different tracers can then be solved simultaneously to determine the proportions of the 'n' different end-members in the mixture.

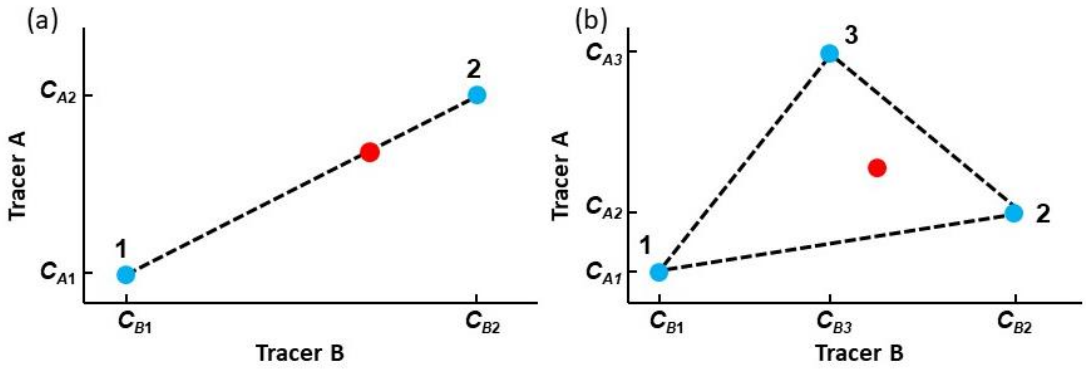

Figure 11 - Effect of mixing of water samples on tracer concentrations. (a) Where mixing occurs between two discrete water sources, then concentrations of conservative elements in the resulting mixed sample will fall on a straight line between the end-members. (b) Where mixing occurs between three discrete water sources, then concentrations of conservative elements in the mixed sample will fall within a triangle bounded by the three end-member concentrations. Blue circles denote end-member concentrations, and red circles denote mixed samples (Cook, 2020).

A good example of the use of environmental tracers to determine mixing fractions is provided by a study of artificial recharge in the Santa Clara Valley, California (Figure 12; Muir and Coplen, 1981; Coplen et al., 2000). Groundwater use in the Santa Clara Valley led to groundwater depletion, and an aqueduct was created to import water from northern California. The imported water was discharged into streambeds and percolation ponds to artificially recharge the groundwater. A study subsequently took place to determine the spread of the imported water from the sites where it was introduced, and its contribution to groundwater pumped by downstream wells. The $\delta^{2}H$ and $\delta^{18}O$ composition of native groundwater was determined to be -41 ‰ and -6.1 ‰, respectively, based on groundwater samples collected in areas unaffected by imported water. The mean value of imported water was -74 ‰ and -10.2 ‰ for $\delta^{2}H$ and $\delta^{18}O$, respectively. Groundwater samples downstream of the artificial recharge sites ranged between -45 and -62 ‰ for $\delta^{2}H$ and -6.6 and -8.6 ‰ for $\delta^{18}O$, and thus were intermediate between the native groundwater and imported water values (Figure 13). The authors used Equation 8 to estimate the contribution of imported water to downstream wells at between 10 and 70%. Lower fractions of imported water were estimated for wells furthest from the artificial recharge sites, with fractions between 10 and 20% recorded for wells up to 4 – 5 km downgradient.

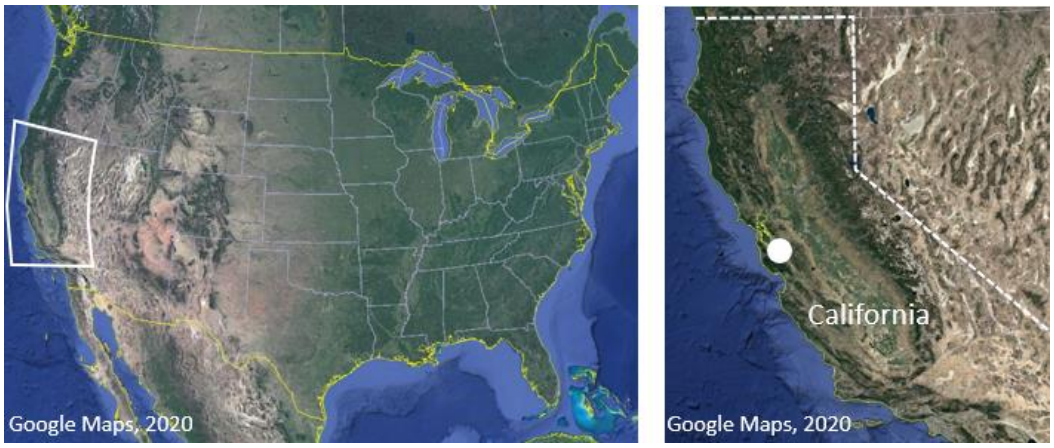

Figure 12 - Location of Santa Clara Valley, California, USA, which has been importing water to recharge local aquifers since the 1960s. Stable isotope studies have been used to evaluate the performance of these managed aquifer recharge schemes (Figure 13). The map on the left shows the location of the inset, on the right.

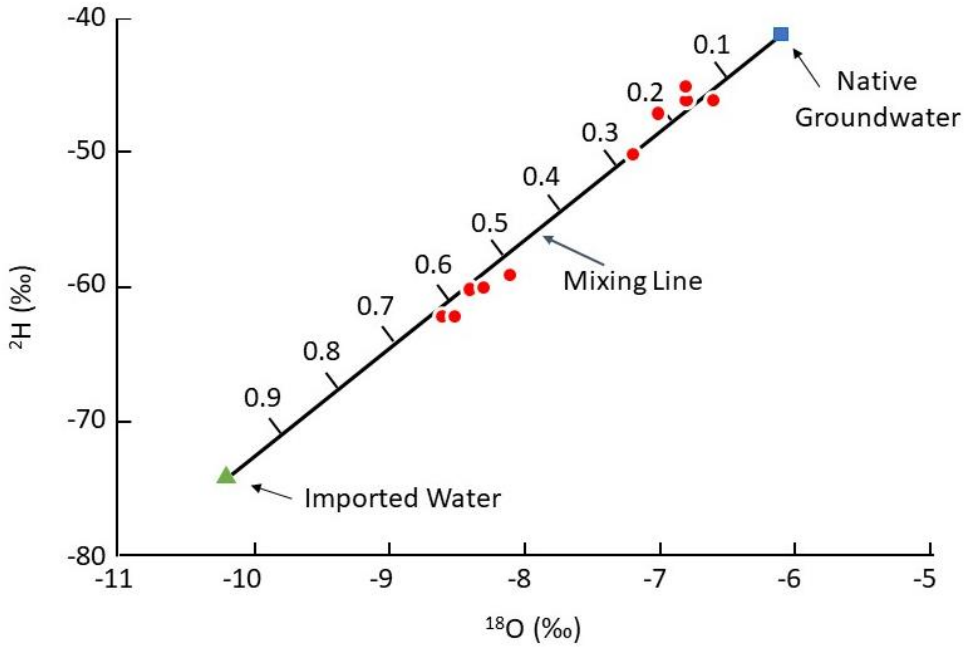

Figure 13 - Mixing between native groundwater in the Santa Clara Valley, California (blue square) and imported water from northern California (green triangle) that was artificially recharged through streams and percolation ponds. Groundwater downstream of the areas of artificial recharge (red circles) had a stable isotope composition between the two end-members. Numerals indicate the fraction of imported water in the downstream wells. Based on the $\delta\ ^{18}O$ and $\delta\ ^{2}H$ composition, the contribution of northern California water in downstream wells varies between 10 and 70%, with lower values calculated for wells that are furthest from the artificial recharge sites. Based on data in Muir and Coplen (1981) (Cook, 2020).

3.2 Quantifying Rates of Groundwater Recharge

In an unconfined aquifer, groundwater age generally increases with depth. If the recharge rate is high, then the age will increase slowly with depth, and if the recharge rate is low, age will increase rapidly with depth. Although it is not necessarily intuitive, Vogel (1967) showed that if recharge is constant across an aquifer, then the age profile will also be constant, and contours of groundwater age will be horizontal (Figure 14). The curvature of flow lines means that vertical water velocity decreases with depth (and is zero at the base of the aquifer). Thus, not only does groundwater age increase with depth, but it does so more rapidly towards the base of the aquifer. The groundwater age profile will therefore be concave upward (Figure 15).

For an aquifer of uniform geology, constant thickness (H), and receiving constant recharge (R), the groundwater age (t) as a function of depth below the water table (z) will be given by Equation 10.

$$t = \frac{H\theta}{R} ln\left(\frac{H}{H-z}\right) \tag{10}$$

where:

θ = porosity

The vertical component of the groundwater velocity will decrease from R/θ at the water table to zero at the base of the aquifer. If groundwater age is measured at any discrete depth, then the recharge rate can be determined by re-arrangement of Equation 10. However, if sampling takes place near the water table (z/H small) then the recharge rate may be approximated by Equation 11.

$$R = \frac{z\theta}{t} \tag{11}$$

where:

z = depth below the water table (L)

In fact, comparison of evaluations of Equation 10 and 11 reveals that the error resulting from using Equation 11 instead of Equation 10 will be less than 20% if samples for age measurement are collected from within the top third of the aquifer.

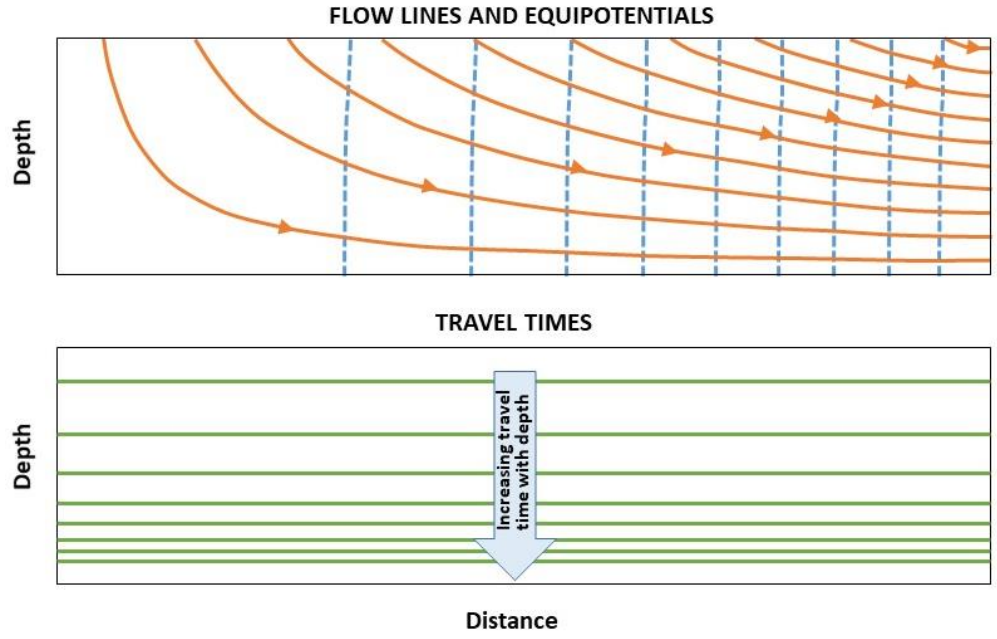

Figure 14 - Flow lines (orange), equipotential lines (blue) and distribution of travel times (green) in a homogeneous unconfined aquifer of constant thickness receiving uniform recharge. The age increases with depth, and the closer spacing of groundwater age contours with depth is because age increases more rapidly with depth towards the base of the aquifer. In this example, the aquifer hydraulic conductivity is very high, so that the curvature of the water table from left to right is not discernible on the scale of the figure. Values are not shown for equipotential lines or travel times because it is the shape of the lines, rather than their value that is important. The left and lower boundaries for the simulation are no flow, and the right boundary is constant head (After Cook and Solomon, 1997).

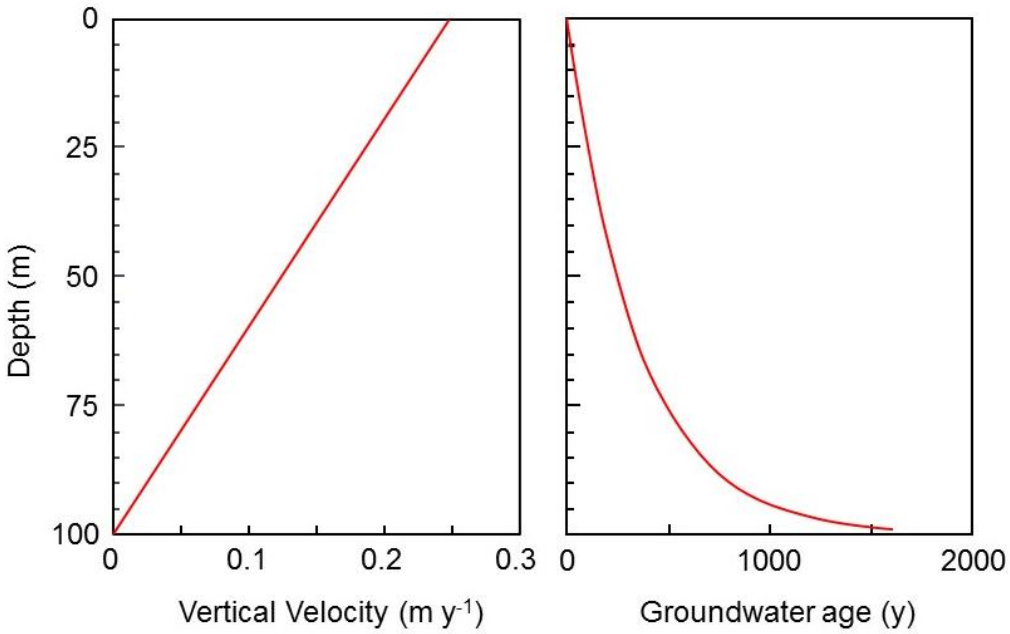

Figure 15 - Vertical water velocity and groundwater age as a function of depth in a homogeneous unconfined aquifer of constant thickness (100 m), porosity θ = 0.35 and recharge R = 0.1 m/y. The velocity at the water table is R/θ, and decreases linearly with depth to be zero at the base of the aquifer. The groundwater age curve is calculated using Equation 10 (Cook, 2020).

In principle, a single measurement of groundwater age at a discrete depth can be used to estimate recharge, but accuracy is significantly improved if vertical profiles can be obtained. For example, a detailed vertical profile of CFC-12 concentrations from a shallow silty sand aquifer near Sturgeon Falls, Ontario, Canada (Figure 16), enabled recharge to be estimated with high precision. At this site, the saturated unconfined aquifer is about 35 m thick and water table depth varies seasonally between approximately 0.2 m in spring and 2 m in late summer. Piezometers are located between approximately 1 and 20 m depth, with screen lengths of 15 cm. The wells were sampled in 1993 for analysis of dissolved concentrations of CFC-11, CFC-12 and CFC-113, although only results from CFC-12, the most conservative of the CFCs, are discussed here. The observed CFC-12 profile shows a gradual decrease in concentration with depth, reflecting a progressive increase in groundwater age with depth (Figure 17). The groundwater age at 12 m is estimated to be approximately 34 years, equivalent to a recharge year of 1959. Below 13 m calculated ages are artificially low, due to trace contamination (probably introduced during sampling) and low measured concentrations. The year 1960 is sometimes considered to be the limit of groundwater dating with CFCs, although reliable dates from the late 1950s can sometimes be obtained.

Figure 16 - Location of Sturgeon Falls, Ontario Canada, which was the site of one of the earlier studies using CFCs to estimate groundwater recharge (Figure 17).

The measured CFC-12 data were used to calibrate a two-dimensional numerical flow and solute transport model for this site, and hence estimate a vertical recharge rate of approximately 130 mm/y. This is reasonable as it is about 14% of the average annual precipitation of about 900mm/y for the locale. A similar recharge rate would have been derived by applying Equation 10 or 11 to measured CFC-12 ages. Simulations were also performed using recharge rates of 110 mm/y and 150 mm/y, and these significantly under-estimate and over-estimate measured values, respectively, indicating an uncertainty of estimated recharge of better than 15% (Cook et al., 1995).

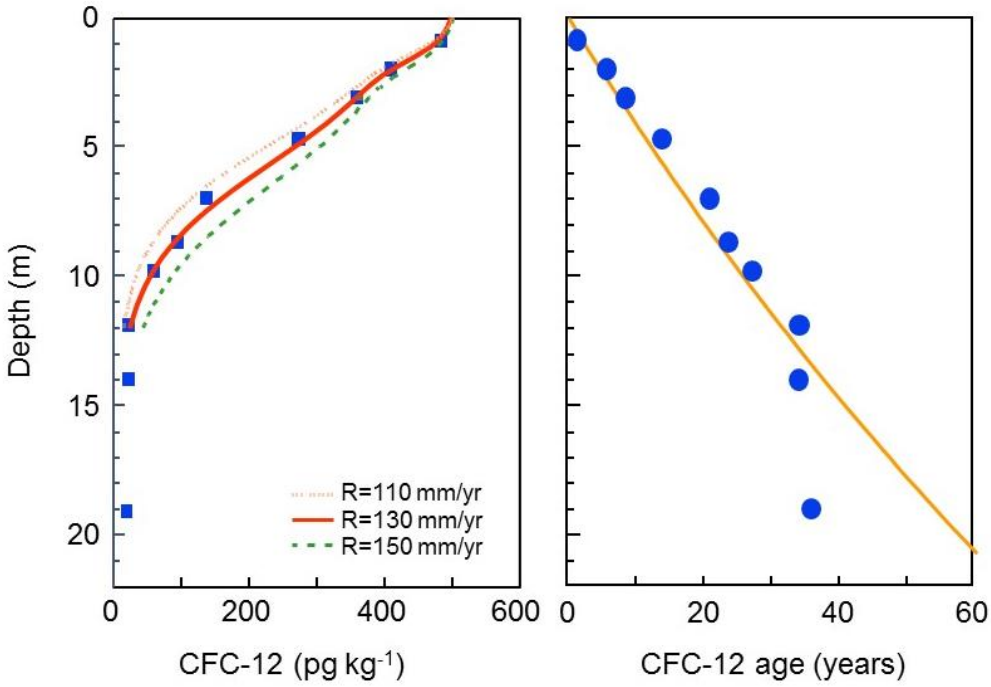

Figure 17 - Measured CFC-12 concentrations, and apparent CFC-12 ages measured in a vertical profile obtained from the Sturgeon Falls aquifer, Canada, in 1993. Estimated CFC-12 ages increase approximately linearly with depth, although below 13 m calculated ages are artificially low, due to trace contamination (probably introduced during sampling) and low measured concentrations. A two-dimensional numerical flow and transport model was calibrated to measured concentrations and used to determine a vertical recharge rate of approximately 130 mm/y (After Cook et al., 1995).

In another example, a vertical profile of ^{3}H and ^{3}He concentration was obtained from a multi-level well in the shallow, sand aquifer at Cape Cod, Massachusetts, USA (Figure 18), as part of an investigation into the transport of organic contaminants (Solomon et al., 1995). The water table ranged from about 20 to 30 m below ground surface, and peaks of ^{3}H and ^{3}He occurred at approximately 27 m below the water table (Figure 19). The increase in apparent $^{3}H/^{3}He$ age with depth can be reproduced using Equation 10. Assuming an aquifer thickness of 33 m and the measured ages, the vertical water velocity at the water table (R/θ) is about 3.3 m/y. Assuming a porosity of $\theta = 0.35$ and solving for recharge, gives R = 115 mm/y. This is a reasonable value given the average annual precipitation of about 1000 mm/y. At this site, sampling occurred in 1993, approximately 30 years after the peak of ^{3}H in rainfall. The $^{3}H/^{3}He$ age at the depth of the peak concentration of ^{3}H in the groundwater is about 16 years, thus the water must have taken about 14 years to travel through the unsaturated zone. Estimates of recharge were used to estimate the horizontal flow velocity, and hence estimate the rate of plume movement at the site, as described in Section 3.9.

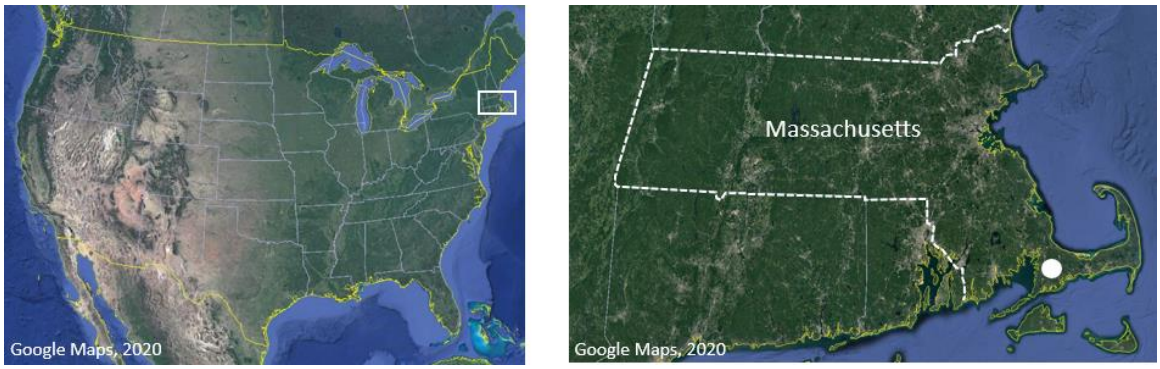

Figure 18 - Location of Cape Cod, Massachusetts, USA, where profiles of ^{3}H and ^{3}He were used to estimate recharge and to track the movement of contaminated groundwater (Figures 19 and 43).

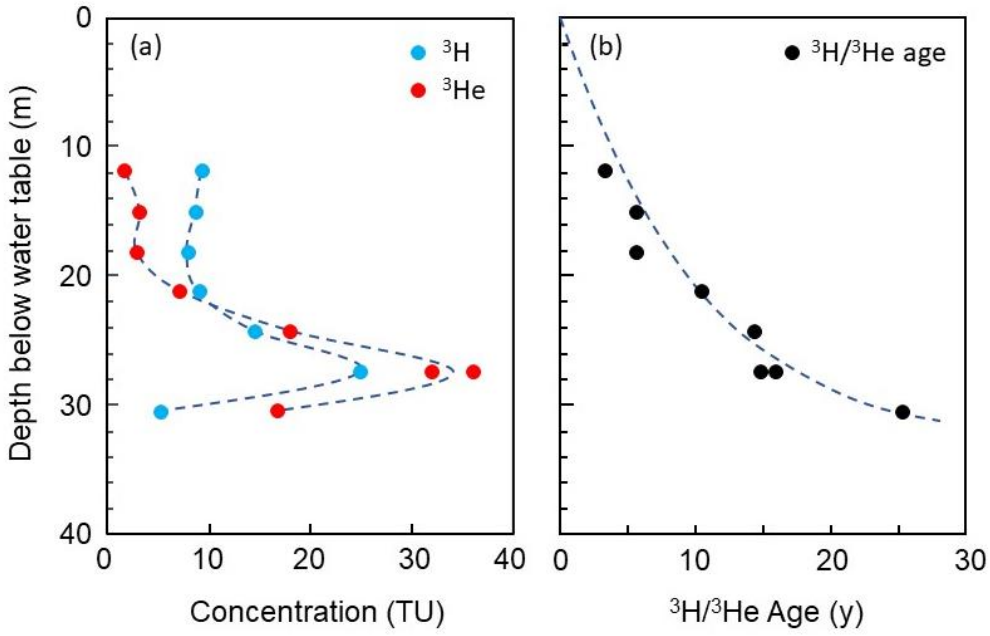

Figure 19 - Concentration profiles of ^{3}H, ^{3}He and $^{3}H/^{3}He$ age measured at Cape Cod, Massachusetts, USA, in 1992–93. Estimated ^{3}He contributions from other sources have been subtracted. The broken line in (b) represents the age profile predicted for an unconfined aquifer with constant aquifer thickness of H = 33 m, porosity 0.35 and recharge rate of 115 mm/y (After Solomon et al., 1995).

Such high-precision estimates of groundwater recharge are only possible where vertical profiles can be obtained using wells with short screened intervals. Typically, existing wells must be used to gather groundwater samples and such wells generally have long screened intervals. On the Eyre Peninsula, South Australia (Figure 20), groundwater is used for irrigation and to augment the drinking water supply. Approximately 20 wells, with screen lengths ranging from about 2 to 10 m, were sampled throughout the region (Figure 21). Since these wells are distributed across a large area and recharge is likely to be spatially variable, a plot of CFC-12 versus depth from all of the wells does not reveal a smooth profile. Nevertheless, in general throughout the area, shallow wells have higher concentrations than deeper wells. Each measured CFC-12 concentration represents the

average age of the groundwater over the entire screened-interval of the well. Recharge rates can be obtained by comparison to results from a one-dimensional numerical groundwater model of flow and transport. However, the recharge rate that is calculated will depend on whether the groundwater is assumed to be derived from near the top of the screen, from near the bottom, or derived evenly across the entire screened interval. The problem is most pronounced for wells that are screened close to the water table. If it is assumed that water is derived evenly across the screened intervals of the wells, then most wells have recharge rates between approximately 20 and 50 mm/y (Cook et al., 1996). This is a reasonable range for an area with precipitation of about 400 mm/y. One well, screened between approximately 11 and 13 m depth, had a measured CFC-12 concentration of 50 pg/kg. This reflects an atmospheric concentration of approximately 100 parts per trillion by volume (pptv) based on an assumed recharge temperature of 15°C, equivalent to a recharge year of 1968, and hence an age of 27 years because sampling took place in 1995. The recharge rate for this well is estimated to be approximately 100 - 140 mm/y. This high rate is surprising considering the arid environment and may represent fracture or macropore flow through the limestone. Comparison of Figures 17, 19 and 21 clearly shows the advantage of short well screens for accurate estimation of groundwater recharge from tracer data.

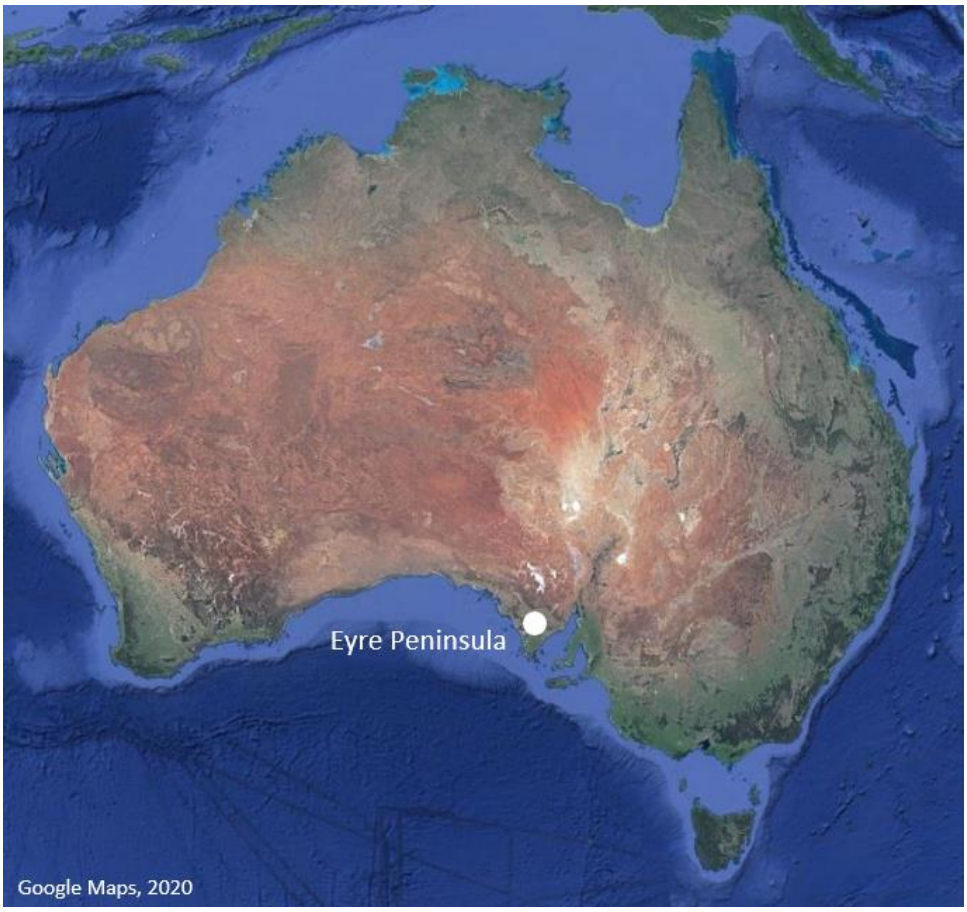

Figure 20 - Location of Eyre Peninsula, South Australia. Recharge rates to aquifers on Eyre Peninsula have been estimated using CFC data from observation wells (Figure 21).

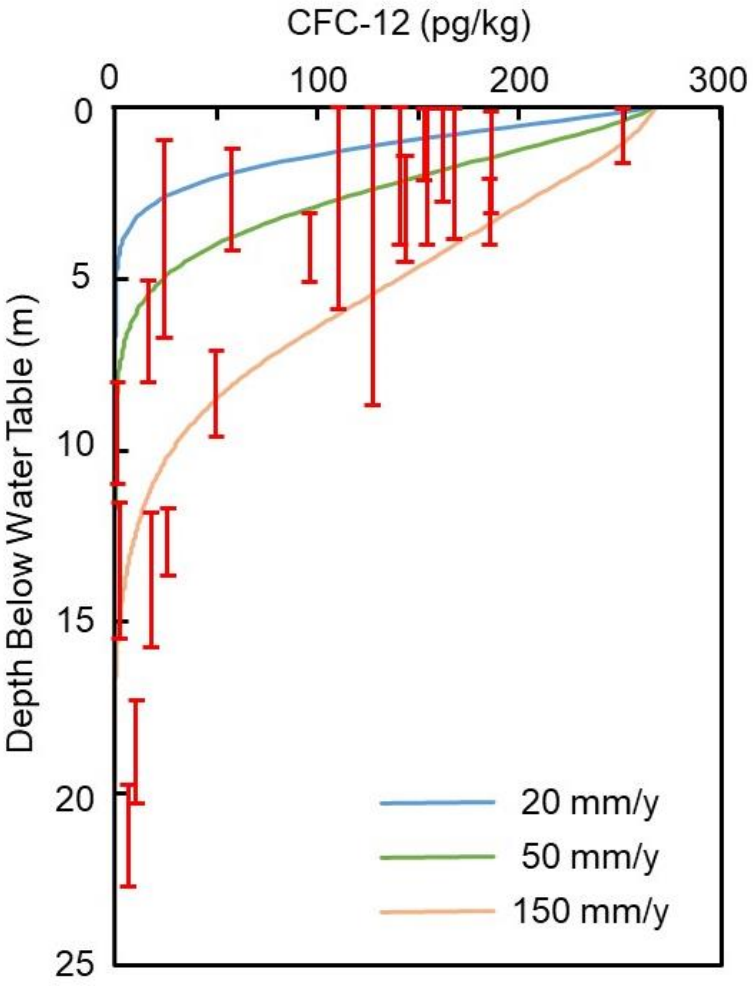

Figure 21 - Comparison between measured CFC-12 concentrations on Eyre Peninsula, southern Australia, and results of a one-dimensional groundwater model simulation with recharge rates between 20 and 150 mm/yr. Vertical red bars indicate the lengths of screened intervals of wells positioned at their measured concentration. The samples are not from a vertical profile, but rather from wells with long screen intervals distributed across a large area. Data are plotted versus depth below the water table at the sampling location. Compared with the data presented in Figure 17, the long-screened intervals of most wells overlap several model curves, and so recharge rates cannot be estimated with high precision. Nevertheless, the data suggests a mean recharge rate of between approximately 20 and 50 mm/y, with some areas of higher recharge (Cook, 2020).

3.3 Quantifying Groundwater Velocities in Confined Aquifers

While groundwater ages in unconfined aquifers can be used to estimate vertical flow velocities and recharge rates, groundwater ages in confined aquifers enable estimation of horizontal groundwater flow velocities. Figure 22 shows the distribution of travel times in a simple confined aquifer of constant thickness. In the confined part of the aquifer, flow lines are horizontal, and groundwater age increases downgradient. The horizontal groundwater velocity (dx/dt) is the inverse of the horizontal age gradient (dt/dx). In

practice, the horizontal groundwater velocity (v_h) is usually estimated as shown in Equation 12.

$$v_h = \frac{x_2 - x_1}{t_2 - t_1} \quad (12)$$

In Equation 12, t_1 and t_2 are groundwater ages at two points in the confined part of the aquifer and (x_2-x_1) is the distance between these points, measured in the direction of flow. It is apparent from Figure 22 that groundwater ages in the confined part of the aquifer also show an increase in age with depth. This vertical age gradient is created within the unconfined part of the aquifer and preserved as the water flows downgradient in the confined part of the aquifer. In many cases, though, the vertical age stratification within the confined part of the aquifer is much less than the horizontal increase in age. Thus, groundwater samples collected from confined aquifers often show an increase in age with distance downgradient, irrespective of the sampling depth.

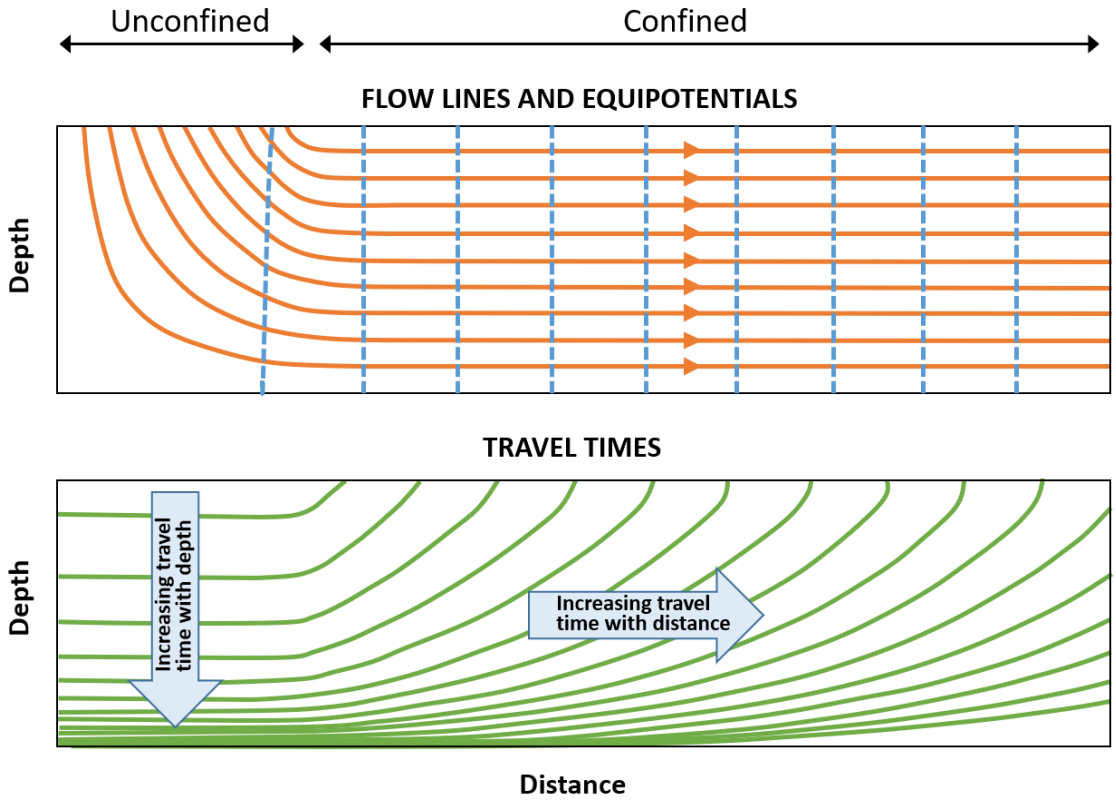

Figure 22 - Flow lines (orange), equipotential lines (blue) and distribution of travel times (green) in a homogeneous aquifer of constant thickness, which is confined in the downstream part. Age increases with depth in the unconfined part of the aquifer, as indicated in Figure 14. Where the aquifer is confined, flow lines are horizontal, and travel times increase in the horizontal direction, as well as with depth. Values are not shown for equipotential lines or travel times because it is the shape of the lines, rather than their value that is important. The left and lower boundaries for the simulation are no flow, and the right boundary is constant head (After Cook and Solomon, 1997).

One of earliest studies that used radioactive ^{14}C as a groundwater dating tool was an investigation into the rate of groundwater flow in the Carrizo-Wilcox aquifer (Figure 23)

in south-central Texas (Pearson and White, 1967). The Carrizo-Wilcox aquifer is a confined aquifer that outcrops roughly 200 – 300 km inland from the coast of the Gulf of Mexico, and dips to the southeast (towards the coast) at an angle of 1 to 2 degrees. In northern Atascosa County, the aquifer outcrops on rolling hills as a band that is only 15 to 20 km wide. The thickness of the aquifer is approximately 200 m in the outcrop area but increases towards the southeast.

Water samples were collected for ^{14}C and $\delta^{13}C$ analysis on dissolved carbonate. pH and alkalinity were also measured and used to calculate the total carbonate content and degree of saturation with respect to calcite. ^{14}C values ranged from 77 pmC (percent modern Carbon; Table 1) in the outcrop area to background values (< 0.7 pmC) in the most downgradient samples. Total carbonate content was lowest (2.6 to 2.8 equivalents per million; epm) and $\delta^{13}C$ was most negative (-18.9 to -17.9 ‰) close to the outcrop area, with most downgradient samples having carbonate contents above 5 epm and $\delta^{13}C$ values between -8 and -12 ‰.

Comparison of total carbonate and $\delta^{13}C$ values indicated that most samples could be explained by dilution of ^{14}C by dissolution of geologic layers of marine carbonate formations. However, some samples had high total carbonate concentrations, but did not have correspondingly enriched $\delta^{13}C$ values, indicating that some other process (perhaps dissolution of plant or petroleum-derived carbonate within aquifer materials) was affecting the carbonate chemistry. Therefore, the ^{14}C values were corrected based on the ratio of the measured carbonate concentration to an assumed initial value. After correcting for dilution with geologic carbonate, ^{14}C ages of groundwater increase from less than a few hundred years in the outcrop area to more than 20,000 years at distances greater than 40 km from the outcrop area (Figure 24). The mean groundwater velocity is therefore calculated to be approximately 2 m/y and is in good agreement with hydraulic calculations based on measured hydraulic heads, porosities and hydraulic conductivities.

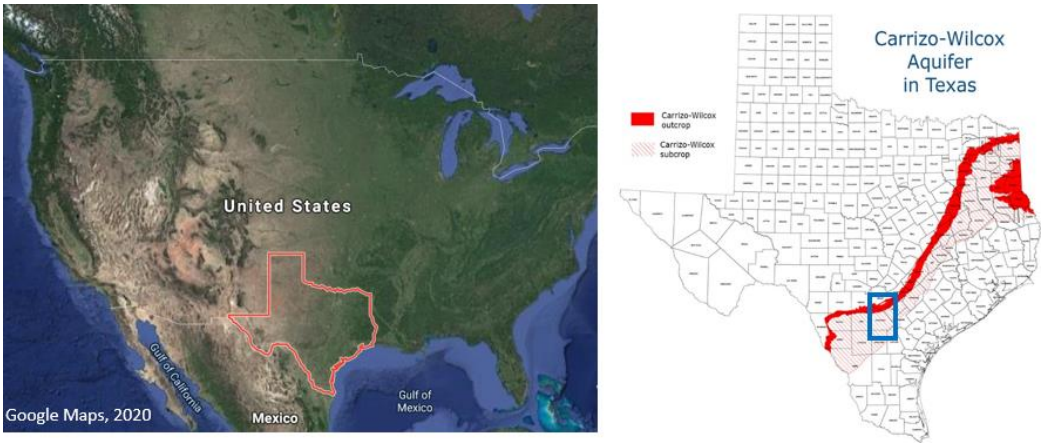

Figure 23 - Location of the Carrizo-Wilcox aquifer in south-central Texas, USA which was the focus of one of the earliest studies to use ^{14}C to estimate groundwater flow rates (Figure 24). The area shown in Figure 24 is indicated by the blue rectangle on the aquifer map (Eckhardt, 2020).

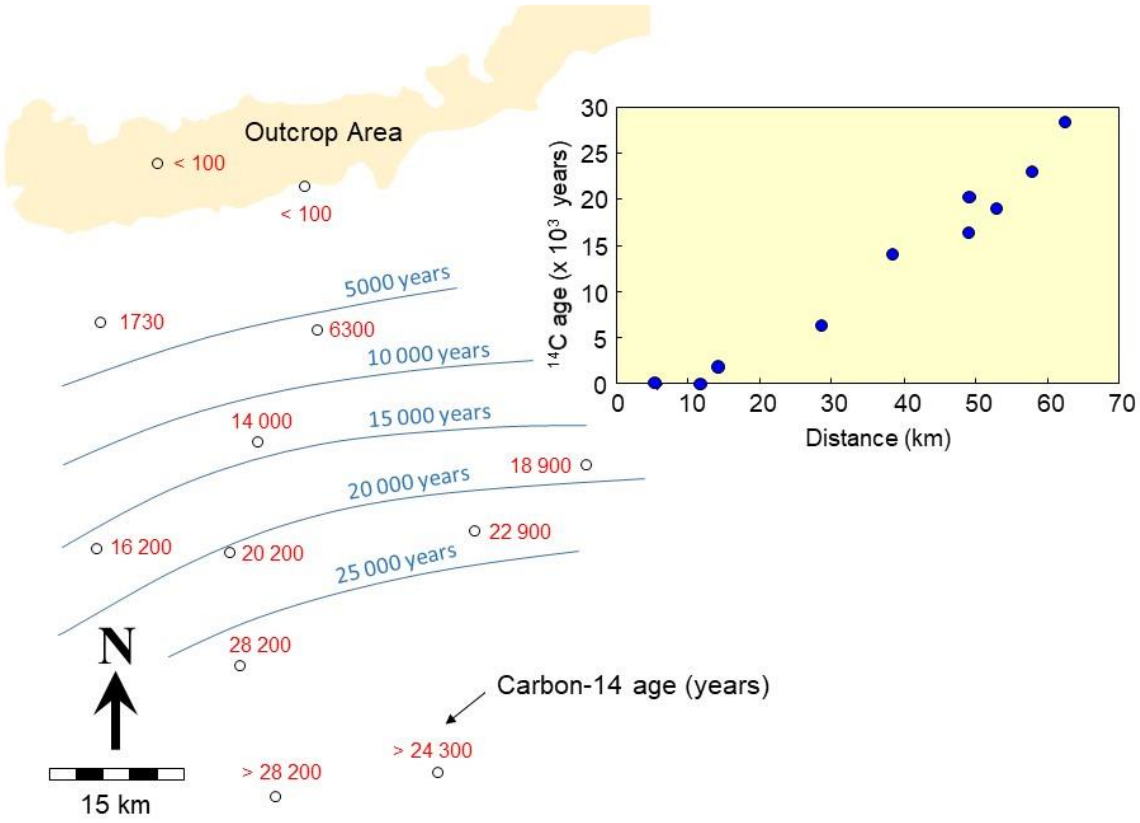

Figure 24 - Carbon-14 ages of groundwater within the Carrizo-Wilcox aquifer, Texas. Blue lines represent approximate lines of equal groundwater age, estimated from contouring the measured age data. The inset shows the increase in age with distance from the outcrop area. Figure 23 for location of the Carrizo-Wilcox aquifer (After Pearson and White, 1967).

The value of combining different groundwater age tracers to cover the range of ages in large flow systems is illustrated in a study of the confined aquifers of the Atlantic Coastal Plain, Maryland, USA (Plummer et al., 2012). The Atlantic Coastal Plain (Figure 25) consists of a series of wedge-shaped unconsolidated sedimentary deposits that thicken in the direction of groundwater flow. Pumping has greatly changed the flow systems in these aquifers, and so wells were selected along two transects in the Upper Patapsco aquifer that were believed to follow pre-development flow lines. Samples were analyzed for ^{14}C, ^{36}Cl and He, as well as several other environmental tracers.

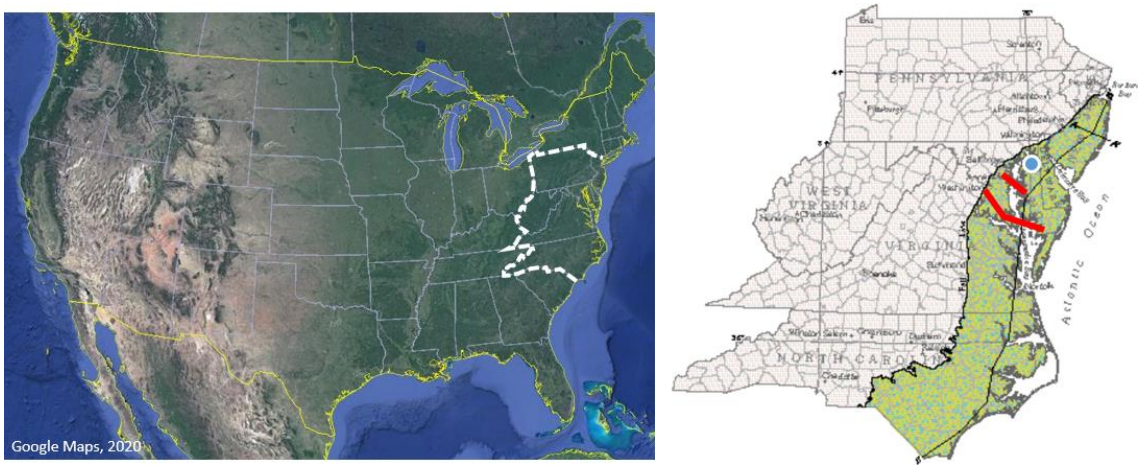

Figure 25 - Location of the Northern Atlantic Coastal Plain Aquifer System, USA (shown in green on right image created by Trapp and Horn, 1997), which has been the focus of several groundwater studies. The red lines are the locations of north and south well transects used for groundwater-dating in the confined Upper Patapsco aquifer, and the blue circle is the location of the Locust Grove agricultural catchment. Data from the Locust Grove catchment is discussed in Sections 3.9 and 3.10.

^{14}C concentrations were measurable only within the first 40 km of the flow system and decreased from 109 pmC near the outcrop area to below detection limit further downgradient (Figure 26). The piezometers with highest concentrations of ^{14}C also contained measurable ^{3}H and CFCs, confirming that the water was very young. The $^{36}Cl/Cl$ ratio also decreased downgradient, but measurable concentrations were observed for at least 80 km, due to the longer half-life of this tracer. ^{36}Cl ages in this part of the aquifer increased from 23,000 years to 328,000 years on the northern flow path and from 185,000 to 503,000 years on the southern flow path. The most downgradient sample (at 120 km) was close to background and appears to have an age of more than 2 million years. Helium concentrations increased from close to atmospheric values (negligible subsurface production) to more than 8×10^{-6} cm^3 STP/g furthest downgradient. The rate of increase in helium concentration with distance is consistent with the ages obtained from ^{14}C and ^{36}Cl data, within the range of uncertainties of the He production rate.

Ages within the aquifer increase in a non-linear fashion, with flow rate significantly decreasing downgradient. This is consistent with an increase in aquifer thickness with distance in the wedge-shaped aquifer, and with a decreasing volume of flow as water leaks out through confining layers into overlying and underlying aquifers. The average groundwater velocity is estimated to be approximately 1 m/y in the upgradient parts of the aquifer (at about 10 km) and decreases to 0.13 m/y and 0.04 m/y at 40 km and 80 km downgradient, respectively.

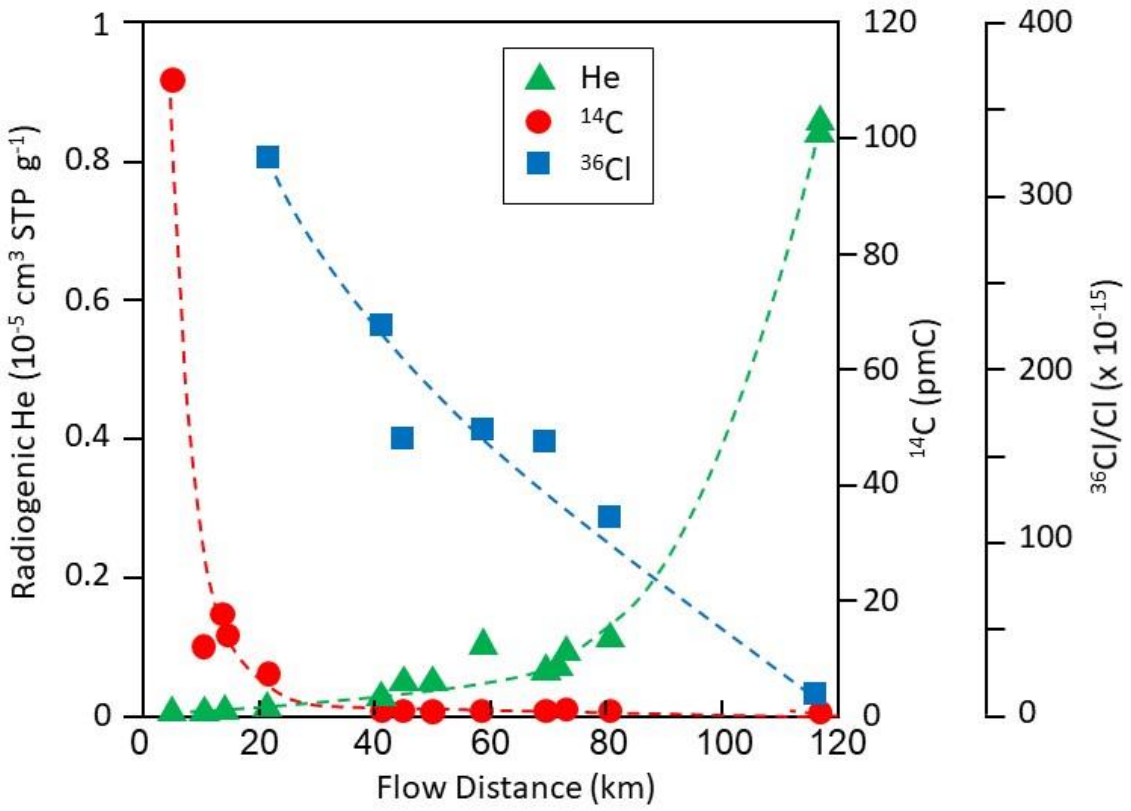

Figure 26 - Comparison of the ^{14}C activity of total dissolved inorganic carbon (TDIC), values of the $^{36}Cl/Cl$ ratio, and radiogenic ^{4}He concentrations in groundwater along flow paths in the Upper Patapsco aquifer, Atlantic Coastal Plain, Maryland, USA. Data is from two flow lines, whose locations are shown in Figure 25, although this Figure combines data from the two flow lines (After Plummer et al., 2012).

3.4 Identifying Recharge Processes

Stable isotopes and noble gases can be used to infer recharge processes and/or locations. They are particularly useful for estimating the degree of evaporation prior to recharge, as well as recharge temperature, pressure and/or elevation. For example, in mountainous terrain, estimation of recharge temperature using either stable isotopes or noble gases can provide information on the elevation of recharge. In central Oregon, USA (Figure 27), measurement of ^{2}H and ^{18}O on melted snow samples collected from different elevations allowed a relationship between isotopic composition and elevation to be established for the region (Figure 28; James et al., 2000). The data indicated a depletion in $\delta^{18}O$ of approximately 0.18 ‰ per 100 m increase in elevation; values between approximately 0.15 and 0.50 ‰ per 100 m have been reported from other studies (Araguas-Araguas et al., 2000). Isotope ratios were then measured on nine springs in the same area of central Oregon and compared with the relationship determined on the melted snow samples. Several springs had ^{18}O compositions indicating recharge at elevations only a few hundred meters higher than the spring location. In most cases, this corresponded with distances of approximately 10 km from the spring outlets, indicating relatively local flow systems. Springs at lower elevations had inferred recharge locations that suggested more remote

recharge. Lower Opal Spring, for example, occurs at an elevation of approximately 600 m, but has an ^{18}O composition indicative of recharge at an elevation of almost 2500 m, which would suggest that it is part of a large regional flow system. The authors also compared the calculated recharge elevation for each spring with the measured water temperature, to provide a qualitative indication of the depth of circulation of the groundwater along its flow path. The measured water temperature at Lower Opal Spring was 12 °C, whereas the mean annual surface temperature at the inferred recharge elevation of 2500 m, is less than 2 °C. Therefore, the authors concluded that this water must travel along a deep flow path, where it is heated geothermally. In contrast, many of the springs that drain local flow systems have water temperatures of between 3 and 4 °C, which is consistent with their inferred recharge elevation of 1500 – 1800 m.

Figure 27 - Location of spring sites in mountainous parts of central Oregon (white square) that were sampled by James et al. (2000) in a study of recharge processes (Figure 28).

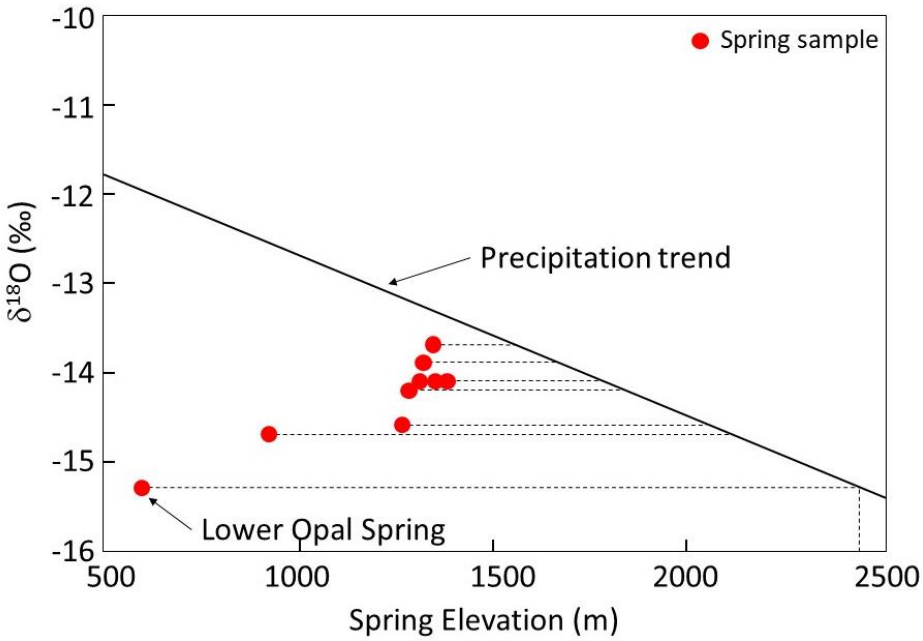

Figure 28 - Determination of groundwater recharge elevations for groundwater discharging from springs. The solid line defines the relationship between $\delta^{18}O$ composition of precipitation and elevation and was determined experimentally from analysis of snow samples. The red circles show spring elevations and $\delta^{18}O$ compositions of spring discharge. Spring samples with $\delta^{18}O$ values below the precipitation trend line therefore indicate recharge from higher elevations. The recharge elevations are determined by drawing a horizontal line from the spring sample to the precipitation line, and then a vertical line to where it intersects the x-axis (After James et al., 2000).

The relationship between rainfall amount and stable isotopic composition can be used to determine the size of a rainfall event leading to recharge. In the arid Ti Tree Basin (Figure 29), central Australia, stable isotope samples of groundwater plot below the local meteoric water line, suggesting evaporation prior to recharge (Figure 30). Fitting a regression line to the data and extrapolating to its intersection with the local meteoric water line, gives a mean composition of ^{2}H = -62 ‰ and ^{18}O = -9.3 ‰ for the precipitation water that recharges the groundwater system. This corresponds to the isotopic composition of rainfall events collected during months that receive more than about 90 mm of precipitation. On average, such periods occur about once every 1 - 2 years, indicating that groundwater recharge occurs regularly in this arid environment. However, the analysis is limited by the lack of isotope data on rainfall during such wet periods.

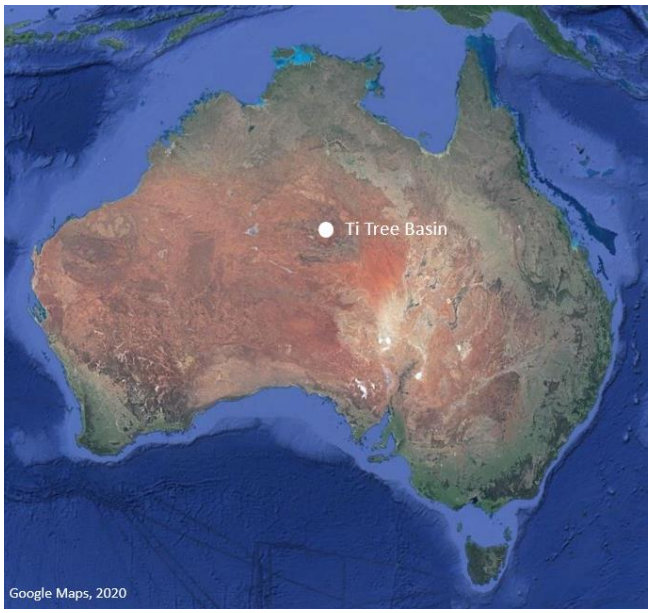

Figure 29 - Location of the Ti Tree Basin in central Australia, where the isotopic composition of groundwater has been used to infer the episodic nature of groundwater recharge (Figure 30).

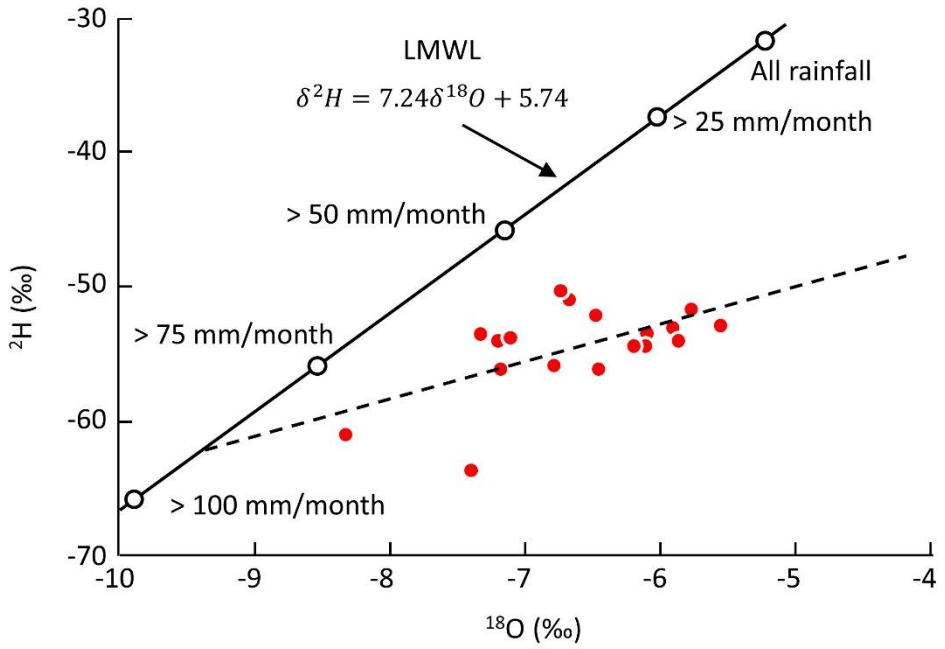

Figure 30 - Stable isotopic composition of groundwater in the Ti Tree Basin, central Australia, compared with the local meteoric water line (LMWL) for Alice Springs rainfall. Rainfall data are only available as mean monthly values, and black circles denote the mean, amount-weighted isotopic composition of rainfall for months with differing magnitudes of large precipitation totals. Groundwater data appear to fall on an evaporation line (with a slope of approximately 3) that intersects the local meteoric water line at an ^{18}O value of approximately -9.3 ‰. This composition reflects the isotopic composition of rainfall events for months that receive more than 90 mm of rain. On average, such events occur about once every 1 - 2 years, indicating that groundwater recharge occurs regularly in this arid environment (After Calf et al., 1991).

3.5 Estimating the Recharge Rate of River Infiltration

Where groundwater recharge is dominated by infiltration from a river, groundwater beneath the river will be young, and groundwater further from the river will be older. The rate of river infiltration can be estimated by calculating the velocity of water flow away from the river, based on this increase in age.

The Danube River in Hungary (Figure 31) is a major recharge source for adjacent coarse-grained alluvial aquifers, and groundwater dating of these aquifers permits estimation of the rate of river infiltration. In this study, groundwater age was estimated using $^{3}H/^{3}He$ dating. ^{4}He and Ne data were used to estimate the recharge temperature and excess air, which was required to distinguish *tritiogenic* ^{3}He (^{3}He derived from ^{3}H decay) from ^{3}He originating from other sources (i.e., atmospheric solubility and excess air components). Since the river dominates recharge to these aquifers, groundwater flow away from the river is essentially horizontal, and plots of groundwater age versus distance appear as straight lines (Figure 32), even though samples are collected from wells with long screens. Based on the rate of increase in age with distance, the groundwater velocity in shallow wells (screened 5 to 15 m below surface) is estimated to be approximately 800 m/y, and in deeper wells (screened 50 to 100 m below surface) it is estimated to be approximately 530 m/y.

Figure 31 - Path of the Danube River in Eastern Europe (Wikimedia Commons, 2019).

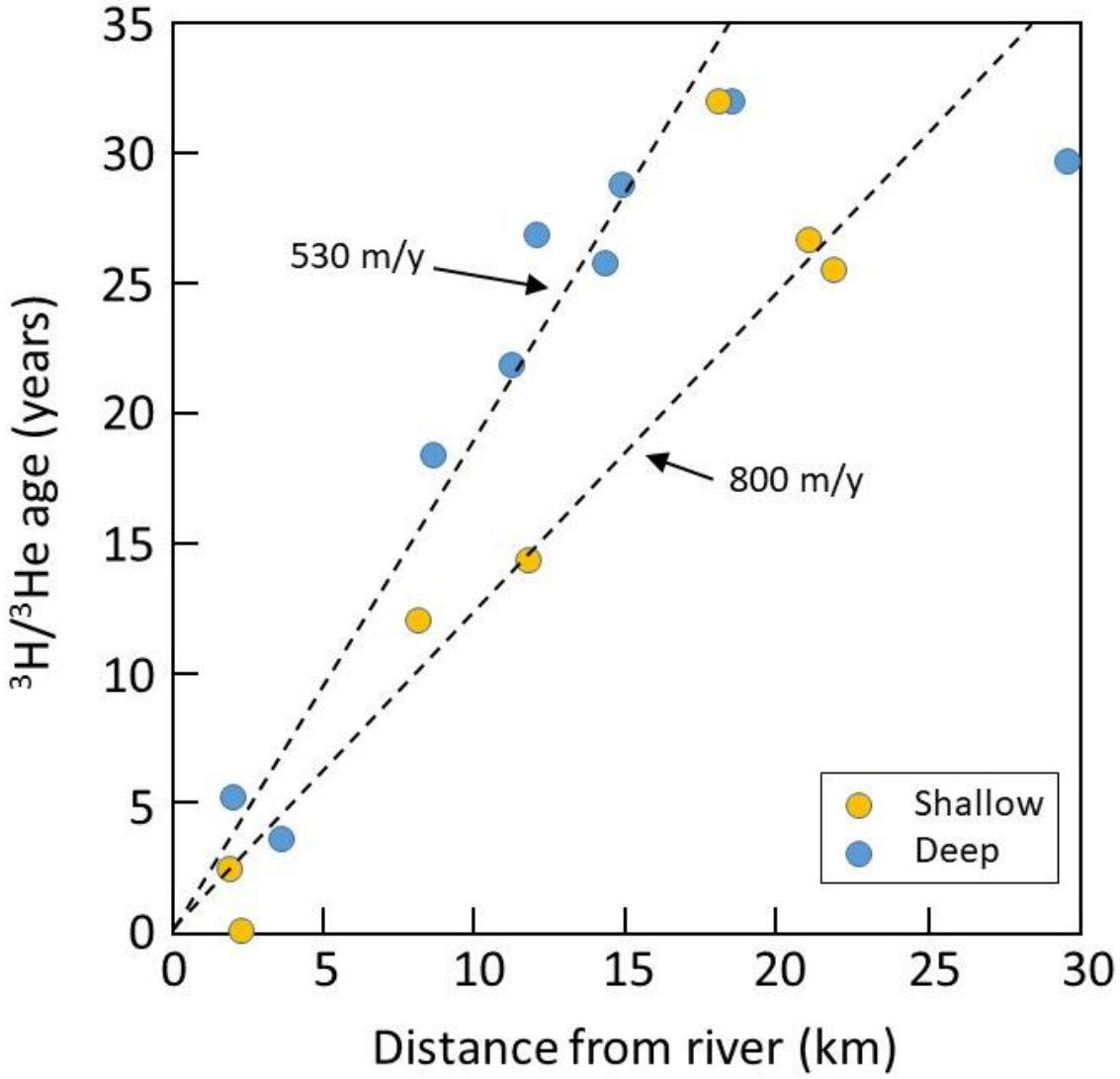

Figure 32 - Estimated $^3H/^3He$ age versus distance from the Danube River in Hungary, measured along the inferred groundwater flow path away from the river. Groundwater velocity appears to be greater in shallow wells (800 m/y) than in deeper wells (530 m/y) (From Cook and Solomon (2000), after Stute et al. (1997)).

One of the best examples of the application of this technique to ephemeral rivers (those that flow for only a short period during the year) is the study of the Finke River, central Australia (Fulton, 2012). Carbon-14 activities in groundwater show a general decrease with distance from the river, reflecting an increase in groundwater age (Figure 33). At distances beyond 40 km, ^{14}C activities are less than 22 pmC, equivalent to groundwater ages of more than 12,000 years. At 20 km from the river, the mean ^{14}C activity is approximately 60 pmC, equivalent to a groundwater age of approximately 4000 years. Assuming an age of zero at the river (distance of zero), this gives a mean velocity of 20 km in 4000 years, or 5 m/y. Assuming an aquifer thickness of 200 m and porosity of 0.22, the author thus calculated mean recharge rates of 5×10^6 to 12×10^6 m^3/y for a 35 km reach of the river. This is equivalent to a recharge rate 0.71 m/y, assuming a nominal river width of 200 m.

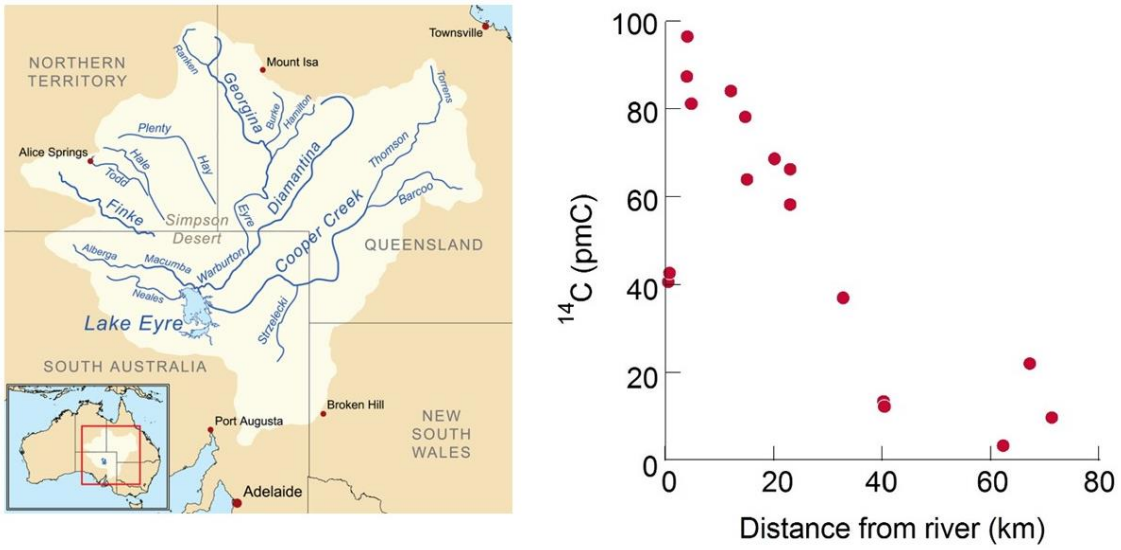

Figure 33 - Carbon-14 activities in groundwater versus distance from the Finke River, central Australia. The location of the Finke River is shown in the left image (Wikimedia Commons, 2010. "Lake Eyre drainage basin including the major rivers↗" by Kmusser↗ is licensed under CC BY-SA 3.0↗). The decrease in ^{14}C activity reflects an increase in residence time and was used to estimate the velocity of groundwater flow away from the river at 5 m/y (After Fulton, 2012).

3.6 Identifying Groundwater Discharge to Rivers

The chemical composition of groundwater will usually be distinct from surface water, and so groundwater flow into rivers and lakes can often be detected from water chemical surveys. A number of different environmental tracers have been used for estimating rates of groundwater discharge to lakes and rivers, including stable isotopes ^{2}H and ^{18}O (Meredith et al., 2009), helium (Gardner et al., 2011), chlorofluorocarbons (Cook et al., 2003) and radon (e.g. Ellins et al., 1990). Radon is particularly useful for this purpose, as its concentration in groundwater is typically much higher than in surface water. After groundwater containing radon discharges to surface water bodies, radon activities will decrease due to radioactive decay and gas loss to the atmosphere. If the groundwater concentration is constant, then measured radon concentrations essentially measure the time that has elapsed since groundwater discharge occurred, and high surface water concentrations only occur in the immediate vicinity of points of groundwater inflow.

Several studies have examined spatial patterns and volumes of groundwater inflow to lakes and rivers based on radon surveys. The Rio Grande de Manati, Puerto Rico (Figure 34), has an annual average discharge of 10.3 m^3/s. Radon samples were collected from the river in May 1985, when discharge rates were lower than average at 1 to 4 m^3/s (Figure 35; Ellins et al., 1990). Concentrations were mostly between 0.15 and 0.50 Bq/L, but ranged up to 1.5 Bq/L, compared to an average value of radon in the groundwater of 6.7 Bq/L. Assuming the groundwater concentration is constant, the location of highest concentration in surface water reflects the location with the greatest rate of groundwater inflow. For the Rio Grande de Manati, this occurs at river-km 17.5.

Figure 34 - Location of the Rio Grande de Manati, Puerto Rico, the site of one of the early studies that used radon to estimate groundwater discharge to rivers as shown in Figure 35.

Quantification of the groundwater flux into surface water usually requires an estimate of the rate of gas loss to the atmosphere. This can sometimes be obtained from the rate of decrease of radon concentration in reaches receiving no groundwater inflow but can also be independently estimated from artificial tracer experiments with other gases.

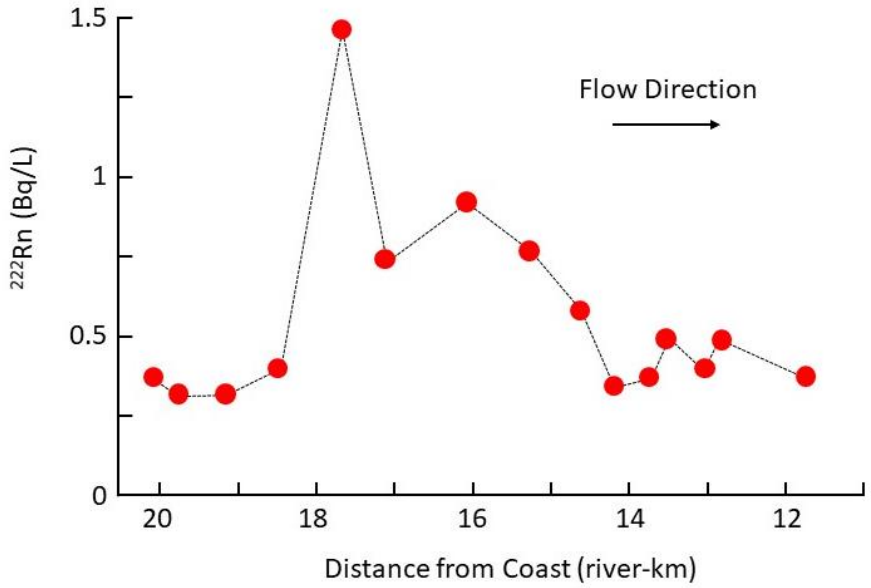

Figure 35 - Radon concentrations in the Rio Grande de Manati, Puerto Rico. The site location is shown in Figure 34 (After Ellins et al., 1990).

3.7 Identifying Groundwater Flow through Fractures

Environmental tracers also provide excellent tracers of groundwater flow in aquifers dominated by fractures - an area where traditional hydraulic approaches for estimating rates and patterns of groundwater flow have limitations. Groundwater age tracers are particularly useful for identifying the depths of active groundwater circulation. A good example of this application comes from a field site in southern Ontario (Figure 36), where clay-rich glacial till deposits extend from within a meter of the ground surface to

depths of several tens of meters. Fractures have been observed to depths of more than 9 m in these sediments, but whether these fractures contribute to significant groundwater flow is difficult to determine. An investigation into flow through these fractured tills involved installing piezometers to 16-m depth at 14 sites, and sampling groundwater from the piezometers for analysis of ^{3}H. Results from four of these sites are presented in Figure 37. All sites show high concentrations of ^{3}H in the upper few meters and concentrations decreasing rapidly with depth. Above-background concentrations of tritium are observed to a depth of 7.5 to 12 m. The authors calculated that ^{3}H could move 1 to 2 m by diffusion, and so concluded that active groundwater flow occurred to a depth of 5 to 10 m. Similar depths were suggested by mapping of fractures, and the maximum depths at which seasonal variations in hydraulic head were observed (Ruland et al., 1991).

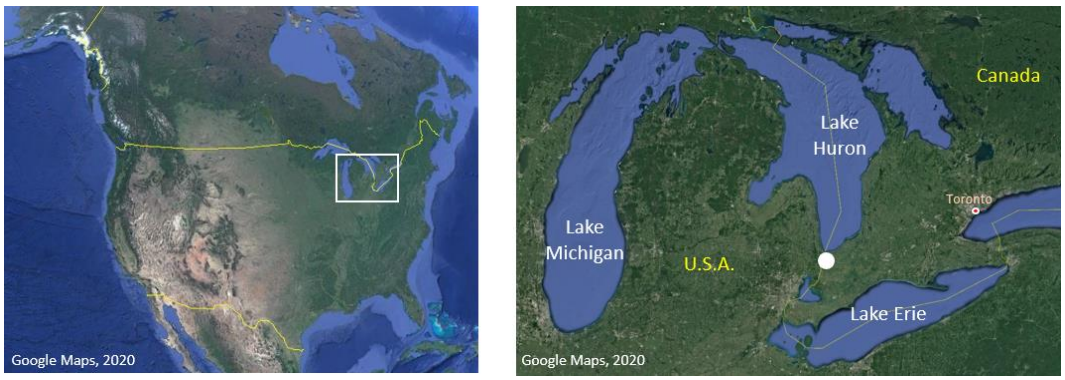

Figure 36 - Location of field site in southern Ontario, Canada, where ^{3}H profiles were measured to determine depth of groundwater flow (white circle). Figure 37 for ^{3}H depth profiles.

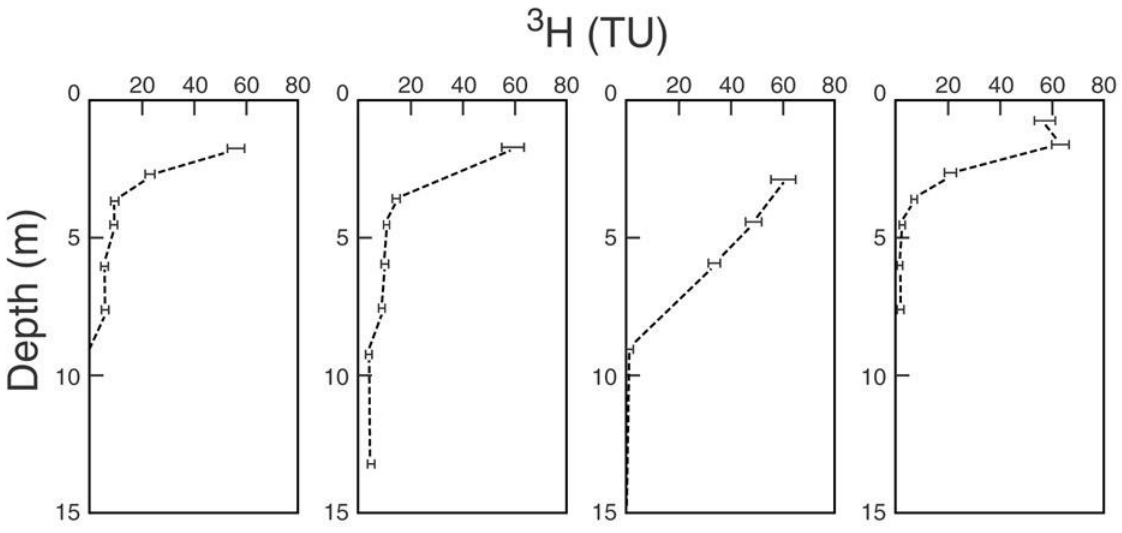

Figure 37 - Profiles of ^{3}H obtained from four sites in southern Ontario. High ^{3}H concentrations indicate active groundwater flow, which extends to depths of approximately 5 to 10 m (After Ruland et al., 1991).

^{36}Cl has more sensitivity than ^{3}H as a tracer of modern recharge, in part because its signal has not been significantly attenuated by radioactive decay since the period of nuclear

fallout, and this makes it an extremely useful tracer for detecting recent rainfall in groundwater. Investigations into the potential for fracture flow at the proposed United States high-level nuclear waste repository at Yucca Mountain, Nevada (Figure 38), relied heavily on results from ^{36}Cl testing (Fabryka-Martin et al., 1997; Wolfsberg et al., 1999). An 8km long, nearly horizontal tunnel was drilled in a loop beneath Yucca Mountain, at the same depth and in the same formation as the proposed repository. The tunnel formed the basis of several tests on fluid flow at the site, including collection of rock samples from the tunnel walls, and leaching of salts dissolved in pore water from the rocks for ^{36}Cl analysis. Samples were collected at regular intervals of approximately 200 m, and collected from selected features where preferential flow was considered to be more likely, such as faults and fractures.

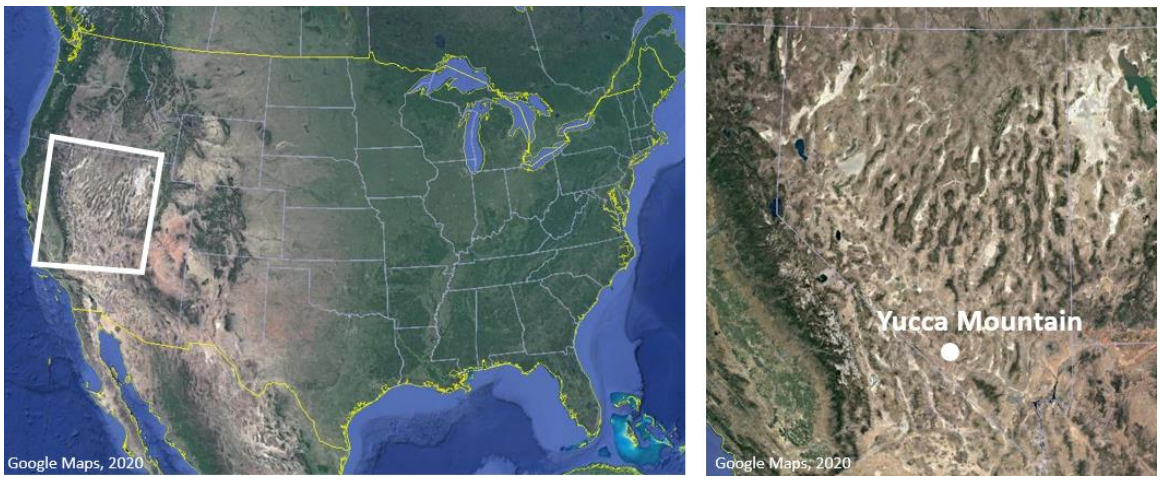

Figure 38 - Location of Yucca Mountain, Nevada, USA. As a proposed storage facility for high-level radioactive waste, Yucca Mountain has been the site of several isotope studies to define rates of infiltration leading to aquifer recharge (Figure 39), and rates of groundwater flow.

The natural $^{36}Cl/Cl$ ratio of modern precipitation at the site is approximately 500 x 10^{-15}, but this value has varied historically, and was as high as 1,200 x 10^{-15} approximately 12,000 years ago. However, during the 1950s and 1960s, high concentrations of ^{36}Cl were added to rainfall from atomic testing of nuclear devices (Figure 6). The peak $^{36}Cl/Cl$ value may have been as high as 200,000 x 10^{-15}, although this signal is diluted by mixing with pre-fallout chloride in the soil. Thus, samples with $^{36}Cl/Cl$ ratios between approximately 500 and 1200 x 10^{-15} probably reflect pre-fallout precipitation, indicative of slow percolation of water through the rock mass, with travel times of several thousand years. Values in excess of 1200 x 10^{-15} are interpreted as reflecting the input of ^{36}Cl from nuclear weapons testing. Whereas samples collected at regular intervals along the tunnel did not yield values greatly in excess of pre-1950s values, many samples collected close to potential conduits (fractures, faults, breccia and unit contacts) yielded high $^{36}Cl/Cl$ values (Figure 39). This suggests higher water velocities (of at least several meters per year) through such features (Fabryka-Martin et al., 1997; Campbell et al., 2003). Subsequent validation studies yielded

mixed results, with some ^{3}H and $^{36}Cl/Cl$ ratios indicative of post-1950s water, but $^{36}Cl/Cl$ values significantly lower than those reported by Fabryka-Martin et al. in 1997. The validation studies also failed to replicate the earlier elevated values measured in the vicinity of the Sundance Fault (Figure 39). However, this does not necessarily invalidate the earlier results. Water flowing rapidly through fractures within the unsaturated zone is unlikely to be detected large distances from individual fractures. Thus, repeat sampling is unlikely to yield identical results, particularly if it occurs after the initial tunneling when the unsaturated zone moisture may have redistributed itself in response to the new conditions created by the presence of the tunnel (Marshall et al., 2012).

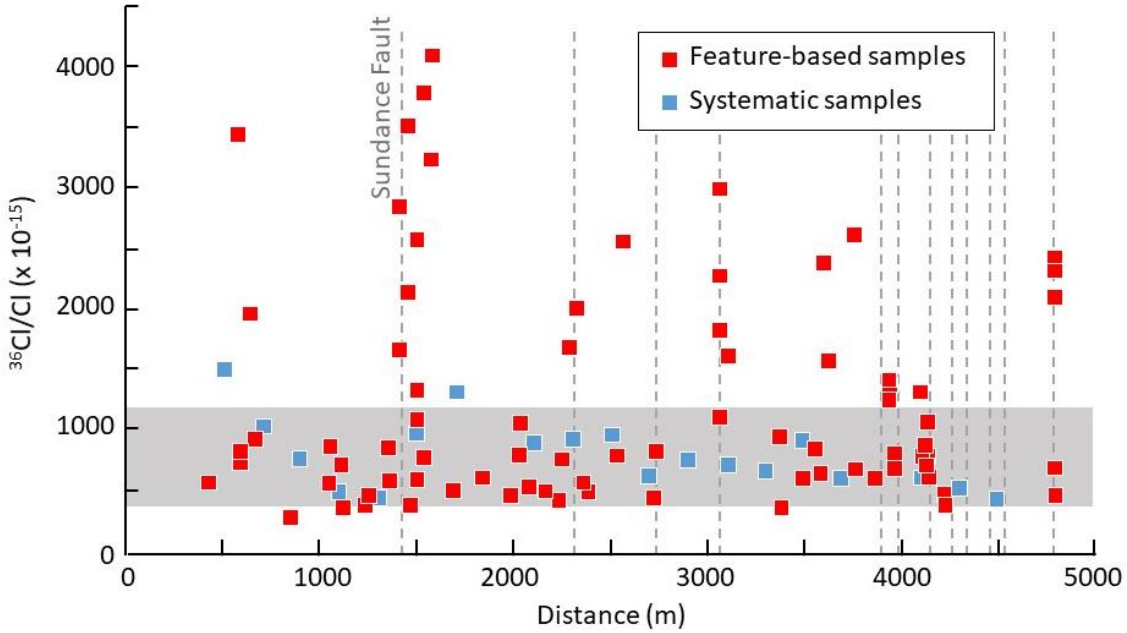

Figure 39 - Chlorine-36 ratios of salts leached from rock samples from a section of the Exploratory Studies Facility at Yucca Mountain, Nevada. The shaded area shows the approximate range of $^{36}Cl/Cl$ values in rainfall prior to the 1950s, and the vertical lines denote the locations of faults that have been mapped at the surface. Feature-based samples were taken from fractures, faults, breccia and unit contacts. From Fabryka-Martin et al. (1997), as reproduced in Philips (2000), and Wolfsberg et al. (1999).

3.8 Reconstructing Climatic Conditions

Environmental tracers can also be used for climatic reconstruction. Noble gases are particularly useful, as their atmospheric concentrations are constant, and so measured concentrations provide direct information on solubility. This is largely determined by the temperature at the water table at the time of recharge. ^{2}H and ^{18}O can also provide information on recharge, as isotopic ratios in rainfall are influenced by temperature, although for quantitative use, the relationship between isotope ratio and temperature needs to be independently determined at each field site. A small number of studies have also estimated past groundwater recharge rates from past changes in the chloride concentration of infiltrating water (e.g., Murphy et al., 1996).

The Great Hungarian Plain (Figure 40) consists of an upper Quaternary aquifer and a deeper Pliocene aquifer. Noble gas temperatures for these aquifer systems have been measured with Ne, Ar, Kr and Xe concentrations. Groundwater ages have been estimated using ^{14}C, which provides the timescale for the climatic reconstruction. Samples with ^{14}C ages less than 10,000 years have an average noble gas recharge temperature of 10.6 °C, which is close to the mean annual temperature in the recharge area under the current climate (11.4 °C). Noble gas temperatures at the glacial maxima (approximately 18,000 years ago) suggest an average mean annual temperature approximately 8.6° lower than present (Figure 41). Temperatures preceding the glacial period (28,000 – 35,000 years ago) were approximately 5° lower than present. The ^{18}O record shows a similar pattern, revealing depleted values in samples with ^{14}C ages exceeding 10,000 years (Stute and Schlosser, 2000).

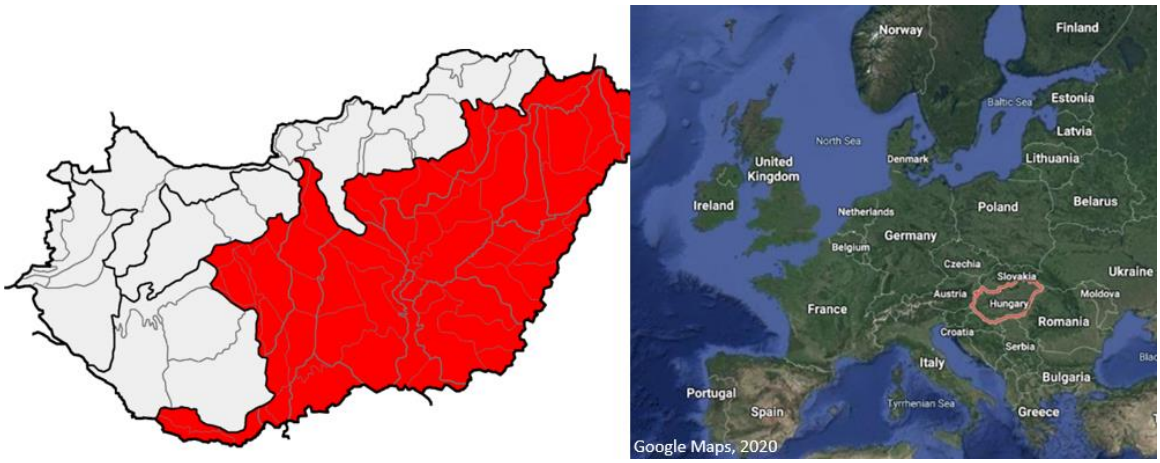

Figure 40 - The Great Hungarian Plain (red area in map of Hungary (Wikimedia Commons, 2010. "Location of geographical macroregion of hu:Alföld (red) within subdivisions of Hungary based on Magyarország kistájainak katasztere↗" by Miaow Miaow↗ is public domain), which has been the focus of palaeoclimate studies using groundwater isotopes and noble gases (Figure 41). The location of Hungary within Europe is shown in the image to the right.

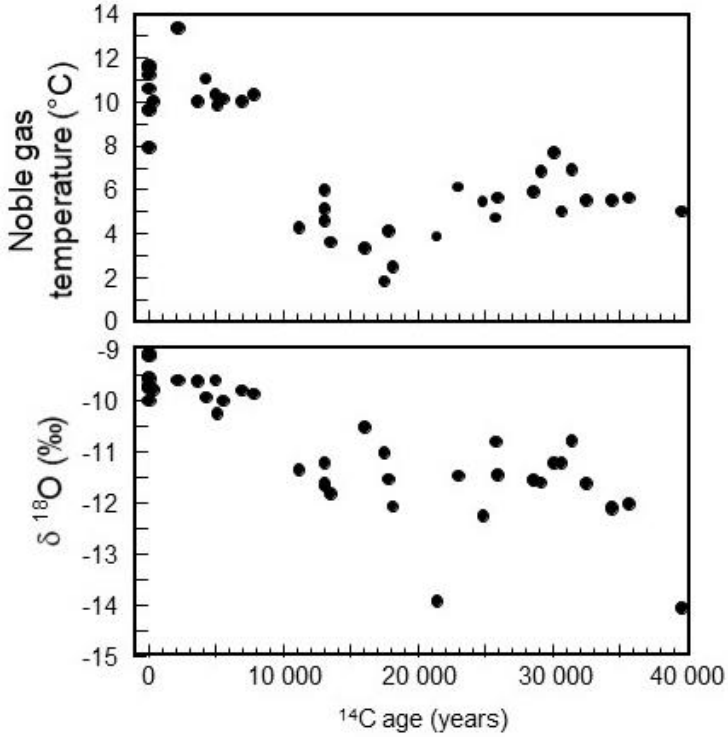

Figure 41 - Noble gas derived palaeotemperatures and ^{18}O ratios and ^{14}C ages for groundwater from the Great Hungarian Plain. Samples with ^{14}C ages less than 10,000 years have an average noble gas temperature of 10.6 °C. The noble gas temperature prior to the last glacial period (28,000 – 35,000 years ago) was approximately 5°C lower than present, and at the glacial maxima (approximately 18,000 years ago) the temperature was 8-9°C lower than present. The ^{18}O record shows a similar pattern, with depleted values in samples with ^{14}C ages exceeding 10,000 years (After Stute and Schlosser, 2000).

3.9 Reconstructing Contamination History

When combined with measurements of contaminant concentrations, groundwater age data can be used to reconstruct contaminant histories. One early study took place in the early 1990s and reconstructed the history of agricultural contamination from measurements of both CFCs-12 and nitrate in groundwater (Böhlke and Denver, 1995). The Locust Grove catchment in Maryland, USA (Figure 25) is dominated by agricultural land uses, and discharges to Chesapeake Bay. CFC-12 dating was used to estimate the mean rate of groundwater recharge to the catchment, and the age distribution within the groundwater and in groundwater discharging to streams. Groundwater ages ranged from pre-1940 (background CFC concentrations) to modern, while ages of groundwater discharging to streams ranged from pre-1940 to approximately 1975. CFC-11 also was measured, but was found to be subject to microbial degradation (Section 5.1), so was less useful as a dating tool. Some measurements of ^{3}H and ^{3}He were made to confirm groundwater ages obtained with CFC-12.

Many groundwater samples from within the catchment have nitrate (NO_3) concentrations above 700 μmol/L (10 mg/L-N). Although most of the streams within the catchment receive groundwater, nitrate concentrations in streams are lower than those observed in groundwater, with concentrations in the two main tributaries between approximately 140 and 700 μmol/L. The high nitrate concentrations in both groundwater and surface water are attributed to agricultural contamination. Some groundwater samples have lower nitrate concentrations, and these values are attributed to infiltration prior to extensive use of nitrogen fertilizers and/or to denitrification of NO_3 by microbes in the subsurface. The authors found a very strong correlation between nitrate concentrations and groundwater age (as determined with CFC-12), with relatively low concentrations (< 500 μmol/L) in water recharged between 1940 and late 1960s, but with increasing concentrations between 1970 and 1990 (Figure 42). The relationship mirrors that of regional fertilizer use (Böhlke and Denver, 1995).

The nitrate flux into streams in the region at the time of this study was less than the nitrate flux into groundwater, in part because of denitrification, but also because groundwater discharge to streams is decades old (and so has lower nitrate concentrations than more recent groundwater recharge). Over time, nitrate fluxes to streams are expected to increase.

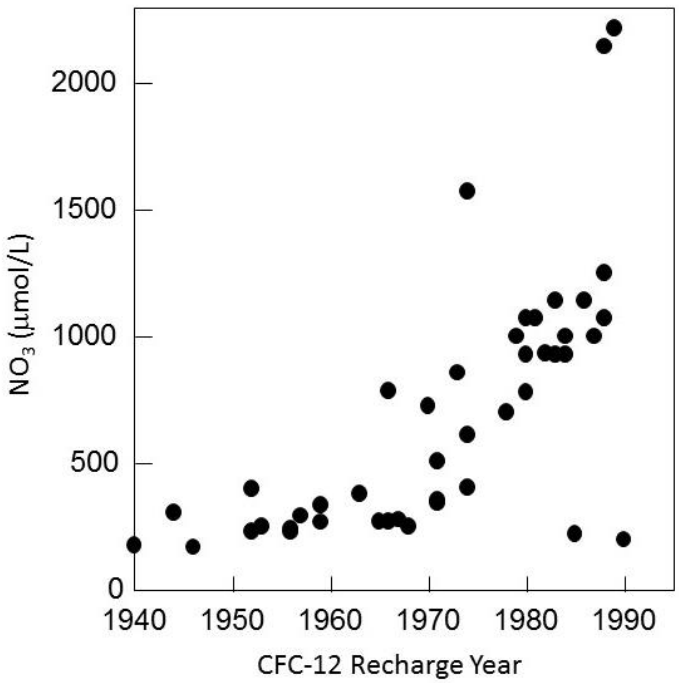

Figure 42 - NO_3 concentration in groundwater recharge as a function CFC-12 age of groundwater samples. The observed relationship shows good agreement with the pattern of regional use of nitrogen fertilizers (After Böhlke and Denver, 1995).

The potential of groundwater dating to assist in investigations of point-source contamination of groundwater is illustrated by a study from Cape Cod, Massachusetts (Figure 18). The site is on a military reservation, and groundwater contamination is believed to have arisen from a leaky pipe which carried aviation gasoline and jet fuel. Installation of piezometer nests, with short intake screens at multiple levels allowed estimation of high-resolution, vertical profiles of groundwater age using $^{3}H/^{3}He$ dating (Figure 19). Comparison between age and contaminant concentration data allowed the evolution of the groundwater plume to be determined. Vertical profiles of groundwater age allow determination of the vertical flow velocity. The plume defines a groundwater flow line, and comparison of ages within the center of the plume at different locations enables estimation of the horizontal flow velocity. With this information, the authors were able to trace the flow lines upgradient of the sampling points and identify both the location of the contaminant source and the approximate year that the contamination first occurred (Figure 43).

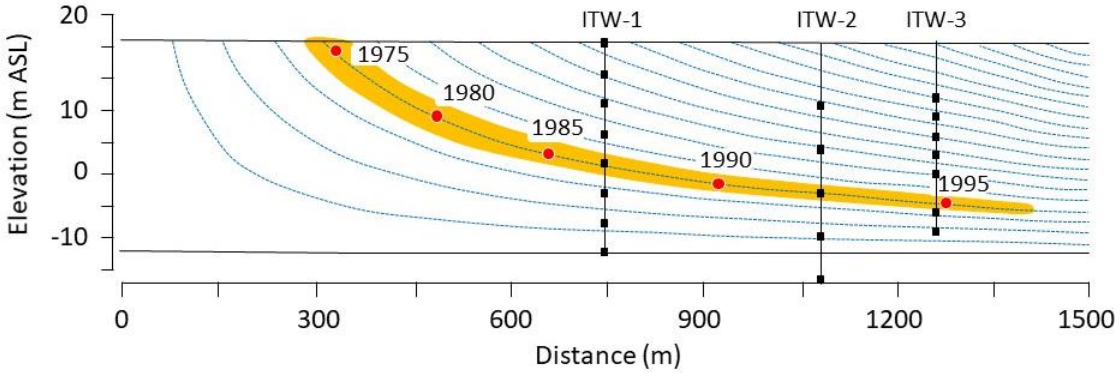

Figure 43 - Groundwater flow lines (blue dashed lines) derived from an analytical model calibrated to contaminant concentrations and $^{3}H/^{3}He$ age determinations (black squares denote sampling locations) at a contaminated site at Cape Cod, Massachusetts, USA. Given the groundwater age profile and the depth of the contaminant plume at three piezometer nests (ITW-1, ITW-2 and ITW-3), the authors were able to calculate the approximate location of the contaminant source and the year that the contamination occurred. The shaded region shows the flow lines originating at the contaminant location, and the red circles show the simulated movement of groundwater recharged at this location in 1975, when the contamination event was estimated to have occurred. Thus, the contaminant moved approximately 100 m in the first ten years (by 1985) and a further 400 m in the next ten years (by 1995). The vertical ^{3}H and ^{3}He profile obtained in piezometer nest ITW-3 is depicted in Figure 19 (After Solomon et al., 1995).

3.10 Calibrating Groundwater Models

A groundwater model is a mathematical representation of a groundwater system created using estimates of hydraulic parameters and boundary conditions. Given the properties and boundaries, a solution of the model provides hydraulic heads and flow rates within the groundwater system. These simulated heads and flows are compared to the heads and flows measured in the field and, if they do not match, the properties and boundaries are adjusted to improve the match between the model output and the measured data. This adjustment process is calibration of the model. However, when both aquifer

properties (e.g. K) and boundary fluxes (e.g. recharge and discharge) are unknown, the calibration process does not produce a unique estimate of properties or fluxes.

Many numerical groundwater models now offer the opportunity to simulate the distribution of groundwater ages and/or tracer concentrations within aquifer systems. When using groundwater ages to estimate aquifer recharge, numerical models allow for consideration of more realistic aquifer geometries than provided by the simple models discussed above (e.g., Figure 14). They also offer the opportunity for comparison between simulated and measured groundwater ages (or tracer concentrations), to evaluate the quality of model calibration. Use of groundwater age tracers for model calibration has the potential to overcome some of the non-uniqueness that is often involved with calibration of models using only hydraulic head data (Sanford, 2011).

One of the earlier studies that illustrated this application of groundwater age data was published in the early-1990s, and used the United States Geological Survey software (USGS, 2019) to create a two-dimensional model of hydraulic heads and flow in the agricultural Locust Grove catchment (Section 3.9). The initial calibration of the model (that did not involve groundwater ages) used values for recharge (457 mm/y) and hydraulic conductivity (K_h = 30.5 m/d with anisotropy ratio of 5:1) based on previous studies, and these values were consistent with observed hydraulic heads. A groundwater travel time analysis was then performed using the United States Geological Survey MODPATH software (USGS, 2019) to track particles in the simulated groundwater system, assuming a porosity value of 0.3. Travel times indicated by MODPATH were much smaller than those estimated from CFC-12 measurements on observation wells within the catchment (Figure 44). This suggested that the recharge rate should have been lower; the fit to heads can be maintained by keeping recharge and hydraulic conductivity in the same ratio. The model was then recalibrated until a much better fit to the CFC-12 ages was obtained, while retaining acceptable fit to heads. The final calibrated model used an average recharge rate of 305 mm/y, and horizontal hydraulic conductivity of 16.8 m/d.

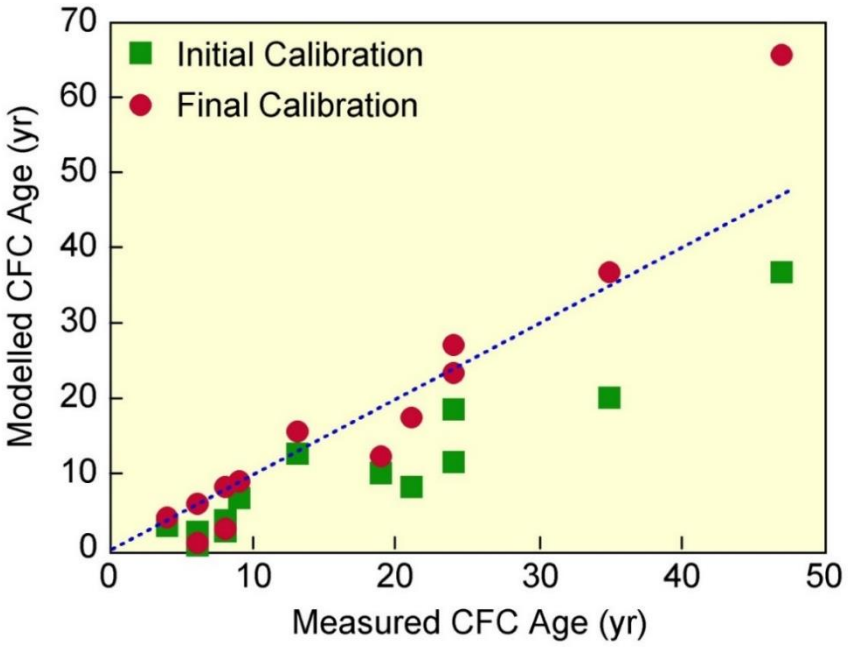

Figure 44 - Correlation between modelled and measured CFC-12 ages in Locust Grove catchment from initial model calibration, and a subsequent calibration that involved fitting to groundwater age data. The broken line denotes the Y=X line (i.e., modelled equals measured CFC age). The catchment location is shown in Figure 25 (From data in Reilly et al., 1994) (Cook, 2020).

The study described above used the particle tracking routine of MODPATH to simulate groundwater ages. In fact, there are three different methods for simulating groundwater age tracers (Figure 45):

1. Particle Tracking. Particle tracking methods calculate ages based on advection in a flow system. This is the simplest and easiest method to apply and will yield reasonable results in simple flow systems, where advective transport dominates diffusion and dispersion. Groundwater modelling packages such as MODFLOW and FEFLOW have particle tracking routines that can be easily applied. Results can be compared to groundwater ages inferred from measured tracer concentrations.
2. Direct Age Simulation. This approach also considers diffusion and dispersion of water molecules so that advective groundwater ages are modified by longitudinal and transverse dispersion and by diffusive exchange with adjacent aquitards. It provides a more realistic distribution of groundwater ages where these processes are important.
3. Solute Transport Modelling. This is conceptually the preferred approach, as it simulates tracer concentrations directly (rather than groundwater age). It differs from Direct Age Simulation in that radioactive decay can be simulated directly and diffusion coefficients specific to the solutes of interest can be used. Recently, some simulations have attempted also to include chemical reactions that can affect tracers (e.g., Salmon et al., 2015). The drawback of this approach is that model run

time can be long (hence making automatic calibration routines that perform multiple runs of a model difficult), and solutions can sometimes be unstable. Often the parameter values required to create the model are so uncertain that this higher level of computation is not useful.

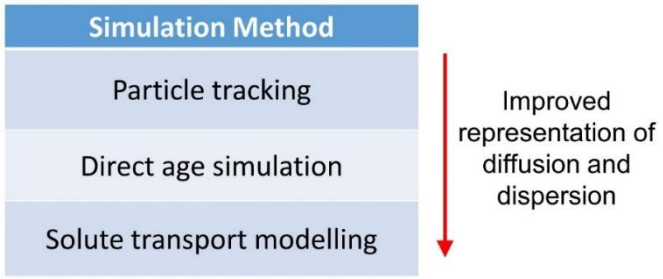

Figure 45 - Different approaches for simulating groundwater age (Cook, 2020).

4 Effects of Mixing on Groundwater Ages

Mixing of water can occur within aquifers and at the point of sampling, particularly if samples are pumped from wells with long intake zones. Because the components of any mixture are likely to have different ages (and hence different tracer concentrations), it is important to understand how mixing affects apparent age measured on the mixed sample.

The effect of mixing on tracer concentrations has already been discussed in Section 3.1. The effect of mixing on groundwater ages depends on the relationship between recharge time and tracer concentration. In the case of a tracer whose concentration decreases exponentially with age, the mean concentration of a mixed sample will not accurately reflect the mean age of the mixture but will be biased towards the younger components (Figure 46b). To illustrate this point, suppose two waters are mixed in equal proportions: one with an age of 1000 years and one with an age of 10,000 years. Clearly, the mean age of the water in this mixture is 5,500 years. However, the young water will have a ^{14}C activity of 88.6 pmC (assuming an initial activity of 100 pmC) and the old water will have a ^{14}C activity of 29.8 pmC (using Equation 1). The mixture will therefore have a ^{14}C activity of 59.2 pmC. The apparent age measured on a sample with this activity is 4,330 years, which is younger than the true (hydraulic) age of the mixture. In fact, the apparent age of any mixture will only accurately reflect the mean age of the mixed sample for tracers whose concentration is a linear function of age (Figure 46a). This is potentially the case with accumulating tracers such as helium, if the production rate of helium is spatially constant. It may also be the case for SF_6, whose atmospheric concentration has increased almost linearly with time since about 1980. However, for most other tracers, the apparent age of a mixed sample is unlikely to equal the mean age of the water in the mixture.

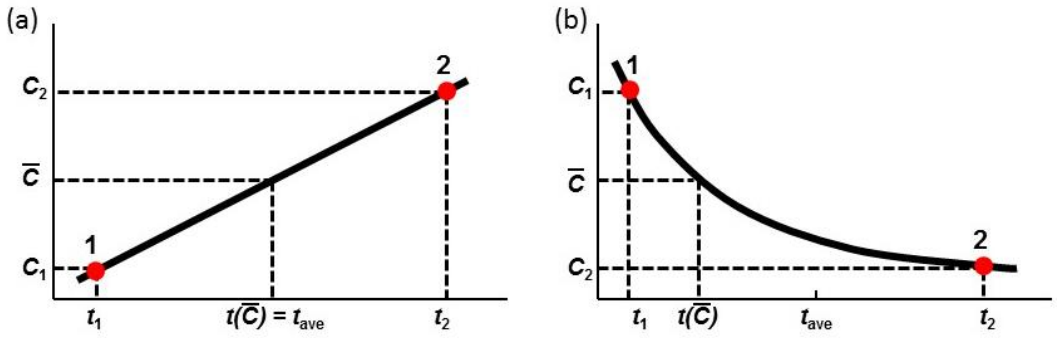

Figure 46 - Schematic representation of the effect of mixing on measured groundwater ages. Assume that water of age t_1 has concentration c_1 and that water of age t_2 has concentration c_2, and that water having groundwater ages t_1 and t_2 (t_2>t_1) mix in equal proportions. If the tracer concentration is a linear function of age (a), then the concentration of the mixture ($\bar{c}$) will correctly give the mean residence time of the mixture. However, if the concentration decreases exponentially with age (such as in the case of a radioactive tracer), then the mixture will have an apparent age which is biased towards the younger component (b). (Note that ages increase from left to right in both figures.) (After Bethke and Johnson, 2002).

The magnitude of the effect of mixing on measured groundwater ages will vary depending on the extent of groundwater mixing and can sometimes be determined by comparing ages obtained from different tracers (Section 5.1). As groundwater mixing often affects different tracers in different ways, the extent to which different tracers indicate different ages is an indicator of the extent of mixing. Groundwater mixing during sampling can be minimized by collecting groundwater samples from wells with relatively short intake zones (i.e., screen lengths). In many cases, however, such piezometers are not available, and samples are collected from municipal, irrigation or mine wells, with very long screen intervals. In these cases, samples are mixed from various levels of the aquifer that produce water along the screened interval. This can be envisioned by considering the ages of water that would enter a long screen in Figure 14. In a homogeneous unconfined aquifer, the extent of mixing caused by long-screened wells can be estimated from the ratio of the screen length to the vertical water velocity as shown in Equation 13.

$$t_{mix} = \frac{z_{well}\theta}{R} \qquad (13)$$

where:

t_{mix} = extent of well mixing (measured in years) (T)

R = aquifer recharge rate (L/T)

θ = Porosity (dimensionless)

z_{well} = length of the well intake zone (L)

Thus, for example, if the aquifer porosity is 0.4 and the recharge rate is 100 mm/y, then a 2 m long well screen will mix water over an age range of approximately 8 years. Therefore, if the well is screened immediately below the water table, the water at the top of the screen would have an age of zero, and the water at the bottom of the screen would have an age of

8 years. In comparison, a well with a 20 m well screen would mix water over an age range of 80 years, which would severely limit the ability to determine groundwater ages within the last 100 years.

4.1 Diffusion and Dispersion

Diffusion causes dissolved constituents to spread and decrease in concentration. Diffusion is caused by the random motion of molecules, known as Fickian motion, in which the system seeks maximum disorder, so that solute or isotopes in one location will spread to decrease that "order". The magnitude of diffusion in porous media is expressed as a coefficient, D^*, in units of length squared over time (e.g. m^2/s) and depends on the nature of the dissolved species (size is a major factor) and the character of the porous medium (its porosity, size of the pores and tortuosity of the pore spaces are influencing factors). Dispersion also spreads dissolved constituents, but this spreading is caused by variations in velocities in heterogeneous materials. It is also expressed in units of length squared over time and includes the diffusion coefficient. Together, diffusion and dispersion cause dissolved constituents to spread in a groundwater system.

The previous section discussed how tracer ages are affected by mixing of discrete water samples. Groundwater flow systems are typically complex and heterogeneous, so rarely produce mixtures of parcels of water of discrete ages, because dispersion will cause mixing of water in one zone with water in adjacent zones. This usually means mixing water with other water that is slightly younger (above and/or upgradient) and slightly older (below and/or downgradient). The effect on bomb tracers such as ^{3}H and ^{36}Cl is that concentrations measured on groundwater samples from the 1950s and 1960s are always lower than the maximum concentrations that occurred in rainfall. Nevertheless, if samples are collected along a flow line, or as vertical profiles, the location of highest concentration in groundwater will indicate the period of highest concentration in rainfall. Furthermore, because the effect of dispersion can be large, the shape of the tracer profile can be used to estimate the dispersivity of the aquifer materials (Robertson and Cherry, 1989).

For tracers whose concentration varies more smoothly with time, the effect of dispersion on tracer concentrations will be less but can still be important. In the simplest case of one-dimensional flow in a homogeneous aquifer, longitudinal dispersion will cause ^{14}C ages to be less than hydraulic ages, although the effect will only be significant for very large dispersivity values and low groundwater velocities. For a water velocity of 1 m/y and dispersivity of 1000 m, the hydraulic age will exceed the tracer age by less than 5%, although the difference increases to 30% for a velocity of 0.1 m/y and the same dispersivity (Castro and Goblet, 2005). For event markers, apparent tracer ages can either overestimate or underestimate hydraulic ages, depending on how the atmospheric input curve has changed with time. For CFCs, a water velocity of 1 m/y and dispersivity of 2 m results in tracer ages that differ from hydraulic ages by up to 10% for water with estimated recharge

dates between the early 1970s and early 1990s, but the effect is greater (up to 30%) for water with estimated recharge dates from the early 1950s. Similar age discrepancies arise for ^{85}Kr, but errors are larger on groundwater that was recharged prior to the mid-1960s (Ekwurzel et al., 1994). $^{3}H/^{3}He$ represents a special case, because the groundwater age is calculated from the ratio of two tracers, and these tracers can be transported at different rates. Errors associated with $^{3}H/^{3}He$ ages can be large for groundwaters recharged prior to the 1970s, as concentration gradients are greatest for groundwaters recharged immediately before and after the bomb peak (Schlosser et al., 1989).

Calculations of the extent of mixing due to dispersion in uniform, homogeneous flow fields can potentially underestimate the extent of mixing within real aquifer systems. The effect of mixing in heterogeneous aquifers on CFC concentrations and ages was examined by Weissmann et al. (2002), who simulated solute transport in a small aquifer system consisting of five different interlayered materials with hydraulic conductivity values that varied over five orders-of-magnitude. The model found that variations in the travel paths of groundwater intercepted by wells with 1.5 m long intake zones resulted in relatively broad age distributions for groundwater samples. Apparent CFC-11 and CFC-12 ages of these mixtures would have underestimated mean hydraulic ages by a factor of approximately two. The extent of this bias in mean age caused by mixing within the aquifer will depend upon the degree of aquifer heterogeneity, the timing and magnitude of tracer input and the diffusion coefficient of the tracer (McCallum et al., 2014). Thus, the effect will differ between tracers. It is still unclear how significant this effect might be in different aquifers. However, similar apparent ages have been obtained using tracers with very different atmospheric input curves (e.g., CFC-12 and $^{3}H/^{3}He$) in some aquifer systems (e.g., Ekwurzel et al., 1994), suggesting that this problem will be aquifer specific.

4.2 Diffusive Exchange with Aquitards

Geologic systems are often a series of layers of alternating high (aquifers) and low (aquitards) hydraulic conductivity. In such systems, groundwater primarily flows horizontally along the aquifer layers with some vertical leakage into or out of overlying and underlying aquitards. Several studies have shown that leakage through aquitards can affect tracer concentrations in aquifers (e.g., Love et al., 1993). Even when the leakage is hydraulically negligible, diffusive exchange between aquifers and aquitards has the potential to affect tracer concentrations. Water in the aquitards is often older than water in the aquifers, and since concentrations of most tracers decrease with age, concentrations in the aquitard are likely to be lower than those in the aquifer. Diffusive exchange between the aquifer and the aquitard will therefore cause a reduction in the concentration in the aquifer, and hence result in tracer ages within the aquifer that will be older than advective water ages. An analytical solution for a 20 m thick aquifer sandwiched between aquitards

showed that the apparent groundwater age in the aquifer estimated using ^{14}C would exceed the hydraulic age by between 50 % and 180 % for aquitard diffusion coefficients between 10^{-2} and 10^{-3} m^2/y, but the effect would be less than 20 % for a 200 m thick aquifer (Sudicky and Frind, 1981; Figure 47). (The reader should be aware that diffusion coefficients can be expressed in two different ways. The above uses the formulation $D = D_0\ \theta\ \tau$, where D_0 is the free solution diffusion coefficient, θ is porosity and τ is tortuosity. Some other papers use the term diffusion coefficient to refer simply to $D_0\ \tau$, and so the diffusion coefficient does not specifically include the porosity term.) For radioactive tracers such as ^{14}C, simple approaches are available for correcting for this effect (Sudicky and Frind, 1981; Sanford, 1997).

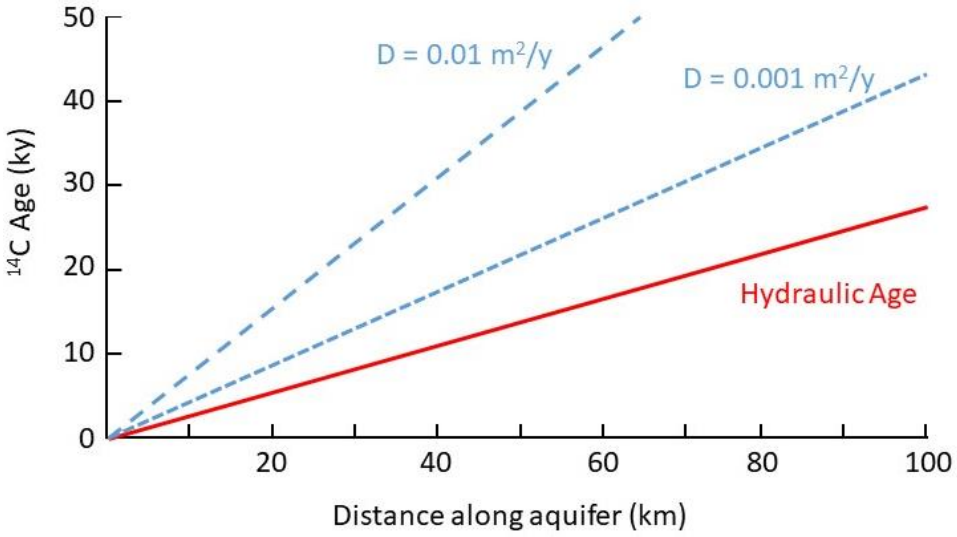

Figure 47 - The effect of aquitard diffusion on apparent ^{14}C ages in an aquifer for a 20 m thick aquifer sandwiched between two aquitards. Apparent ^{14}C ages are greater than hydraulic ages by 58 % for an aquitard diffusion coefficient of D = 0.001 m^2/y and by 180 % for D = 0.01 m^2/y. The model also assumes an aquifer porosity of 0.35, aquitard porosity of 0.5 and negligible dispersivity. Although the plot assumes a groundwater velocity of 3.65 m/y, the relative difference between apparent ^{14}C age and hydraulic age is relatively insensitive to the groundwater velocity, and mostly determined by the aquitard diffusion coefficient, aquifer thickness, and the ratio between the aquitard and aquifer porosity. Modified from Sudicky and Frind (1981).

Diffusive exchange between aquifers and aquitards will have a smaller effect on event marker tracers (such as CFCs, SF_6, and ^3H) because the extent of tracer diffusion over the timescale that the tracer has been present in groundwater is likely to be relatively small. The distance over which diffusion will occur can be approximated by Equation 14.

$$x = \sqrt{4Dt} \tag{14}$$

where:

x = distance (L)

D = diffusion coefficient of the tracer (L^2/T)

t = Time (T)

Assuming $D = 10^{-2}$ to 10^{-3} m²/y and t = 70 years gives x = 0.5 – 1.7 m. Therefore, diffusive exchange between aquifers and aquitards is only likely to be significant for these tracers if aquifer thicknesses are much less than 10 m.

Helium differs from most other tracers, in that its concentration increases with age. Thus, diffusive exchange with aquitards usually increases the He concentration in the aquifer, although this still causes an apparent increase in age (like with other tracers). As concentrations of helium increase linearly with time, concentrations within thick aquitards can become very high, and so diffusion of helium from aquitards can have a pronounced effect on ages in confined aquifers.

There have been several studies that have obtained core samples through aquitards, and estimated rates of aquitard leakage from isotope concentrations in aquitard pore water (e.g., Hendry et al., 2004; Mazurek et al., 2011). These studies can distinguish between purely diffusive and advective transport through aquitards and hence allow us to better quantify the effect of aquifer-aquitard interaction on environmental tracer concentrations in aquifers.

5 Practical Considerations

5.1 Non-Conservative Tracer Behavior

To this point, this discussion of groundwater age tracers has mostly assumed that they are neither produced nor consumed in the subsurface, other than by radioactive decay processes. This is not always the case. Carbon-14 activities can be altered by chemical reactions with geologic materials containing mineral or organic carbon. In some cases, these reactions can be identified, and a correction can be made using geochemical modelling. Numerous authors have shown that CFC-11 is subject to microbial degradation in anaerobic environments. This will lead to CFC-11 ages that are significantly older than true groundwater ages. There is some evidence for sorption of CFC-113 (sorption is delayed migration because a dissolved constituent is either temporarily or permanently attached to solids), particularly in aquifers with a high organic carbon content, and this will also lead to apparent ages that are greater than true water ages. In contrast, CFC-12 appears to behave conservatively in most groundwater systems.

Some tracers can also be produced in groundwater systems. SF_6 production has been observed in some groundwaters, particularly those in igneous rocks. Also, subsurface production of ^{36}Cl can occur. This does not affect use of this isotope as an indicator of recent recharge because ^{36}Cl concentrations in rainfall were very high during the 1960s, but it can affect groundwater dating on timescales of hundreds of thousands to millions of years. ^{3}He and ^{4}He can be contributed from other sources, including excess air. Excess air can also lead

to elevated concentrations of SF_6 in groundwater, and this needs to be accounted for correctly in order to make accurate age determinations. Corrections for excess air are sometimes required for CFC-11, CFC-12 and CFC-113. All dissolved gases can be contaminated during drilling and well development using compressed air. This is most significant in low permeability environments, and where sampling occurs shortly after well installation, and is most significant for the low solubility gases (e.g., SF_6).

Artificially elevated tracer concentrations can occur in contaminated environments, and this can preclude the use of such tracers as groundwater dating tools. Elevated CFC concentrations are widely reported in groundwater in urban and industrial areas, and groundwater contamination is possible for other tracers with industrial sources, such as SF_6. Some of the radioactive tracers (e.g., ^{14}C, ^{3}H, ^{85}Kr) may be contaminated at sites with a history of nuclear activities.

When more than one tracer is measured, it is often instructive to prepare tracer – tracer plots that compare the relationship between different tracers in atmospheric input with the measured values (Figure 48). Because the different tracers are affected by the above processes to different extents, it is often possible to identify non-conservative behavior by comparing concentrations or apparent ages obtained from different tracers. Thus, for example, degradation of CFC-11 may be apparent from CFC-11 ages that are significantly older than ages obtained with other tracers such as CFC-12 or SF_6, for example. Contamination of one or more of the CFCs can similarly often be identified from discrepancies in ages.

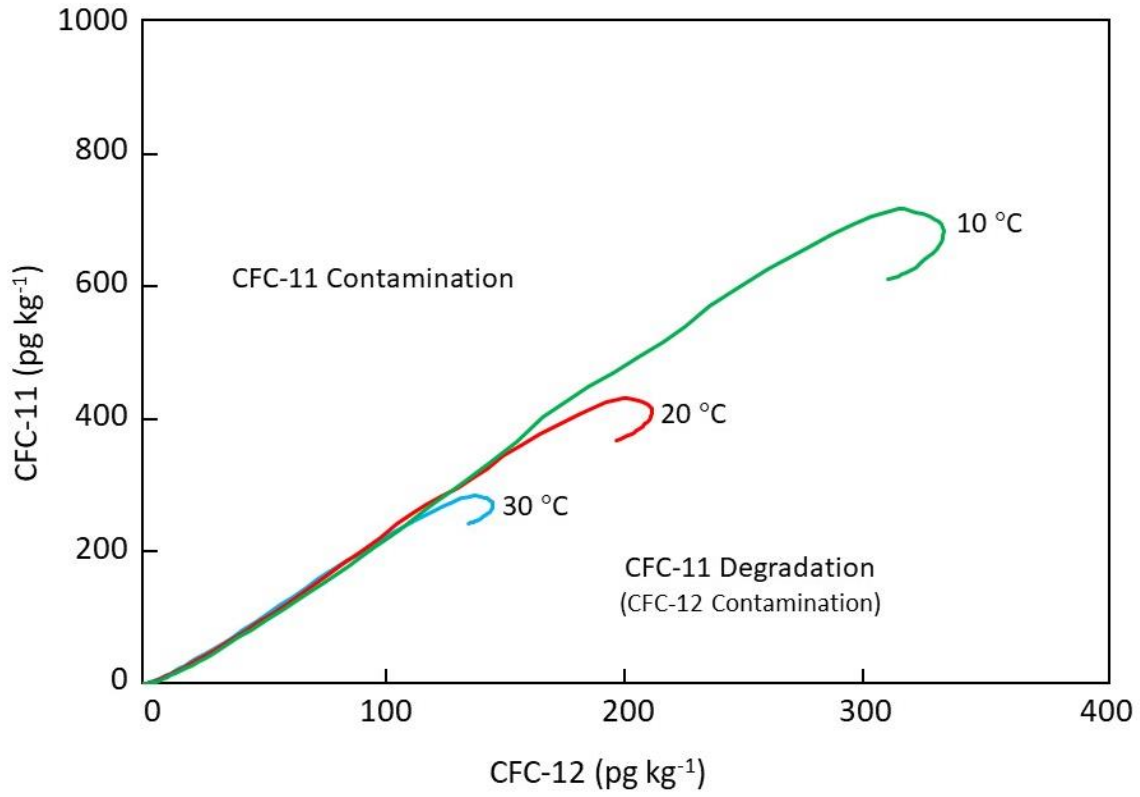

Figure 48 - Plot showing expected CFC-11 and CFC-12 concentrations in groundwater, against which field data can be compared. The solid lines depict the relationship between concentrations of the tracers for rainfall in equilibrium with atmospheric gas concentrations between 1950 and 2018, at recharge temperatures between 10 and 30 °C. Concentrations of these tracers in the atmosphere (and hence in groundwater recharge) increased until the mid to late 1990s, but have decreased by 5 – 15 % since then. This recent decrease in concentration causes the apparent 'hooks' at the end of each line. Samples that fall significantly below these equilibrium lines probably indicate degradation of CFC-11, although contamination of CFC-12 cannot be ruled out. Samples that fall above the lines probably indicate CFC-11 contamination (Cook, 2020).

Groundwater mixing can also be identified with tracer – tracer plots. The solid black line in Figure 49 depicts the relationship between CFC-12 and ^{14}C concentration that should be observed in groundwater if these tracers are non-reactive and there is no significant mixing within the aquifer. Note that there is not a unique relationship between CFC-12 concentration and ^{14}C activity because concentrations of these tracers have risen and fallen over time (Figure 6). The shaded area denotes possible concentrations that might occur if both tracers are non-reactive, but mixing occurs within the aquifer or during sampling, with the red circles denoting two mixing possibilities as explained in the caption of Figure 49. Water samples with concentrations outside of the shaded area cannot occur by mixing alone and would imply non-conservative behavior of at least one of the tracers and/or contamination.

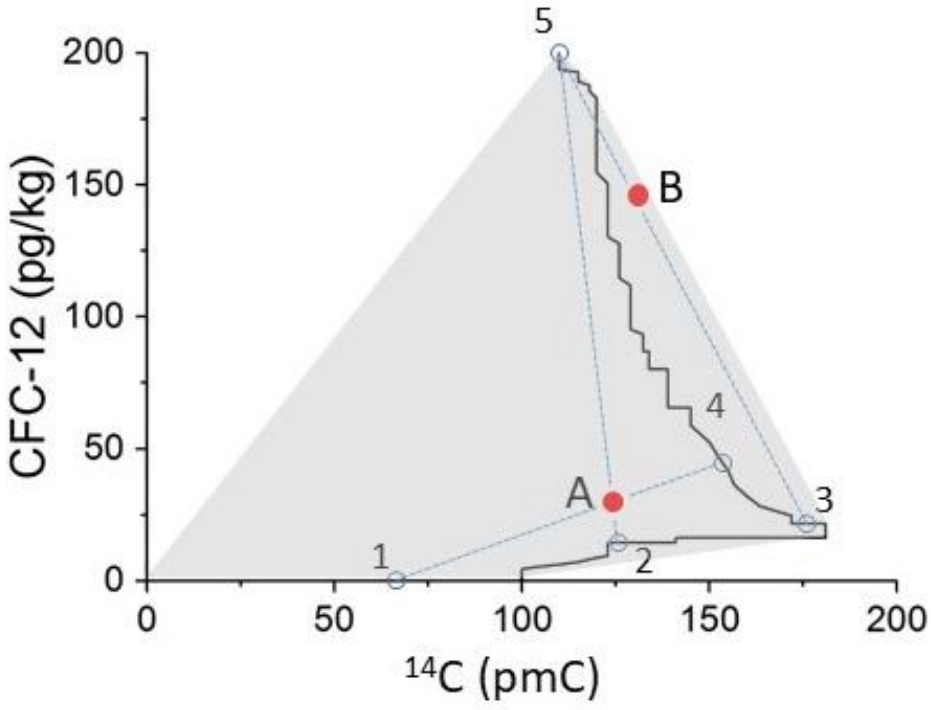

Figure 49 - Example of a mixing plot between CFC-12 and ^{14}C. The solid black line depicts the relationship between concentrations of the tracers for Australian rainfall in equilibrium with atmospheric gas concentrations between 1950 and 2014, at a temperature of 24 °C. This is assumed to be the concentration in recharge between these times. Prior to 1950, recharge would have had zero CFC-12, and so the line would extent along the x-axis to the origin. Points 1 to 5 therefore represent water with progressively younger ages (5 being the youngest). Two-component mixing lines can be drawn to connect any two points on the solid black line. Mixed samples can then occur anywhere on these lines, with the location on the line depending on the mixing proportion. For example, Sample A could be produced by mixing between end members at point 2 and point 5 (with a larger proportion from the end member at point 2). Alternatively, it could be produced by mixing between end members at point 1 and point 4. However, many other mixing combinations are also possible. Sample B could be produced by mixing between points 3 and 5. The shaded region indicates all possible concentrations that could arise due to mixing of water of different ages. Groundwater samples falling outside of this mixing envelope indicate that processes other than mixing have affected either ^{14}C or CFC-12 ages. This could include chemical reactions affecting ^{14}C or, degradation or contamination of CFC-12 (Cook, 2020).

5.2 Planning Field Investigations

Several factors need to be considered when planning a field investigation involving environmental tracers. For groundwater dating, there is often a choice of tracer, and those that are selected will depend upon the required precision of analyses, the site conditions and the project budget. A summary of the advantages and limitations of the different tracers is provided in Table 3. The factors that should be considered in the selection of tracer include:

Availability of Piezometers

Are groundwater samples to be obtained from existing wells, or will piezometers be installed specifically for the project? The length of the well screen of existing wells will impact on the precision that can be obtained with different residence time tracers and may

therefore affect the choice of tracer. If piezometers are to be specifically installed, then the length of the well screen is usually a trade-off between the desire to sample a discrete interval of the aquifer and the need for sufficient well-yield for purging and sampling. Piezometer diameter may be influenced by pump availability and minimum diameter requirements of downhole geophysical or sampling equipment. Drilling methods may be influenced by a need to avoid introducing air into the aquifer.

The Expected Age of the Groundwater and Required Precision

Although the purpose of measuring environmental tracers is often to estimate the age of the groundwater, it is sometimes necessary to know the approximate age so that the most appropriate tracers can be chosen for the study. Information related to choosing tracers is provided in Figure 2 and Table 3. The expected age of the groundwater and the required precision of groundwater age measurements will affect the choice of tracers. Only event markers with monotonically increasing atmospheric concentrations can uniquely provide groundwater ages over the full age range of the tracer. The sensitivity of different tracers for estimating groundwater age is largely dependent on shape of their input function and measurement precision. Radon is the most reliable tracer for ages of days to weeks; $^{3}H/^{3}He$ for ages of months to a few years; SF_6, ^{85}Kr, $^{3}H/^{3}He$ have good precision for ages from a few years to about 20 years; SF_6, ^{85}Kr, $^{3}H/^{3}He$ and CFCs have good precision from about 20 – 40 years; and CFCs, SF_6 and ^{85}Kr have good precision for ages from about 40 – 60 years (Figure 6). Fewer tracers are available for older groundwater.

Local Geology and Geochemical Environment

The use of environmental tracers for estimating groundwater flow usually relies on conservative tracer behavior, and this can be affected by the geological and geochemical environment. CFC-11 is likely to degrade in groundwater with a low dissolved-oxygen concentration, and all CFCs can degrade in highly anoxic groundwater (Hinsby et al., 2007). CFCs can also sorb to aquifer materials with a high organic carbon content (Choung and Allen-King, 2010), and so other age indicators may be preferred in this environment. Subsurface production of SF_6 has been reported in some aquifers, particularly in granites and rocks containing fluorite (Chambers et al., 2019). Interpretation of ^{14}C is more difficult in carbonate aquifers due to chemical reactions that can modify the ^{14}C activity of TDIC, although there are few alternative tracers over the time range represented by ^{14}C (Figure 2).

Sampling Requirements and Analytical Facilities

Some environmental tracers are straightforward to sample, whereas others require more care and/or specialized sampling equipment. For others (e.g., radon), the short half-life means that samples need to be analyzed by the laboratory within a short time (usually a few days) after samples are collected. This requires careful planning. Although most environmental tracers only require collection of relatively small sample volumes (< 1 litre), this can vary depending on analytical method, and some environmental tracers require much larger volumes (e.g., ^{39}Ar, ^{81}Kr). In some aquifers, piezometers will not yield

enough water for these analyses. Where specialized sampling equipment is required, it can usually be obtained from the laboratory where the analyses are to be performed.

For groundwater dating, analytical costs are similar for most tracers (around US$300-400 per sample in 2020). Exceptions are ^{36}Cl and the isotopes of noble gases (^{39}Ar, ^{81}Kr, ^{85}Kr), which are more costly, in part because of the scarcity of analytical facilities. However, these tracers offer some advantages over other tracers, as the noble gases are non-reactive in all environments, and ^{36}Cl and ^{81}Kr are the only available tracers for ages beyond 50,000 years. ^{222}Rn is cheaper than the other age tracers (US$50-$150), but only provides ages for groundwater less than several weeks old. This limits its application in most environments. Field-portable analytical units are available for ^{222}Rn, ^{2}H, ^{18}O and some of the noble gases.

Ancillary Information Requirements

Interpretation of some tracers is assisted by the availability of ancillary information. For example, dissolved gases such as CFCs and SF_6 require information on recharge temperature, the amount of excess air and salinity, to calculate tracer solubility in water. Temperature and excess air can be estimated with concurrent N_2 and Ar measurements, or more precisely, with measurements of other noble gases. For relatively high solubility tracers such as CFCs, recharge temperature can sometimes be estimated from air temperature data, although more precise ages can be determined using noble gas data. This information is not needed for ^{81}Kr, ^{85}Kr or ^{39}Ar, because their ages are based on isotope ratios, rather than chemical activity. Local measurements of atmospheric levels of ^{85}Kr and ^{3}H concentrations in precipitation can improve the accuracy of these methods. ^{2}H and ^{18}O studies will benefit from collection of rainfall data, particularly if the site is remote from an existing rainfall measurement station. Information on carbonate chemistry of the aquifer solids and soil gas (including ^{13}C) will greatly improve the ability of ^{14}C data to accurately constrain groundwater residence times. Dissolved oxygen measurements can provide useful information regarding the potential for degradation of CFC-11. Information on production rate is needed for accumulating tracers.

The Potential for Site Contamination

Several of the environmental tracers used as event markers for estimation of groundwater age are atmospheric contaminants. Their use as groundwater age indicators relies on either their atmospheric concentrations being relatively uniform (e.g., CFCs, SF_6, ^{85}Kr), or the time of maximum atmospheric concentration being the same over large areas (e.g., ^{3}H). There is the potential for these tracers to be present as local contaminants, either in the groundwater or through locally elevated atmospheric concentrations. Elevated atmospheric concentrations of CFCs can occur in large urban areas or close to industrial facilities (Ho et al., 1988), and groundwater contamination can also occur at urban and industrial sites. Low solubility gases can also be contaminated by well development using compressed air, particularly in low permeability formations (Figure 50). There is also

potential for contamination of ^{85}Kr at radioactive waste disposal sites or at sites close to nuclear reactors or nuclear test facilities, and for contamination of ^{3}H at landfills, nuclear facilities and disposal sites. The use of CFCs as groundwater dating tools is severely limited where groundwater is contaminated by urban or industrial sources.

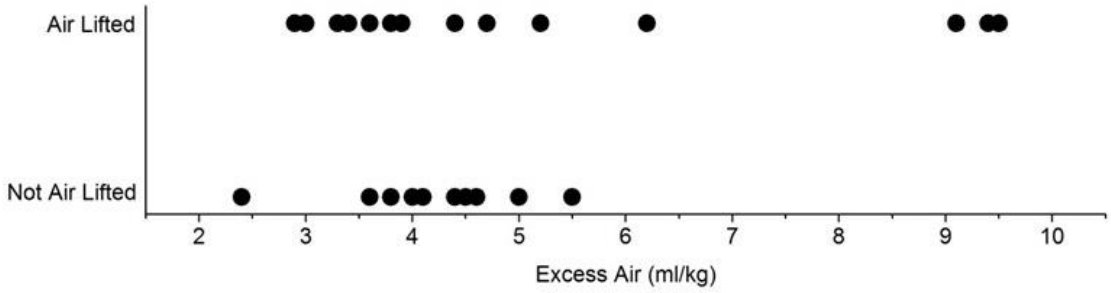

Figure 50 - Comparison of excess air measurements on groundwater samples from wells that had previously been purged using either compressed air (air lifted) or using a submersible pump (not air lifted). Three samples that had been purged using compressed air have much higher excess air concentrations than other samples, possibly indicating introduction of air to the formation during well purging. Data are from an industrially contaminated site in Adelaide, South Australia (Cook, 2020).

Given the potential limitations of some tracers, and the difficulty of predicting their limitations at specific sites, it is useful to analyze for more than a one tracer. Measuring multiple age tracers can also provide information on mixing processes, that would not be apparent from measurement of a single tracer.

Table 3 - Advantages and limitations of different environmental tracers for groundwater dating.

Tracer	Approximate Age Range	Advantages	Limitations
^{222}Rn	1 - 10 days	Completely unreactive	Sample must be delivered to the laboratory rapidly, due to the short half-life.
^{3}H	Provides indication of presence of 1950s-1960s precipitation.	Inert, and easy to sample. Reliable indicator of the presence of young (<70 year) precipitation.	Cannot provide precise age estimates without parallel ^{3}He measurements.
$^{3}H/^{3}He$	0.1 - 70 years	In suitable environments, can have high precision over a large age range.	Highly sensitive to mixing, and so precise age estimates require short well screens.
CFC-12	1950 - present. Non-unique ages since mid-1990s.	Most inert of three common CFCs.	Contamination is commonly observed in urban and industrial environments.
CFC-11	1950 - present. Non-unique ages since late 1980s.	Usually included with analysis of CFC-12 and can provide useful supporting information.	Contamination is commonly observed in urban and industrial environments; Degrades in anaerobic environments.
CFC-113	1970 - present. Non-unique ages since early 1990s.	Sometimes included with analysis of CFC-12 and can provide useful supporting information.	Contamination is commonly observed in urban and industrial environments; Can sorb onto aquifer materials.
SF_6	1970 - present.	Monotonically increasing atmospheric concentrations Largely unreactive.	Highly sensitive to excess air; Subsurface production can be locally important.
^{85}Kr	1950 - present.	Monotonically increasing atmospheric concentrations; Completely unreactive; Insensitive to recharge temperature and excess air.	Analysis is relatively costly.
^{39}Ar	50 - 1000 years	Completely unreactive.	Requires large sample volume; Subsurface production can sometimes occur.
^{14}C	200 - 30,000 years	Most widely available tracer for this time range.	Interaction with carbon in aquifer materials can complicate interpretation.
^{36}Cl	50,000 - 1,000,000 years; Can also provide indication of presence of 1950s – 1960s precipitation.	Very sensitive indicator of recharge from 1950s - 1960s.	Mixing with chloride from other sources can complicate analysis.
^{81}Kr	50,000 - 1,000,000 years	Completely unreactive.	Requires very large sample volumes.

6 Exercises

Exercise 1

Water samples are collected from two piezometers and from a river. The piezometer that is closest to the river (P2) is believed to be a mixture of groundwater flowing towards the river (represented by piezometer P1), and river water that moves into the aquifer during high river flows. Assuming that the water obtained from piezometer P2 is a mixture of water from piezometer P1 and from the river, calculate the relative proportions of the two sources in the mixed sample from P2. Use Equation 7 and calculate the mixing proportions independently using chloride and deuterium.

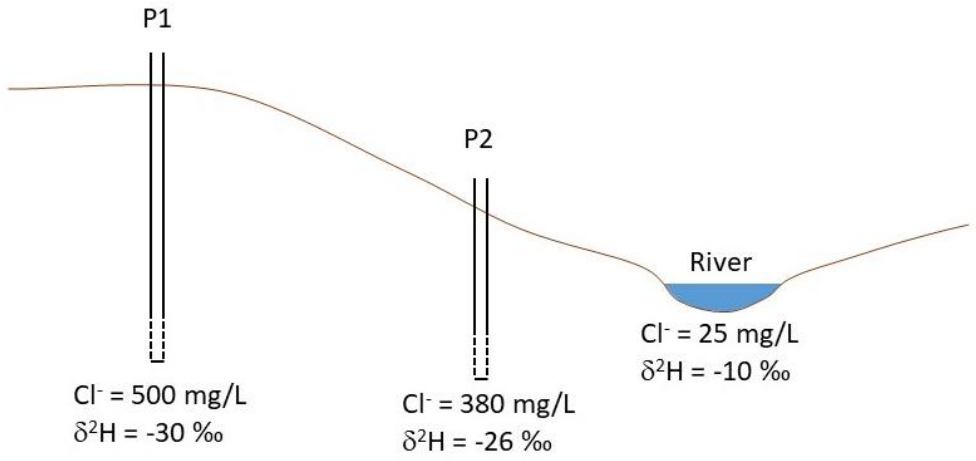

Click here for solution to exercise 1

Exercise 2

Groundwater samples were collected from two wells in a confined aquifer. The wells are located along a flow line and are 13 km apart. The ^{14}C activities on groundwater from these wells were determined to be 79 and 56 pmC. Assuming an initial ^{14}C activity of 90 pmC at the time of groundwater recharge and that there are no chemical reactions affecting ^{14}C activities, calculate the horizontal groundwater velocity. (The half-life of ^{14}C is $t_{1/2}$ = 5730 years, and its decay constant is 1.21 x 10^{-4} per year.)

If the head difference between the two wells is 2 m, what value of hydraulic conductivity would be consistent with the tracer data. Assume an effective porosity, n_e, of 0.2.

Click here for solution to exercise 2

Exercise 3

A piezometer nest in an unconfined aquifer has a short screen which is 10 m below the water table. The CFC-12 concentration measured on groundwater obtained from this piezometer was 93 pg/kg. Based on a salinity of 400 mg/L, recharge temperature of 21 °C, and atmospheric pressure at recharge of 0.917 atm, the atmospheric concentration at the time of recharge is calculated to have been 225 parts per trillion by volume (pptv). This corresponds to the atmospheric concentrations in 1976 (Figure 6). If sampling took place in 2015, this reflects a water age of 39 years. Assuming an age of zero at the water table, a porosity of 0.2 and an aquifer thickness of 50 m, use Equation 10, to calculate the aquifer recharge rate.

Click here for solution to exercise 3

Exercise 4

A water sample extracted from an irrigation well had a ^{3}H concentration of 10 TU. The $^{3}He/^{4}He$ ratio of dissolved helium was also measured, and after correcting for helium due to other sources, the ^{3}He concentration due to decay of ^{3}H (termed the tritiogenic ^{3}He concentration) was estimated to be 5 TU. Calculate the apparent age of the water sample using Equation 3. (The decay constant for ^{3}H is $\lambda = 0.0558$ y^{-1}.)

Click here for solution to exercise 4

7 References

Aeschbach-Hertig, W., 2004, NOBLEBOOK online MicroSoft Excel Workbook for inverse modeling of dissolved noble gases, https://www.iup.uni-heidelberg.de/research/hydrotrap/noblebook↗.

Aeschbach-Hertig, W., F. Peeters, U. Beyerle, and R. Kipfer, 1999, Interpretation of dissolved atmospheric noble gases in natural waters. Water Resource Research, volume 35, number 9, pages 2779-2792.

Aeschbach-Hertig, W. and D.K. Solomon, 2013, Noble gas thermometry in groundwater hydrology. *In,* P. Burnard, editor, The Noble Gases as Geochemical Tracers. Springer, Berlin, Heidelberg, pages 81-122.

Araguas-Araguas, L., K. Froelich, and K. Rozanski, 2000, Deuterium and oxygen-18 isotope composition of precipitation and atmospheric moisture. Hydrological Processes, volume 14, pages 1341-1355.

Barnes, C.J. and G.B. Allison, 1988, Tracing of water movement in the unsaturated zone using stable isotopes of hydrogen and oxygen. Journal of Hydrology, volume 100, pages 143-176.

Bethke, C.M. and T.M. Johnson, 2002, Ground water age. Groundwater, volume 40, issue 4, pages 337-339.

Beyer, M., U. Morgenstern, P. van der Raaij, and H. Martindale, 2017, Halon-1301: further evidence of its performance as an age tracer in New Zealand groundwater. Hydrology and Earth Systems Sciences, volume 21, pages 4213-4231.

Böhlke, J.K. and J.M. Denver, 1995, Combined use of groundwater dating, chemical, and isotopic analyses to resolve the history and fate of nitrate contamination in two agricultural watersheds, Atlantic coastal plain, Maryland. Water Resources Research, volume 31, number 9, pages 2319-2339.

Bollhöfer, A., C. Schlosser, S. Schmid, M. Konrad, R. Purtschert, and R. Krais, 2019, Half a century of Krypton-85 activity concentration measured in air over Central Europe: Trends and relevance for dating young groundwater. Journal of Environmental Radioactivity, volumes 205-206, pages 7-16.

Busenberg, E. and L.N. Plummer, 2008, Dating groundwater with trifluoromethyl sulfurpentafluoride (SF_5CF_3), sulfur hexafluoride (SF_6), CF_3Cl (CFC-13), and CF_2Cl_2 (CFC-12). Water Resources Research, volume 44, W02431, doi:10.1029/2007WR006150↗.

Calf, G.E., P.S. McDonald, and G. Jacobsen, 1991, Recharge mechanism and groundwater age in the Ti-Tree Basin, Northern Territory. Australian Journal of Earth Sciences, volume 38, pages 299-306.

Campbell, K., A. Wolfsberg, J. Fabryka-Martin, and D. Sweetkind, 2003, Chlorine-36 data at Yucca Mountain: statistical tests of conceptual models for unsaturated-zone flow. Journal of Contaminant Hydrology, volume 62-63, pages 43-61.

Castro, M.C. and P. Goblet, 2005, Calculation of ground water ages – A comparative analysis. Groundwater, volume 43, issue 3, pages 368-380.

Chambers, L.A., D.C. Gooddy, and A.M. Binley, 2019, Use and application of CFC-11, CFC-12, CFC-113 and SF_6 as environmental tracers of groundwater residence time: A review. Geoscience Frontiers, volume 10, pages 1643-1652.

Choung, S., and R.M. Allen-King, 2010, Can chlorofluorocarbon sorption to black carbon (char) affect groundwater age determinations? Environmental Science and Technology, volume 44, number 12, pages 4459-4464.

Clark, I., 2015, Groundwater Geochemistry and Isotopes. Chemical Rubber Company (CRC) Press, Taylor and Francis Group, 437 pages.

Clark, I., and P. Fritz, 1997, Environmental Isotopes in Hydrogeology. Lewis, Boca Raton, 328 pages.

Cook, P.G., and J.K. Böhlke, 2000, Determining timescales for groundwater flow and solute transport. *In* P.G. Cook and A.L. Herczeg, editors, Environmental Tracers in Subsurface Hydrology. Kluwer, Boston, pages 1-30.

Cook, P.G., G. Favreau, J.C. Dighton, and S. Tickell, 2003, Determining natural groundwater influx to a tropical river using radon, chlorofluorocarbons and ionic environmental tracers. Journal of Hydrology, volume 277, pages 74-88.

Cook, P.G., D.K. Solomon, L.N. Plummer, E. Busenberg, and S.L. Schiff, 1995, Chlorofluorocarbons as tracers of groundwater transport processes in a shallow, silty sand aquifer. Water Resources Research, volume 31, pages 425-434.

Cook, P.G., A. Love, and J. Dowie, 1996, Recharge estimation of shallow groundwaters using CFC age dating. MESA Journal, volume 3, pages 32-33.

Cook, P.G., and D.K. Solomon, 1997, Recent advances in dating young groundwater: $^{3}H/^{3}He$, chlorofluorocarbons and ^{85}Kr. Journal of Hydrology, volume 191, pages 245-265.

Cook, P.G., and A.L. Herczeg, 2000, Environmental Tracers in Subsurface Hydrology. Kluwer Academic Press, Boston, 529 pages.

Cook, P.G., 2020, Original figures and tables created for publications in 2020, peter.cook@flinders.edu.au.

Coplen, T.B., A.L. Herczeg, and C. Barnes, 2000, Isotope Engineering – Using stable isotopes of the water molecule to solve practical problems. *In*, P.G. Cook and A.L. Herczeg, editors, Environmental Tracers in Subsurface Hydrology. Kluwer, Boston, pages 79-110.

Dunkle, S.A., L.N. Plummer, J.M. Denver, P.A. Hamilton, R.L. Michel, and T.B. Coplen, 1993, Chlorofluorocarbons (CCl_3F and CCl_2F_2) as dating tools and hydrologic tracers

in shallow groundwater of the Delmarva Peninsula, Atlantic Coastal Plain, United States. Water Resources Research, volume 29, number 12, pages 3837–3860.

Eckhardt, Gregg, 2020, The Edwards Aquifer Website, https://www.edwardsaquifer.net/images/carrizo_map.jpg↗.

Ekwurzel, B., P. Schlosser, W.M. Smethie Jr, L.N. Plummer, E. Busenberg, R.L. Michel, R. Weppernig, and M. Stute, 1994, Dating of shallow groundwater: comparison of the transient tracers $^{3}H/^{3}He$, chlorofluorocarbons, and ^{85}Kr. Water Resources Research, volume 30, number 6, pages 1693-1708.

Ellins, K.K., A. Roman-Mas, and, R.Lee, 1990, Using ^{222}Rn to examine groundwater/surface discharge interaction in the Rio Grande De Manati, Puerto Rico. Journal of Hydrology, volume 115 pages 319–341.

Engesgaard, P., A.L. Hojberg, K. Hinsby, K.H. Jensen, T. Laier, F. Larsen, E. Busenberg, and L.N. Plummer, 2004, Transport and time lag of chlorofluorocarbon gases in the unsaturated zone, Rabis Creek, Denmark. Vadose Zone Journal, volume 3, number 4, pages 1249-1261.

Fabryka-Martin, J.T., A.V. Wolfsberg, P.R. Dixon, S.S. Levy, J.A. Musgrave, and H.J. Turin, 1997, Summary report of chlorine-36 studies: Sampling, analysis, and simulations of chlorine-36 in the Exploratory Studies Facility. Report LA-13352-MS, Los Alamos National Laboratory, Los Alamos, USA.

Fritz, P., and J. C. Fontes, 1980, Handbook of Environmental Isotope Geochemistry. Elsevier, Amsterdam.

Fulton, S.A., 2012, Technical Report: Great Artesian Basin Resource Assessment. Department of Land Resource Management, Darwin, Australia.

Gardner, W.P., G.A. Harrington, D.K. Solomon, and, P.G. Cook, 2011, Using terrigenic ^{4}He to identify and quantify regional groundwater discharge to streams. Water Resources Research, volume 47, doi:10.1029/2010WR010276↗.

Graven, Heather, Colin E. Allison, David M. Etheridge, Samuel Hammer, Ralph F. Keeling, Ingeborg Levin, Harro A. J. Meijer, Mauro Rubino, Pieter P. Tans, Cathy M. Trudinger, Bruce H. Vaughn, and James W. C. White, 2017, Compiled records of carbon isotopes in atmospheric CO_2 for historical simulations in CMIP6. Geoscientific Model Development, volume 10, pages 4405-4417.

Hall, C.M., M. Clara Castro, K.C. Lohmann, and, T. Sun, 2012, Testing the noble gas paleothermometer with a yearlong study of groundwater noble gases in an instrumenting monitoring well. Water Resources Research, volume 48, W04517, doi:10.1029/2011WR010951↗.

Heaton, T.H.E. and J.C. Vogel, 1981, 'Excess air' in groundwater. Journal of Hydrology, volume 50, pages 201-216.

Hendry, M.J., C.J. Kelln, L.I. Wassenaar, and, J. Shaw, 2004, Characterizing the hydrogeology of a complex clay-rich aquitard system using detailed vertical profiles of the stable isotopes of water. Journal of Hydrology, volume 293, pages 47-56.

Hinsby, K., A.L. Højberg, P. Engesgaard, K.H. Jensen, F. Larsen, L.N. Plummer, and, E. Busenberg, 2007, Transport and degradation of chlorofluorocarbons (CFCs) in the pyritic Rabis Creek aquifer, Denmark. Water Resources Research, volume 43, W10423, doi:10.1029/2006WR005854↗.

Ho, D.T., P. Schlosser, W.M. Smethie, and H.J. Simpson, 1988, Variability in atmospheric chlorofluorocarbons (CCl_3F and CCl_2F_2) near a large urban area: implications for groundwater dating. Environmental Science and Technology, volume 32, number 16, pages 2377-2382.

International Atomic Energy Association (IAEA) and World Meteorological Organization (WMO), 2018, Global Network of Isotopes in Precipitation. The Global Network of Isotopes in Precipitation (GNIP) Database. https://nucleus.iaea.org/wiser↗.

Ingraham, N.L., 1998 Isotopic variations in precipitation, Chapter 3, *in*, C. Kendall and J.J. McDonnell, editors, Isotope Tracers in Catchment Hydrology. Elsevier, Amsterdam, pages 87-118.

James, E.R., M. Manga, T.P. Rose, and, G.B. Hudson, 2000, The use of temperature and the isotopes of O, H, C, and noble gases to determine the pattern and spatial extent of groundwater flow. Journal of Hydrology, volume 237, pages 100-112.

Kendall, C. and E.A. Caldwell, 1998, Fundamentals of Isotope Geochemistry, Chapter 2, *in*, C. Kendall and J.J. McDonnell, editors, Isotope Tracers in Catchment Hydrology. Elsevier, Amsterdam, pages 51-86.

Ko, M.K.W. et al., 1993, Atmospheric sulfur hexafluoride: Sources, sinks and greenhouse warming. Journal of Geophysical Research, volume 98, number D6, pages 10499-10507.

Love, A.J., A.L. Herczeg, D. Armstrong, F. Stadter, and, E. Mazor, 1993, Groundwater flow regime within the Gambier Embayment of the Otway Basin, Australia: evidence from hydraulics and hydrochemistry. Journal of Hydrology, volume 143, pages 297-338.

Maiss, M. and C.A.M. Brenninkmeijer, 1998, Atmospheric SF_6: Trends, sources and prospects. Environmental Science and Technology, 32, 3077-3086.

Marshall, B.D., R.J. Moscati, and G.L. Patterson, 2012, Fluid geochemistry of Yucca Mountain and vicinity, *in*, J.S. Stuckless, editor, Hydrology and Geochemistry of Yucca Mountain and Vicinity, Southern Nevada and California. Geological Society of America Memoir 209, pages 143-218.

Massmann, G., and J. Sültenfuss, 2008, Identification of processes affecting excess air formation during natural bank filtration and managed aquifer recharge. Journal of Hydrology, volume 359, pages 235-246.

Mazor, E., 2004, Chemical and Isotopic Groundwater Hydrology. Dekker, New York, 453 pages.

Mazor, E., and A. Bosch, 1992, Helium as a semi-quantitative tool for groundwater dating in the range of 10^4–10^8 years, *in,* Isotopes of Noble Gases as Tracers in Environmental Studies, International Atomic Energy Association (IAEA), Vienna, pages 163-178.

Mazurek, M. et al., 2011, Natural tracer profiles across argillaceous formations. Applied Geochemistry, volume 26, number 7, pages 1035-1064.

McCallum, J.L., P.G. Cook, C.T. Simmons, and A.D. Werner, 2014, Bias of apparent tracer ages in heterogeneous environments. Groundwater, volume 52, number 2, pages 239-250.

Meredith, K.T., S.E. Hollins, C.E. Hughes, D.I. Cendon, S. Hankin, and, D.J.M. Stone, 2009, Temporal variation in stable isotopes (O-18 and H-2) and major ion concentrations within the Darling River between Bourke and Wilcannia due to variable flows, saline groundwater influx and evaporation. Journal of Hydrology, volume 378, number 3-4, pages 313-324.

Muir, K.S., and T.B. Coplen, 1981, Tracing ground-water movement by using the stable isotopes of oxygen and hydrogen, Upper Penitencia Creek Alluvial Fan, Santa Clara Valley, California. United States Geological Survey Water-Supply Paper 2075.

Murphy, E.M., T.R. Ginn, and, J.L. Phillips, 1996, Geochemical estimates of paleorecharge in the Pasco Basin: Evaluation of the chloride mass balance technique. Water Resources Research, volume 32, number 9, pages 2853-2868.

Pearson, F.J. Jr., and D.E. White, 1967, Carbon 14 ages and flow rates of water in Carrizo Sand, Atascosa County, Texas. Water Resources Research, volume 3, number 1, pages 251-261.

Peters, E., A.Visser, B.K. Esser, and, J.E. Moran, 2018, Tracers reveal recharge elevations, groundwater flow paths and travel times on Mount Shasta, California. Water, volume 10, number 97, doi:10.3390/w10020097↗.

Philips, F.M., 2000, Chlorine-36. *in*, P.G. Cook and A.L. Herczeg, editors, Environmental Tracers in Subsurface Hydrology. Kluwer, Boston, pages 299-348.

Plummer, L.N., J.R. Eggleston, D.C. Andreasen, J.P. Raffensperger, A.G. Hunt, and G.C. Casile, 2012, Old groundwater in parts of the upper Patapsco aquifer, Atlantic Coastal Plain, Maryland, USA: evidence from radiocarbon, chlorine-36 and helium-4. Hydrogeology Journal, volume 20, pages 1269-1294.

Reilly, T.E., L.N. Plummer, P.J. Phillips, E. Busenberg, 1994, The use of simulation and multiple environmental tracers to quantify groundwater flow in a shallow aquifer. Water Resources Research, volume 30, number 2, pages 421-433.

Robertson, W.D., and J.A. Cherry, 1989, Tritium as an indicator of recharge and dispersion in a groundwater system in central Ontario. Water Resources Research, volume 25, number 6, pages 1097-1109.

Rosman, K.J.R., and P.D.P. Taylor, 1998, Isotopic compositions of the elements 1997. Pure Applied Chemistry, volume 70, number1, pages 217-235.

Ruland, W.W., J.A. Cherry, and S. Feenstra, 1991, The depth of fractures and active ground-water flow in a clayey till plain in southwestern Ontario. Groundwater, volume 29, number 3, pages 405-417.

Salmon, S.U., H. Prommer, J. Park, K.T. Meredith, J.V. Turner, and J.L. McCallum, 2015, A general reactive transport modelling framework for simulating and interpreting groundwater ^{14}C age and $\delta^{13}C$. Water Resources Research, doi:10.1002/2014WR015779↗.

Sanford, W.E., 1997, Correcting for diffusion in carbon-14 dating of ground water. Groundwater, volume 35, number 2, pages 357-361.

Sanford, W.E., 2011, Calibration of models using groundwater age. Hydrogeology Journal, volume 19, pages 13-16.

Schlosser, P., M. Stute, C. Sonntag, and K.O. Münnich, 1989, Tritiogenic ^{3}He in shallow groundwater. Earth and Planetary Science Letters, volume 94, pages 245-256.

Solomon, D.K., R.J. Poreda, P.G. Cook, and A. Hunt, 1995, Site characterization using $^{3}H/^{3}He$ ground water ages, Cape Cod, MA. Groundwater, volume 33, pages 988-996.

Solomon, D.K., A. Hunt, and R.J. Poreda, 1996, Source of radiogenic helium 4 in shallow aquifers: implications for dating young groundwater. Water Resources Research, volume 32, number 6, pages 1805-1813.

Stute, M., K. Deak, K. Revesz, J.K. Böhlke, E. Deseo, R. Weppernig, and P. Schlosser, 1997, Tritium/^{3}He dating of river infiltration: an example from the Danube in the Szigetkoz area, Hungary. Groundwater, volume 35, number 5, pages 905-911.

Stute, M. and P. Schlosser, 2000, Atmospheric noble gases. i*n*, P.G. Cook and A.L. Herczeg, editors, Environmental Tracers in Subsurface Hydrology. Kluwer, Boston, pages 349-377.

Sudicky, E.A., and E.O. Frind, 1981, Carbon 14 dating of groundwater in confined aquifers: Implications of aquitard diffusion. Water Resources Research, volume 17, number 4, pages 1060-1064.

Trapp, Henry, Jr., and Marilee A. Horn, 1997, Ground Water Atlas of the United States: Delaware, Maryland, New Jersey, North Carolina, Pennsylvania, Virginia, West Virginia. United States Geological Survey Hydrologic Atlas 730-L, https://pubs.usgs.gov/ha/ha730/ch_l/gif/L018.GIF↗.

United States Geological Survey (USGS), 2019, MODFLOW Software, www.usgs.gov/mission-areas/water-resources/science/modflow-and-related-programs?qt-science_center_objects=0#qt-science_center_objects↗.

Verhagen, B.T., 1992, Detailed geohydrology with environmental isotopes. A case study at Serowe, Botswana. Isotope Techniques in Water Resources Development 1991, International Atomic Energy Association (IAEA), Vienna, pages 345-362.

Vogel, J.C., 1967, Investigation of groundwater flow with radiocarbon. Isotopes in Hydrology, International Atomic Energy Association (IAEA), Vienna, pages 355-369.

Walker, S.J., R.F. Weiss, and P.K. Salameh, 2000, Reconstructed histories of the annual mean atmospheric mole fractions for the halocarbons CFC-11, CFC-112, CFC-113, and carbon tetrachloride. Journal of Geophysical Research, volume 105, number C6, pages 14285-14296.

Weissmann, G.S., Y. Zhang, E.M. LaBolle, and G.E. Fogg, 2002, Dispersion of groundwater age in an alluvial aquifer system. Water Resources Research, volume 38, number 10, doi:10.1029/2001WR000907↗.

Wikimedia Commons, 2010, "Lake Eyre drainage basin including the major rivers↗" by Kmusser↗, own work using Digital Chart of the World, The Rand McNally New International Atlas (1993) and Department of the Environment, Water, Heritage and the Arts map used as references, is licensed under CC BY-SA 3.0↗)

Wikimedia Commons, 2010, "Location of geographical macroregion of hu:Alföld (red) within subdivisions of Hungary↗, own work based on Magyarország kistájainak katasztere" by Miaow Miaow↗ is public domain.

Wikimedia Commons, 2019, Danube Map, https://commons.wikimedia.org/wiki/File:Danubemap.png↗.

Wolfsberg, A.V., J.T. Fabryka-Martin, and S.S. Levy, 1999, Use of chlorine-36 and other geochemical data to test a groundwater flow model for Yucca Mountain, Nevada. *in*, Use of Hydrogeochemical Information in Testing Groundwater Flow Models. Workshop held at Borgolm, Sweden, 1-3 September 1997. Organisation for Economic Co-operation and Development (OECD), Nuclear Energy Agency.

8 Exercise Solutions

Exercise 1 Solution

Answer: The proportion of river water in piezometer P2 is calculated to be 25% using ^{2}H values, and 20% using chloride concentrations. The corresponding proportions of regional groundwater in piezometer P2 are then 75% and 80% using ^{2}H and chloride, respectively.

Details: Equation 7 can be re-arranged to $f = \frac{c_m - c_2}{c_1 - c_2}$

where f is the proportion of end-member 1, c_1 and c_2 are the respectively end-member concentrations and c_m is the concentration of the mixed sample. Using c_m = 380 mg/L, c_1 = 25 mg/L and c_2 = 500 mg/L gives f = (-120)/(-475) = 0.25. Using c_m = -26 ‰, c_1 = -10 ‰ and c_2 = -30 ‰ gives f = 4/20 = 0.2.

Rack to exercise 1

Exercise 2 Solution

Answer: The velocity is 4.6 meters per year and the hydraulic conductivity is 16.3 meters per day.

Details: First use Equation 1 to calculate the groundwater age at each well. Using c_0 = 90 pmC and $\lambda = 1.21 \times 10^{-4}$, gives t = 1077 years for the upstream well and 3921 years for the downstream well. The age gradient is then (3921 – 1077) / 13000 years per meter = 0.219 y m^{-1}. From Equation 9, the horizontal velocity is the inverse of the age gradient, which equals 4.57 m y^{-1}.

Darcy's Law gives the relationship between the seepage velocity and the hydraulic conductivity as:

$v = Ki/n_e$

so

$K = v n_e / i$

$i = (h_1 - h_2)$/distance between h_1 and h_2 = 2 m / 13000 m = 0.000154

K = 4.57 m/y x 0.2 / 0.000154 = 5943 m/y = 16.3 m/day

Return to exercise 2

Exercise 3 Solution

Answer: The recharge rate is 60 millimeters per year.

Details: Equation 9 can be re-arranged to give $R = \frac{H\theta}{t} ln\left(\frac{H}{H-z}\right)$

Using H = 50 m, z = 10 m, θ = 0.2 and t = 39 years, gives R = 0.057 m/y or 57 mm/y or rounding 60 mm/yr.

Return to exercise 3

Exercise 4 Solution

Answer: The groundwater age is 7.3 years.

Working: In Equation 3, c_p = 10 TU, c_d = 5 TU and λ = 0.0558 y^{-1}. The groundwater age is therefore calculated to be 7.3 years.

Return to exercise 4

9 About the Author

Dr. Peter Cook is a Professorial Research Fellow at Flinders University, South Australia, and Director of the Australian National Centre for Groundwater Research and Training. He previously spent more than 20 years as Research Scientist with CSIRO. With more than 30 years of experience, he has worked on groundwater investigations in Australia, Europe, North America and Africa. He regularly advises Australian and international governments on water management, and has consulted to attorneys, industries, engineering companies, government agencies and citizen groups on groundwater issues. He has conducted projects on a broad range of groundwater topics, many of which have involved the application of environmental tracers and isotopes. These have included assessment of rates of groundwater recharge and discharge, surface water-groundwater interactions, groundwater-dependence of vegetation, impacts of mining and unconventional gas on groundwater and regional groundwater management. He has written or co-written books on environmental tracers and ecohydrology and was the NGWA Darcy Lecturer in 2009.

Please consider signing up to the Groundwater Project mailing list and stay informed about new book releases, events and ways to participate in the Groundwater Project. When you sign up to our email list it helps us build a global groundwater community. Sign-up↗.

Modifications from original release

Adjusted numbering and indenting of headings to be consistent with latest GW-Project books

p. 11, Table 2, 3rd column: 34Sr changed to 84Sr

p. 17, Definitions of variables below Equation (7): C's changed to lower case.

p. 18, Definitions of variables below Equation (11): C's changed to lower case.

p. 71, Exercise 2 Solution: space was removed from the number 13 000 to be 13000.